The standard model effective field theory at work

Gino Isidori,* Felix Wilsch,† and Daniel Wyler‡

Physik-Institut, Universität Zürich, CH-8057 Zürich, Switzerland

(published 19 March 2024)

The striking success of the standard model in explaining precision data and, at the same time, its lack of explanations for various fundamental phenomena, such as dark matter and the baryon asymmetry of the Universe, suggest new physics at an energy scale that greatly exceeds the electroweak scale. In the absence of a short-range–long-range conspiracy, the standard model can be viewed as the leading term of an effective "remnant" theory (referred to as the SMEFT) of a more fundamental structure. In recent years, many aspects of the SMEFT have been investigated, and it has become a standard tool for analyzing experimental results in an integral way. In this review, after a presentation of the salient features of the standard model, the construction of the SMEFT is reviewed. The range of its applicability and bounds on its coefficients imposed by general theoretical considerations are discussed. Since new-physics models are likely to exhibit exact or approximate accidental global symmetries, especially in the flavor sector, their implications for the SMEFT are also discussed. The main focus of the review is the phenomenological analysis of experimental results. How to use various effective field theories to study the phenomenology of theories beyond the standard model is explicitly shown. Descriptions of the matching procedure and the use of the renormalization group equations are given, allowing one to connect multiple effective theories that are valid at different energy scales. Explicit examples from low-energy experiments and from high-p_T physics illustrate the workflow. Also commented upon are the nonlinear realization of electroweak symmetry breaking and its phenomenological implications.

DOI: 10.1103/RevModPhys.96.015006

CONTENTS

*gino.isidori@physik.uzh.ch
†felix.wilsch@physik.uzh.ch
‡wyler@physik.uzh.ch

I. INTRODUCTION

The standard model (SM) of particle physics, formulated approximately 50 years ago and judiciously completed over the years, forms the basis of our understanding of the fundamental interactions:

> Maybe the main point of our analysis is that it demonstrates explicitly how remarkable the standard electroweak theory is (Buchmüller and Wyler, 1986).

More precisely, the SM is the quantum field theory (QFT) that describes how the basic matter constituents (quarks and leptons) interact at the microscopic level via weak, strong, and electromagnetic forces. While all data from Earth-based laboratory experiments agree with the SM predictions (with a few possible exceptions that we later comment upon), there is some indirect evidence derived from cosmological observations that the model is not complete: It does not explain the baryon asymmetry of the Universe, dark matter, or dark energy. These are all phenomena that could find their explanation in the domain of particle physics or, more generally, within QFT. There are also theoretical concerns about the SM itself, such as the strong sensitivity of the Higgs mass term to high-energy modes in the renormalization procedure (the so-called hierarchy problem), the absence of an explanation for the hierarchical structure of the fermion spectrum, and the lack of a bridge to quantum gravity. Finally, nonvanishing neutrino masses cannot be accounted for by the "classical version" of the standard model, containing only left-handed neutrinos and only renormalizable interactions.

To address these problems, a large number of new "fundamental" theories beyond the standard model (BSM) were formulated over the past 40–50 years. In fact, the 1980s and, to a lesser extent, the 1990s saw an explosion of model building. While some of the theories addressed specific questions, others offered veritable extensions of the basics of the SM, such as supersymmetric models, models with composite Higgs sectors, and composite quarks and leptons: concepts that might become important again in the future, possibly within a new context, such as string theory. These models have new particles and interactions, generally at energies well above the Fermi scale. They were designed to explain some of the facts that the SM cannot, such as the quantization of the electric charge, the hierarchical generational structure of quarks and leptons, the possible unification of interaction strengths, etc. However, many of these models have been shown to be inconsistent with data or will not be testable at present or near-future experimental facilities.

To explore these new-physics scenarios, most likely manifested in small discrepancies between the SM predictions and the observations, both theoretical and experimental progress will be necessary. Over many years and with increasing intensity and success in the new century, theoretical work on the standard model has improved enormously. Apart from devising new calculational tools, this progress has been made possible by developing and applying the concepts of effective field theory (EFT) in several relevant areas. Roughly speaking, a quantum EFT is a quantum field theory that is not considered to be fundamental, as it is valid in only a limited range of energies or distances, or even in specific kinematic configurations. The wide separation between the Fermi scale (or the W-boson mass m_W) and the masses of the B mesons or the charmed particles has allowed EFT and renormalization group techniques to be successfully used to calculate the expected inclusive decay rates of these mesons with astonishing accuracy. The formulation of new quantum EFTs like heavy quark effective theory and soft collinear effective theory have also led to accurate predictions for exclusive decays. In addition, high-energy calculations, such as those used for jet dynamics at the Large Hadron Collider (LHC), have benefited from EFT techniques. The oldest effective field theory of the SM, namely, chiral perturbation theory (ChPT), has been extensively used to obtain precise results for low-energy meson dynamics. We expect this quest for ever higher precision, on both the theoretical and the experimental side, to continue, in the hope of finding deviations from the SM for which there are well motivated reasons.

In this perspective, it is natural to consider the original formulation of the SM as the effective low-energy "remnant" of a more fundamental theory whose new heavy degrees of freedom are removed in favor of generating additional effective contact interactions between the known SM fields. As argued by Wilson (1983), the true physics of the "full" theory below the cutoff scale can be recovered by including all possible interactions allowed by the particles and symmetries of the theory. The effective Lagrangian thus obtained consists of a string of local interaction terms (operators), each characterized by an appropriate coefficient (effective coupling or Wilson coefficient), organized in a series of increasing dimensionality corresponding to the expected decreasing relevance. As is common for EFTs, this construction is not renormalizable in the usual strict sense, because it involves an infinite number of coupling constants. It is, however, renormalizable order by order in an energy or momentum expansion reflected in the operator expansion. The independence from the renormalization scale of physical amplitudes can be exploited using the renormalization group flow of the operator coefficients, allowing the largest quantum corrections to be identified and resummed.

Given the success of effective theories thus far, this approach seems to be a good way to access the next layer of physics, as proposed by Buchmüller and Wyler (1986) even before the last building blocks of the SM where experimentally identified. In this review, we trace its development and highlight some of the most recent results. Our main scope is to illustrate how considering the SM as an EFT can help in identifying properties of the new physics and single out future

research directions. The EFT approach provides not only a systematic way for analyzing experimental results but also a precious tool to correlate different observables while obtaining deeper insights on where to look for the next layer.

This review is organized as follows: In the rest of this section we introduce the SM, also recalling the motivations for why we want to go beyond it; we review general aspects of EFT; and finally we introduce the so-called standard model effective field theory (SMEFT). A detailed analysis of the SMEFT, with a special focus on the structure of operators of dimension 6, is presented in Sec. II. The role of global symmetries in the SMEFT, with a particular emphasis on exact and approximate flavor symmetries, is discussed in Sec. III. Section IV is devoted to a discussion of the differences between the SMEFT and the more general case of a nonlinearly realized electroweak symmetry. In Sec. V we review the low-energy ($E \ll M_W$) effective theory of the SMEFT, particularly in comparison with the standard model. Finally, in Sec. VI we present two concrete examples of the SMEFT at work, i.e., of applications of the SMEFT to analyze concrete phenomenological problems. In the Appendix we discuss some technical details of dimensional regularization showing up in SMEFT computations.

A. The standard model of particle physics

Within the standard model[1] the three fundamental forces are described via the principle of gauge invariance, requiring the theory to be invariant under the local symmetry group

$$\mathcal{G}_{\mathrm{SM}} = \mathrm{SU}(3)_c \times \mathrm{SU}(2)_L \times \mathrm{U}(1)_Y. \tag{1.1}$$

The quantum fields can be divided into three categories: (i) the gauge fields associated with the local gauge symmetry groups (G_μ, W_μ, B_μ), (ii) the matter (fermion) fields (ℓ, e, q, u, d), and (iii) the Higgs boson doublet H responsible for the breaking of the electroweak subgroup of $\mathcal{G}_{\mathrm{SM}}$ down to the QED group $\mathrm{U}(1)_e$,

$$\mathrm{SU}(2)_L \times \mathrm{U}(1)_Y \to \mathrm{U}(1)_e. \tag{1.2}$$

The field content of the SM is shown in Table I together with the transformation properties of each field under the different gauge groups and the hypercharge assignments.[2] The basic fermion family (ℓ, e, q, u, d) is replicated three times.

The SM Lagrangian is the most general renormalizable expression that can be constructed out of the fields in Table I that is invariant under $\mathcal{G}_{\mathrm{SM}}$,

TABLE I. Standard model field content with the transformation properties of the fields under $\mathrm{SU}(3)_c \times \mathrm{SU}(2)_L$ and the hypercharge assignments. The fields are divided into fermions (ℓ, e, q, u, d), the Higgs doublet (H), and the gauge fields (G, W, B).

	ℓ	e	q	u	d	H	G	W	B
$\mathrm{SU}(3)_c$ representation	**1**	**1**	**3**	**3**	**3**	**1**	**8**	**1**	**1**
$\mathrm{SU}(2)_L$ representation	**2**	**1**	**2**	**1**	**1**	**2**	**1**	**3**	**1**
$\mathrm{U}(1)_Y$ charge	$-\frac{1}{2}$	-1	$\frac{1}{6}$	$\frac{2}{3}$	$-\frac{1}{3}$	$\frac{1}{2}$	0	0	0

$$\begin{aligned}\mathcal{L}_{\mathrm{SM}} = & -\tfrac{1}{4}G^A_{\mu\nu}G^{A\mu\nu} - \tfrac{1}{4}W^I_{\mu\nu}W^{I\mu\nu} - \tfrac{1}{4}B_{\mu\nu}B^{\mu\nu} \\ & - \frac{\theta_3 g_3^2}{32\pi^2}G^A_{\mu\nu}\tilde{G}^{A\mu\nu} - \frac{\theta_2 g_2^2}{32\pi^2}W^I_{\mu\nu}\tilde{W}^{I\mu\nu} - \frac{\theta_1 g_1^2}{32\pi^2}B_{\mu\nu}\tilde{B}^{\mu\nu} \\ & + i(\bar{\ell}_p \not{D} \ell_p + \bar{e}_p \not{D} e_p + \bar{q}_p \not{D} q_p + \bar{u}_p \not{D} u_p + \bar{d}_p \not{D} d_p) \\ & + (D_\mu H)^\dagger (D^\mu H) + m^2 H^\dagger H - \frac{\lambda}{2}(H^\dagger H)^2 \\ & - ([Y_e]_{pr}\bar{\ell}_p e_r H + [Y_u]_{pr}\bar{q}_p u_r \tilde{H} + [Y_d]_{pr}\bar{q}_p d_r H + \mathrm{H.c.}).\end{aligned} \tag{1.3}$$

1. The gauge sector

The first three lines of Eq. (1.3) contain all gauge interactions in the SM. The gauge couplings associated with the gauge groups $\mathrm{SU}(3)_c$, $\mathrm{SU}(2)_L$, and $\mathrm{U}(1)_Y$ are g_3, g_2, and g_1, respectively. The indices $A = 1, \ldots, 8$ and $I = 1, 2, 3$ denote adjoint $\mathrm{SU}(3)_c$ and $\mathrm{SU}(2)_L$ gauge indices, respectively. In the first line of Eq. (1.3) the field-strength tensors are defined by

$$G^A_{\mu\nu} = \partial_\mu G^A_\nu - \partial_\nu G^A_\mu + g_3 f^{ABC} G^B_\mu G^C_\nu, \tag{1.4a}$$

$$W^I_{\mu\nu} = \partial_\mu W^I_\nu - \partial_\nu W^I_\mu + g_2 \varepsilon^{IJK} W^J_\mu W^K_\nu, \tag{1.4b}$$

$$B_{\mu\nu} = \partial_\mu B_\nu - \partial_\nu B_\mu, \tag{1.4c}$$

where f^{ABC} and ε^{IJK} are the totally antisymmetric structure constants of $\mathrm{SU}(3)_c$ and $\mathrm{SU}(2)_L$. They contain the kinetic terms for the gauge fields as well as all interactions among the gauge fields themselves.

On the second line, the dual field-strength tensors are defined by $\tilde{F}^{\mu\nu} = (1/2)\varepsilon^{\mu\nu\rho\sigma}F_{\rho\sigma}$ for $F = G^A, W^I, B$ with the totally antisymmetric Levi-Civita tensor defined by $\varepsilon^{0123} = -\varepsilon_{0123} = +1$. The Lagrangian terms containing dual field-strength tensors are proportional to total derivatives, meaning that we can rewrite them as $G^A_{\mu\nu}\tilde{G}^{A,\mu\nu} = 2\varepsilon^{\mu\nu\alpha\beta}\partial_\mu[G^A_\nu \partial_\alpha G^A_\beta + (1/3)g_3 f^{ABC} G^A_\nu G^B_\alpha G^C_\beta]$. Therefore, they can contribute only to topological effects. For simplicity, we drop them from here on.

The third line comprises the kinetic terms of the fermion fields as well as their gauge interactions. The latter are encoded in the gauge covariant derivative

$$D_\mu = \partial_\mu - i g_3 T^A G^A_\mu - i g_2 t^I W^I_\mu - i g_1 \mathsf{y} B_\mu, \tag{1.5}$$

where $T^A = \lambda^A/2$ and $t^I = \tau^I/2$ are the generators of the fundamental representation of $\mathrm{SU}(3)_c$ and $\mathrm{SU}(2)_L$, respectively, with the Gell-Mann matrices λ^A and the Pauli matrices τ^I. The hypercharge generator is denoted as y.

[1]For a pedagogical introduction to the SM, see Donoghue, Golowich, and Holstein (2014) and Grossman and Nir (2023).

[2]In principle, one could extend the fermion content including right-handed neutrinos. However, those fields would be completely neutral under $\mathcal{G}_{\mathrm{SM}}$. We prefer to define the SM as the theory of the chiral fermions with nontrivial transformation properties under $\mathcal{G}_{\mathrm{SM}}$ that acquire mass via the Higgs mechanism. As such, right-handed neutrinos are not SM fields.

2. The Higgs sector

The last two lines of Eq. (1.3) include the Higgs and Yukawa sectors of the SM written in symmetric notation before electroweak symmetry breaking. The complex Higgs doublet is denoted by H, and we define $\tilde{H} = i\tau_2 H^*$. Minimizing the scalar potential

$$V(H) = -m^2 H^\dagger H + \frac{\lambda}{2}(H^\dagger H)^2 \tag{1.6}$$

yields a nonvanishing vacuum expectation value (VEV) for the Higgs field, $v^2 = 2\langle 0|H^\dagger H|0\rangle$, whose tree-level expression reads $v^2 = 2m^2/\lambda$. Considering the breaking of the electroweak symmetry, it is convenient to rewrite the Higgs doublet as

$$H = \frac{1}{\sqrt{2}} \begin{pmatrix} \varphi^2 + i\varphi^1 \\ v + h - i\varphi^3 \end{pmatrix}, \tag{1.7}$$

where h is the massive physical Higgs boson and φ^a denote the three Goldstone bosons that, in the unitary gauge, are "eaten" by the massive gauge bosons. The tree-level mass of the physical Higgs is $m_h^2 = 2m^2$.

The Yukawa couplings $[Y_i]_{pr}$ for $i = e, u, d$ are complex 3×3 matrices in flavor space contracted to the fermion fields via the global flavor indices p and r, which run from 1 to 3. After electroweak symmetry breaking the Yukawa interactions in Eq. (1.3) yield the fermion mass terms as well as the Yukawa interactions with the physical Higgs boson h. The Yukawa matrices $Y_{u,d}$ are the only source of flavor violation in the SM, as the gauge interactions are all flavor diagonal. They are also the only source of CP violation in the SM apart from the topological terms associated with the dual field-strength tensors, which are shown on the second line of Eq. (1.3).

3. The success of the standard model

With the discovery of the Higgs boson by the ATLAS (Aad *et al.*, 2012) and CMS (Chatrchyan *et al.*, 2012) experiments at the LHC in 2012, the last missing piece of the standard model was observed. The measurement of the Higgs mass also made it possible to complete the determination of all the free parameters of the SM Lagrangian, except for the topological terms. The overall agreement of the theoretical predictions of the SM with the plethora of available experimental data is noteworthy. The achieved precision is high, especially in the electroweak sector (Haller *et al.*, 2018; de Blas *et al.*, 2022), as highlighted by the results in Fig. 1. We emphasize that the results shown in the figure are only a small subset of the many tests successfully passed by the SM in the past few years, including flavor-violating transitions of both quarks and leptons (Isidori and Teubert, 2014; Bona *et al.*, 2022) and high-energy processes (Boyd, 2022). In particular, no clear deviation from the SM predictions has been observed in the high-energy distributions analyzed thus far during the ATLAS and CMS experiments, which collected an integrated luminosity of about 140 pb^{-1} each in proton-proton collisions at an energy of $\sqrt{s} = 13$ TeV at the LHC.

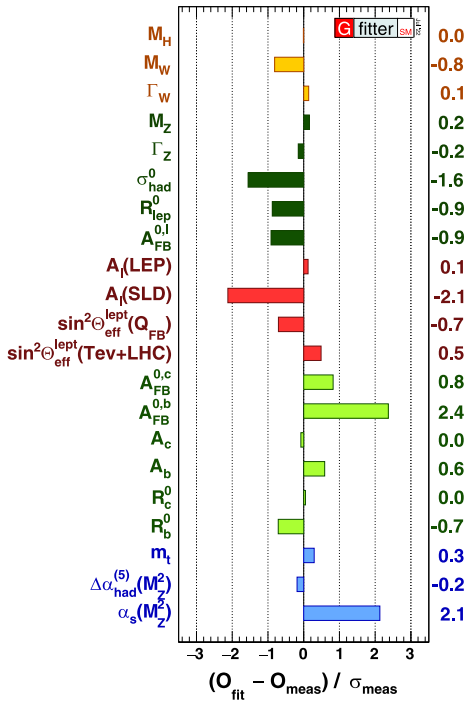

FIG. 1. *Pulls* of the electroweak observables as obtained by a global SM fit, namely, differences between SM predictions and direct measurements, normalized to the experimental uncertainties. From Haller *et al.*, 2022.

B. Motivations for and hints of new physics

Despite the strong agreement of the SM with experimental data, there are well-known deficiencies that hint at a more fundamental theory. The most important is arguably the failure to incorporate gravity, the fourth known fundamental force of nature, into a coherent QFT framework that is valid at arbitrary energy scales. As anticipated, the SM does not provide an explanation for cosmological observations such as the baryon asymmetry, dark matter, and dark energy. These phenomena do not necessarily need to be explained in the domain of particle physics. However, no convincing alternative explanations have yet been provided and, if interpreted in a QFT framework, they unavoidably point to the existence of new degrees of freedom beyond the SM ones.

The clear experimental evidence of nonvanishing neutrino masses is also an unambiguous indication that the SM Lagrangian in Eq. (1.3) is not complete. As we discuss in Sec. II.A, a natural solution to this problem is obtained when one interprets Eq. (1.3) as the first part (more precisely, the leading part containing operators up to dimension 4) of a more general EFT Lagrangian. A serious consistency problem of the SM is the instability of the Higgs quadratic term in Eq. (1.6) with respect to the quantum corrections, the so-called electroweak hierarchy problem (Barbieri, 2019). While none of the previously mentioned problems point to a well-defined energy scale for the breakdown of the SM, a solution of the electroweak hierarchy problem would necessarily require new physics not far from the Fermi scale ($v \approx 246$ GeV). More precisely we should expect some new degrees of freedom in the few-TeV energy domain able to screen the quadratic

sensitivity of the mass term in Eq. (1.6) to possible higher scales in the theory. The fact that no clear evidence of new physics has yet been found at the LHC has led researchers to consider explanations of this problem beyond the EFT framework (Giudice, 2019). However, we emphasize that the few-TeV energy domain is still largely unexplored, and many solutions within the EFT domain are still possible. This provides motivation for a deeper study of the SM as the low-energy limit of a more complete theory with new degrees of freedom not far from the Fermi scale, and thus potentially detectable in near-future experiments.

Besides these general considerations, there are a few specific hints of deviations from the SM predictions observed in precision measurements. None of these hints are statistically compelling yet. However, they provide an illustration of the types of deviations that we can expect in the near future, and of the types of effects that we can describe within the EFT approach to new physics. This is why we now discuss two such hints in more detail: we use these results in Sec. VI to illustrate, in practice, the power of the EFT approach.

1. Muon anomalous magnetic moment

A long-standing discrepancy between SM predictions and observations concerns the anomalous magnetic moment of the muon. The magnetic moment of the muon $\boldsymbol{\mu}_\mu$ is defined as

$$\boldsymbol{\mu}_\mu = g_\mu \left(\frac{e}{2m_\mu}\right)\boldsymbol{s}, \tag{1.8}$$

where $\boldsymbol{s}$ denotes the muon spin and g_μ is the so-called g factor. The prediction from the Dirac equations is $g_\mu = 2$; however, in QFT this value is modified by quantum effects sensitive to heavy degrees of freedom. The interesting quantum effects are parametrized by the anomalous magnetic moment $a_\mu = (1/2)(g_\mu - 2)$. According to the detailed analysis by Aoyama *et al.* (2020), the current SM prediction is $a_\mu^{\mathrm{SM}} = 116\,591\,810(43) \times 10^{-11}$. The E989 experiment at the Fermi National Accelerator Laboratory (FNAL) (Abi *et al.*, 2021) recently measured a deviation from this value that, combined with the previous Brookhaven National Laboratory E821 experiment (Bennett *et al.*, 2006), yielded the following 4.2σ discrepancy:

$$\Delta a_\mu = a_\mu^{\mathrm{Exp}} - a_\mu^{\mathrm{SM}} = (251 \pm 59) \times 10^{-11}. \tag{1.9}$$

The chance of a statistical fluctuation of this size is below 0.003%, making this an interesting hint of possible BSM dynamics. We discuss the possible interpretation of this effect in terms of the SM effective field theory in Sec. VI.D. However, we point out that there is an intense debate on the reliability of the error in the SM prediction entering Eq. (1.9). The main uncertainty is due to hadronic contributions to the photon vacuum-polarization amplitude. The latter is computed either via $\sigma(e^+e^- \to \text{hadron})$ data and dispersion relations or via lattice QCD. Recent results from lattice QCD (Borsanyi *et al.*, 2021) [see also Cè *et al.* (2022), Davies *et al.* (2022), and Alexandrou *et al.* (2023)] hinted at a possibly smaller deviation from the SM than what was obtained by Aoyama *et al.* (2020) using dispersive techniques; see also Colangelo *et al.* (2022). More recently a new measurement of $\sigma(e^+e^- \to \text{hadron})$ presented by Ignatov *et al.* (2023) also showed some discrepancies with previous experimental inputs used in the dispersive approach.

2. Lepton universality violation

Deviations from the SM predictions were recently reported in tests of lepton flavor universality in semileptonic B-meson decays. These tests were performed via universality ratios such as

$$R_{D^{(*)}} = \frac{\mathcal{B}(B \to D^{(*)}\tau\nu_\tau)}{\mathcal{B}(B \to D^{(*)}\ell\nu_\ell)}, \tag{1.10}$$

where $\ell \in \{\mu, e\}$, probing the quark-level amplitude $b \to c\ell\nu$ and similar ratios in neutral-current processes of the type $b \to s\ell\ell$. These ratios can be predicted with high accuracy within the SM due the cancellation of hadronic uncertainties. The latest results on $R_{D^{(*)}}$ indicate a 3.1σ deviation from the SM predictions (Amhis *et al.*, 2023b). We discuss a possible interpretation of this effect in terms of the SM effective field theory in Sec. VI.E.1. Until recently, an even more significant deviation was reported by the LHCb experiment in universality ratios in $b \to s\ell\ell$ decays; however, this effect was not confirmed by the latest analysis (Aaij *et al.*, 2023).

C. Effective field theories

In physics we are interested in much different length or energy scales. Progressing from the scale of the entire Universe for cosmological studies all the way down to the scales of elementary particle physics at the LHC, the relevant energy scales vary by many orders of magnitude. Each energy region usually requires its own physical theory to describe its phenomena. Note that we often do not need to know in detail the laws at all energies if we want to describe processes at a given scale: it often suffices to set scales that are small or large compared to the process of interest to zero or infinity, respectively, to get correct results. This is the basic principle of effective theory. We state it as a principle; however, in a wide class of quantum field theories, and specifically when considering effective theories with an ultraviolet cutoff, this principle follows from the decoupling theorem (Appelquist and Carazzone, 1975).[3]

Computations in an effective theory are usually simpler than in the full theory and reproduce the complete results with a degree of accuracy that can be systematically improved. A common example is Newtonian mechanics, which is the effective theory of special relativity in the limit of small energies and small velocities. Relativistic (or post-Newtonian) corrections are included in an expansion in the small parameter v^2/c^2 to the desired accuracy. Descriptions of the essence of effective quantum field theories were given by Georgi (1993), Skiba (2010), Weinberg (2016), Manohar (2018), and Falkowski (2023), on which our forthcoming discussion is

[3]Possible exceptions were discussed by Donoghue (2009).

based. Recent and further information can be found in the *All Things EFT* lecture series.[4]

Quantum EFTs as we use them today grew out of attempts to simplify and systematize the calculations of low-energy pion observables, which were originally based on current algebra techniques. Weinberg (1979b) argued[5] that, adhering strictly to the relevant symmetry properties embodied in current algebra, it is possible to construct an effective Lagrangian of the pion fields that is able to reproduce all known results and that greatly simplifies the treatment. This, together with the work of Wilson (1969), who clarified the concept of integrating out heavy states in QFT obtaining universal results, and the related decoupling theorem by Appelquist and Carazzone (1975), put EFTs on a solid basis. Starting with this basis, the systematic construction of the effective theory of low-energy QCD, namely, ChPT, was developed by Gasser and Leutwyler (1984, 1985). This theory, whose leading expansion parameter is E/Λ_{QCD}, where E is the energy of the process, has been applied with great success to describe a multitude of low-energy systems with high precision. For a recent review, see Ananthanarayan, Alam Khan, and Wyler (2023).

Another well-known example of an effective theory is Fermi's theory of weak interactions (Fermi, 1934), which is part of the EFT of the standard model, and actually the first quantum EFT considered in particle physics (although its recognition as quantum theory, valid also beyond lowest order in the loop expansion, arrived much later). While certain amplitudes of the Fermi theory diverge at high energies, thereby violating unitarity, this does not spoil the low-energy limit of the SM, and particularly the infrared (IR) behavior of QCD and QED, which are still correctly reproduced.

To elucidate in simple terms the basic concepts of quantum EFT, we now consider a theory containing two types of fields ϕ_L and ϕ_H. We further assume that $m \ll M$, where m denotes the mass of the excitations of ϕ_L and M indicates the mass associated with ϕ_H. The generating functional of the sources J_L associated with the light fields and the corresponding EFT Lagrangian can be obtained by performing the path integral over the heavy fields,

$$\begin{aligned} Z[J_L] &= \int \mathcal{D}\phi_L \exp\left(\int \mathrm{d}^4x[\mathcal{L}_{\mathrm{EFT}}(\phi_L) + \phi_L J_L]\right) \\ &= \int \mathcal{D}\phi_H \mathcal{D}\phi_L \exp\left(\int \mathrm{d}^4x[\mathcal{L}(\phi_L,\phi_H) + \phi_L J_L]\right). \end{aligned} \tag{1.11}$$

This formal manipulation, usually referred to as integrating out the heavy degrees of freedom, essentially amounts to averaging over all ϕ_H configurations. The $\mathcal{L}_{\mathrm{EFT}}(\phi_L)$ thus obtained contains nonlocal operators built only out of the light fields. Using an operator-product expansion we can then express $\mathcal{L}_{\mathrm{EFT}}$ as a generally infinite sum of higher-dimensional operators,

$$\mathcal{L}_{\mathrm{EFT}} = \mathcal{L}_{d\le 4} + \sum_{d=5}^{\infty} \frac{1}{M^{d-4}} \sum_{i=1}^{n_d} C_i^{(d)} Q_i^{(d)}, \tag{1.12}$$

where d is the mass dimension of the operator $Q_i^{(d)}$, and n_d is the number of independent operators at a given dimension d, which is always finite. The effective couplings $C_i^{(d)}$ associated with each operator are named Wilson coefficients. This procedure of integrating out the heavy fields changes the ultraviolet (UV) structure of the theory, but it ensures that the EFT is constructed in such a way as to reproduce the same low-energy behavior as the original theory.

As can be seen in Eq. (1.12), the higher-dimensional operators are suppressed by inverse powers of the mass scale M of the heavy fields. Computing physical observables using $\mathcal{L}_{\mathrm{EFT}}$ thus leads to an expansion in powers of E/M, where E is the typical energy scale of the process of interest. The EFT description is valid if $E \sim m \ll M$, i.e., if the energies probed are far below the mass scale of the heavy states and only the light particles can be produced on shell. This energy region is exactly where the EFT offers a valid approximation of the underlying theory. It is then sufficient to truncate the sum over d in Eq. (1.12) at a finite order, depending on the required accuracy of the result, since higher-dimensional operators contribute with higher powers of the suppression factor E/Λ. More details on the validity of the EFT approach are given in Sec. II.C.1.

Since the operators $Q_i^{(d)}$ in Eq. (1.12) are of mass dimension $d > 4$, these terms are nonrenormalizable in the traditional sense, that is, all infinities cannot be absorbed into a finite number of coefficients. For example, a divergent Feynman graph with two insertions of a $d = 5$ operator is of the order of $\mathcal{O}(M^{-2})$ and therefore requires a counterterm of mass dimension $d = 6$. A diagram with two insertions of this counterterm would then require a $d = 8$ counterterm, etc. Thus, an infinite set of operators would be required to render the theory finite. However, the EFT comes with an associated expansion in powers of E/M: if all terms with more than k powers of this parameter are neglected, only a finite set of parameters remains and the theory can be renormalized in the usual sense. This means that all infinities up to terms of the order of $(E/M)^k$ can be canceled by a finite set of couplings, and that the corresponding renormalization group (RG) equations can be derived.

The procedure of integrating out heavy particles as shown in Eq. (1.11) can be performed repeatedly. Suppose that we have a theory with particles at several well separated mass scales $\Lambda_1 \gg \Lambda_2 \gg \Lambda_3 \gg \cdots$. We can first integrate out the heavy particles at the scale Λ_1 and then compute the RG equations of the resulting EFT to run the theory down from Λ_1 to Λ_2. Next we can integrate out the particles at the mass scale Λ_2, obtaining a second EFT only containing practices with masses $\lesssim\Lambda_3$. Again we can compute the RG equations of the new EFT to run down to the scale Λ_3, etc., until we reach the desired mass scale. The advantage of this multistep procedure is the systematic resummation of large logarithms that would appear in the matching steps if we would only do a single matching at the desired scale and integrate out all heavy particles at once.

[4]See https://sites.google.com/view/all-things-eft.

[5]For early work, see Weinberg (1967) and Dashen and Weinstein (1969); see also Weinberg (1980a, 2010).

The previously described scenario can be viewed as the *top-down* approach to EFTs. We start with a known theory at the high scale and integrate out the heavy particles. This is the adequate procedure when we strive to make precise predictions from a known theory with known UV behavior. However, EFTs can also be a useful tool if the full theory at the high scale is unknown, with only some of its features known. This was the case for the strong interactions before the discovery of the $SU(3)_c$ gauge theory, which was helped by the work on current algebra and chiral perturbation theory. This scenario is often referred to as the *bottom-up* approach. This is also the case for the present situation, where the standard model is known and one wants to understand the underlying theory. This is the approach of the SM effective theory. In this case the operators $Q_i^{(d)}$ in Eq. (1.12) do not emerge in the matching procedure but have to be constructed using symmetry arguments. Suppose that we want to find the EFT operators for the SM. In this case we have $\mathcal{L}_{d\leq 4} = \mathcal{L}_{\rm SM}$, and for the EFT operators $Q_i^{(d)}$ at a given mass dimension d we simply have to construct all structures that are invariant under the local and global symmetries of the theory of interest, i.e., the SM. In this bottom-up setup we usually replace the explicit mass M in Eq. (1.12) by a generic UV scale Λ that can be identified with a heavy BSM mass scale once the EFT is matched to a UV theory. In the remainder of this review we focus on these EFT extensions of the SM, with particular emphasis on the so-called SMEFT.

D. The standard model as an effective theory

As mentioned, the standard model can be interpreted as the leading-order dimension-4 piece of a larger effective theory. This EFT must have the same gauge symmetries as the SM. The gain of embedding the unknown physics into an effective theory is that it applies to all particle-physics processes and thus allows us to use a common framework to relate results of different experiments. There are actually two candidate EFTs that are distinguished only by their assumptions on the realization of the electroweak symmetry group. The SMEFT assumes that the electroweak symmetry is realized linearly, whereas the Higgs effective field theory (HEFT) allows us to consider the more general case of a nonlinear realization.[6] Within the SM the two versions are equivalent, as they are related by a field redefinition. However, they lead to different EFT descriptions, as in the EFT framework it is not always possible to find a field redefinition to go from a nonlinear to a linear realization of the electroweak symmetry (we review this issue in more detail in Sec. IV). The HEFT is thus a more general theory containing the SMEFT as a special case. In particular, the HEFT scenario also applies to BSM theories where the Higgs is part of a strongly interacting and not fully decoupled sector.

In this review we focus mainly on the SMEFT: on the one hand, because of its "simplicity" and, on the other hand, because present data on SM precision tests and Higgs couplings seem to favor a linearly realized electroweak symmetry, i.e., a fundamental (or quasifundamental) Higgs field transforming as doublet of $SU(2)_L$. For an extensive discussion about differences between HEFT and SMEFT, see Brivio and Trott (2019).

Applying the general concepts of EFT discussed in Sec. I.C, we can decompose the SMEFT Lagrangian as

$$\mathcal{L}_{\rm SMEFT}(\psi,H,A) = \mathcal{L}_{\rm SM}(\psi,H,A) + \sum_{d=5}^{\infty}\sum_{i=1}^{n_d}\frac{C_i^{(d)}}{\Lambda^{(d-4)}}Q_i^{(d)}(\psi,H,A). \quad (1.13)$$

In Eq. (1.13) ψ, H, and A collectively denote the SM fermion, Higgs, and gauge fields, respectively, as listed in Table I. The key assumption of this construction is indeed the hypothesis that physics beyond the SM is characterized by one or more heavy scales. As in most of the literature, we adopt the convention where the Wilson coefficients $C_i^{(d)}$ are dimensionless quantities; this is why we explicitly pull the factor $\Lambda^{(4-d)}$ out in the effective couplings. In principle, the sum on d runs over all possible values; however, the majority of our discussion here focuses on operators up to dimension 6, and therefore we often drop the superscript d denoting the operator dimension.

After fixing the mass dimension up to which we expand the EFT, which is equivalent to determining the desired accuracy of our result, $\mathcal{L}_{\rm SMEFT}$ is capable of describing the low-energy signatures of generic UV completions of the SM. One of the less trivial aspect of this approach is the construction of a suitable basis of operators at a given dimension. Not surprisingly a long time passed from the initial formulation of a complete basis for the SMEFT at dimension 6 by Buchmüller and Wyler (1986) until the identification of a complete and nonredundant basis by Grzadkowski *et al.* (2010). We review how this is done in general, and specifically for the SMEFT up to dimension 6, in Sec. II.A.

In many realistic UV completions, the physics above the electroweak scale is characterized by several mass scales. What matters to determine the convergence of the EFT expansion is the lowest of such scales, which we can identify with Λ. However, the presence of additional energy scales can play a role in determining the size of the $C_i^{(d)}$ given the conventional choice of assuming a unique normalization scale Λ in Eq. (1.13). We return to this point at the end of Sec. II and in Sec. III.

The two key assumptions of this construction in describing generic extensions of the SM is that no unknown light particles exist and the electroweak symmetry is linearly realized. Under these hypotheses, any experimental result on the search for new physics can be given in the framework of the SMEFT, i.e., in terms of bounds on the Wilson coefficients, if the energies probed in the experiment are well below the scale of new physics. At the same time, different models of new physics can be matched onto the SMEFT Lagrangian by integrating out the heavy particles in each theory. Note that if a deviation from the SM emerges, the SMEFT can be used to test its consistency in pointing out correlated observables and discriminating among large

[6]The HEFT is sometimes also called the electroweak chiral Lagrangian.

varieties of UV completions. Illustrating all this with concrete examples is the subject of Sec. VI.

The absence of light new particles is definitely a strong hypothesis. Several examples of light new states, such as axionlike particles or the dilaton, are well founded and can originate by physics at energies far beyond the weak scale. However, such new states are necessarily weakly coupled to the SM fields (otherwise, they would have already been discovered). This implies that we can neglect their effect in a large class of observables, for which the description in terms of the SMEFT remains an efficient tool. To describe in full generality these frameworks requires the corresponding light fields in the EFT to be added. This can be done case by case according the nature of the new degrees of freedom but is beyond the scope of this review.

II. STANDARD MODEL EFFECTIVE FIELD THEORY

In this section, we provide a comprehensive introduction to the SMEFT. We start by presenting general arguments on how to find an operator basis and then focus on the construction of the commonly used *Warsaw basis* (Grzadkowski *et al.*, 2010). In Sec. II.B, we analyze how the size of the different operator coefficients can be estimated using general theoretical considerations. We conclude in Sec. II.C by analyzing some constraints on the Wilson coefficients and discussing the validity of the EFT approach to describe BSM physics.

A. Operator bases

On general grounds, we consider the SMEFT in a bottom-up EFT perspective: we know the low-energy limit of the theory, which is the standard model, while we do not know its UV completion. The goal is to find a general description, in terms of higher-dimensional operators, of the effects generated by integrating out heavy degrees of freedom that are *a priori* unknown. In the absence of a clear UV theory to start with, we constrain the set of operators using only symmetry arguments. The symmetries we assume are Lorentz invariance, the SM gauge symmetry $\mathcal{G}_{\rm SM}$, and possible additional global symmetries such as baryon and lepton number. With the known symmetries, it becomes a pure group theory exercise (although a nontrivial one) to construct all of the allowed operators.

Concerning the global symmetries, it is unclear whether properties of the SM, such as baryon and lepton number, are fundamental symmetries of the underlying theory or are approximate symmetries arising accidentally at low energies. We postpone a detailed discussion of this point to Sec. III. However, there is no doubt that the SM local symmetry provides a useful and unambiguous tool to classify the higher-dimensional operators since the UV theory must have a local symmetry group that includes $\mathcal{G}_{\rm SM}$ as a subgroup.

For the construction of an operator basis, we restrict ourselves for now to work only up to mass dimension 6. To this end, we express the SMEFT Lagrangian as

$$\mathcal{L}_{\rm SMEFT} = \mathcal{L}_{\rm SM} + \frac{1}{\Lambda}\mathcal{L}_5 + \frac{1}{\Lambda^2}\mathcal{L}_6 + \mathcal{O}(\Lambda^{-3}), \qquad (2.1)$$

where $\mathcal{L}_{5(6)}$ contains all dimension-5 (dimension-6) operators.

As an illustration, we construct following Buchmüller and Wyler (1986) the dimension-5 piece $\mathcal{L}_5$, which consists of a single term, the so-called Weinberg operator (Weinberg, 1979a), and its Hermitian conjugate. For dimensional reasons it is impossible to form a dimension-5 operator only out of fermions or only out of field-strength tensors. It can also not be built only out of Higgs doublets H, due to gauge invariance. For the same reason, or due to Lorentz invariance, it is also impossible to combine three scalars with a field-strength tensor. In principle, the combination of a field-strength tensor and a fermion bilinear is of the right dimension, but for it to be Lorentz invariant the fermion bilinear would have to be a tensor current, which necessarily transforms as an $\mathrm{SU}(2)_L$ doublet, therefore violating gauge invariance. Thus, the only remaining option is to combine two scalars and two fermions. If we choose H and H^* as the scalars, the net hypercharge of the fermion product must vanish, which is possible only by choosing a fermion and its charge conjugate, but this combination does not yield a Lorentz scalar. Therefore, both scalars must be H and combine into an $\mathrm{SU}(2)_L$ triplet, as the singlet combination vanishes. Therefore, both fermions also have to be $\mathrm{SU}(2)_L$ doublets that combine into a triplet and carry no color to form a gauge invariant operator. The resulting operator can be written as

$$Q_{\rm Weinberg} = \varepsilon^{ik}\varepsilon^{jl}H_k H_l \bar{\ell}_i^c \ell_j, \qquad (2.2)$$

where we explicitly show the $\mathrm{SU}(2)_L$ indices (i,j,k,l) and suppress the flavor ones.[7] After electroweak symmetry breaking, the Weinberg operator introduces the following Majorana mass for the left-handed neutrinos ν_L: $\langle Q_{\rm Weinberg}\rangle = (v^2/2)\bar{\nu}_L{}^c\nu_L$, where $v/\sqrt{2}$ is the vacuum expectation value of H. The operator $Q_{\rm Weinberg}$ violates one of the global symmetries of the SM Lagrangian: it violates the total lepton number by two units. As we discuss in Sec. III, this fact could naturally justify its smallness and, correspondingly, the smallness of the neutrino masses. Postponing a discussion about global symmetry violations to Sec. III, in the rest to this section we focus on lepton- and baryon-number-conserving operators, which start at dimension 6.

Besides the aforementioned continuous global symmetries, one can also constrain the SMEFT structure via the discrete global charge-parity (CP) symmetry, which experimentally is violated only in specific flavor-changing processes, as predicted in the SM. Contrary to continuous symmetries, imposing CP invariance limits not the operator structures but rather the form of the allowed couplings: non-Hermitian operators are not allowed to appear in the Lagrangian with imaginary couplings. However, requiring only real Wilson coefficients does not offer sufficient protection from CP violation, since CP-even operators can still interfere with the CP-violating phase of the SM. This form of indirect CP violation, also called opportunistic CP violation, allows us to derive additional constraints on CP-even operators from measurements

[7]The fully antisymmetric rank-2 tensor ε^{ij} is defined by $\varepsilon^{ij} = -\varepsilon^{ji}$ and $\varepsilon^{12} = \varepsilon_{12} = +1$, and the superscript c denotes the charge conjugate of a fermion given by $\psi^c = C\bar{\psi}^{\rm T}$, with the charge conjugation matrix $C = i\gamma^2\gamma^0$.

of CP-violating observables. For more details about CP violation in the SMEFT, see Bonnefoy *et al.* (2022, 2023).

The operators of $\mathcal{L}_6$ can be obtained by considerations analogous to those presented in the derivation of Eq. (2.2). We list a minimal and independent set of them in Sec. II.A.2. The first complete SMEFT operator set up to dimension 6 was constructed in the original analysis by Buchmüller and Wyler (1986).[8] Some extensive lists of previously known operators were given by Leung, Love, and Rao (1986) and references therein. However, these lists contain many redundant operators that were eliminated by Buchmüller and Wyler (1986), who, however, still did not provide a minimal basis. This goal was later achieved by Grzadkowski *et al.* (2010). We now discuss general arguments on how different effective operators can be related and how an independent set can be obtained.

1. Toward a nonredundant basis

A set of effective operators constructed with the procedure illustrated in the previous example usually contains many redundancies.[9] Two or more operators or a larger set of operators are redundant if they yield the same contribution to all physical observables; hence, some of them can be dropped with no physical consequences if the coefficients of the remaining operators are modified accordingly. Redundant operators can be eliminated using various techniques. The most relevant ones are (a) integration by parts, (b) field redefinitions (and equations of motion), (c) Fierz identities, and (d) Dirac structure reduction. We now proceed by discussing each of them in more detail. Note, however, that it might be necessary to perform further simplifications, for example, by applying either the Jacobi or Bianchi identity or the Chisholm identity, to obtain a minimal operator basis for the EFT. Furthermore, it might be required to exploit the internal symmetries of the EFT operators, such as (anti)symmetric indices. Thus, the following discussion is not meant as a complete description for reducing a given operator set to a basis, but instead only highlights the most common methods used in this procedure.

a. Integration by parts

Within QFT we commonly assume that total derivatives vanish; i.e., all fields vanish at infinity. Thus, the action S of the theory $S = \int \mathrm{d}^4x\, \mathcal{L}$ is invariant under integration by parts (IBP) identities. As a consequence, we can use IBP to relate different operators. In the SM this can be used to write the kinetic term for the Higgs in the two equivalent forms $(D_\mu H)^*(D^\mu H)$ and $-H^* D^2 H$. The same technique can also be applied to rewrite higher-dimensional effective operators in the SMEFT.

[8]In fact, one operator was missing in the printed version of that paper but mentioned by Buchmüller, Lampe, and Vlachos (1987).

[9]The effective operators form a complex vector space, and the redundancy in the operator choice is equivalent to the redundancy in defining a basis for this vector space (Einhorn and Wudka, 2013). We also call a minimal set of operators an operator basis.

b. Field redefinitions

Probably the most relevant form of equivalence among different effective operators is due to field redefinitions. According to the Lehmann-Symanzik-Zimmermann (LSZ) reduction formula (Lehmann, Symanzik, and Zimmermann, 1955), we are free to choose any form for the interpolating quantum fields of our theory without affecting physical observables, as long as the fields that we use can create all the relevant states from the vacuum. This freedom allows us to perform field redefinitions for our effective Lagrangian modifying the operators and, in practice, reducing the operator basis but leaving the physical observables invariant (Politzer, 1980; Georgi, 1991; Arzt, 1995). The field redefinitions of interest for the SMEFT are perturbative transformations of the type

$$\phi \to \tilde{\phi}(\phi) = \phi + \epsilon F(\phi), \tag{2.3}$$

where the new field $\tilde{\phi}$ is given by the original field ϕ plus a small ($\epsilon \ll 1$) perturbation $F(\phi)$ that can depend not only on the field ϕ itself but also on all the other fields of the SM and their covariant derivatives. We furthermore assume that F is an analytic function of the SM fields, their derivatives, and ϵ. For the SMEFT the expansion parameter ϵ is usually related to a power n of the EFT expansion parameter $(E/\Lambda)^n$, where E is the typical energy scale for the process of interest.

Following Criado and Pérez-Victoria (2019), we now show that field redefinitions leave the S matrix, and by that all observables, invariant. Let the generating functional of the SM be

$$Z_{\mathrm{SM}}[J] = \int \mathcal{D}\phi\, \exp(iS_{\mathrm{SM}}[\phi] + J\phi), \tag{2.4}$$

with ϕ representing all SM fields collectively and J the corresponding source terms. Assuming that the field redefinition in Eq. (2.3) is always invertible in a perturbative sense, we can perform a coordinate transformation for the path integral in Eq. (2.4),

$$Z_{\mathrm{SM}}[J] = \int \mathcal{D}\phi\, \det\left(\frac{\delta\tilde{\phi}(\phi)}{\delta\phi}\right) \exp\{iS_{\mathrm{SM}}[\tilde{\phi}(\phi)] + J\tilde{\phi}(\phi)\}. \tag{2.5}$$

Thus, a field redefinition in the action $\tilde{S}_{\mathrm{SM}}[\phi] = S_{\mathrm{SM}}[\tilde{\phi}(\phi)]$ leaves the resulting generating functional invariant if it is accompanied by the Jacobian of the transformation and an appropriate transformation of the source terms.

Using ghost fields η and $\bar{\eta}$, we can write the Jacobian as

$$\det\left(\frac{\delta\tilde{\phi}(\phi)}{\delta\phi}\right) = \int \mathcal{D}\bar{\eta}\mathcal{D}\eta \exp\left(-i\bar{\eta}\frac{\delta\tilde{\phi}(\phi)}{\delta\phi}\eta\right). \tag{2.6}$$

We can then simply add the ghost part to the action S_{SM}. Using Eq. (2.3), we find that the ghost propagator is proportional to the identity and ghost loops can depend only on $\delta F(\phi)/\delta\phi$, which is a polynomial in the internal momenta since $\tilde{\phi}$ is analytic in the fields and their derivatives. In dimensional

regularization, which we assume throughout this work, these scaleless loops thus vanish. Therefore, the Jacobian of the coordinate transformation is the identity and we can simply neglect the ghosts.

The modification of the source terms affects off-shell quantities; however, owing to the LSZ formula (Lehmann, Symanzik, and Zimmermann, 1955) the source terms do not alter the S matrix or, by extension, the physical observables. This means that the generating functional with the action obtained after the field transformation

$$\tilde{Z}_{\mathrm{SM}}[J] = \int \mathcal{D}\phi \, \exp(i\tilde{S}_{\mathrm{SM}}[\phi] + J\phi) \tag{2.7}$$

yields the same S matrix as the original generating functional $Z_{\mathrm{SM}}[J]$, and therefore they are physically equivalent. For a more detailed analysis and further information on the treatment of fields with nonzero vacuum expectation values and a discussion of the inclusion of renormalization, see Criado and Pérez-Victoria (2019).

Next we give a concrete example of how field redefinition can be used to eliminate redundant operators from the SMEFT. Consider the SM amended by the two effective operators

$$[Q_{Dl}]_{pr} = [\bar{\ell}_p(\overleftrightarrow{\not{D}} + \overleftrightarrow{\not{D}})\ell_r](H^\dagger H), \tag{2.8}$$

$$[Q_{eH}]_{pr} = (\bar{\ell}^i_p e_r)H_i(H^\dagger H), \tag{2.9}$$

with the corresponding Wilson coefficients $[C_{Dl}]_{pr}$ and $[C_{eH}]_{pr}$. In Eqs. (2.8) and (2.9) p and r are flavor indices and i is a fundamental $\mathrm{SU}(2)_L$ index shown only when the contraction is nontrivial. Our goal is to show that both of these operators are equivalent. We first notice that both operators are of mass dimension 6 and are allowed by the SM symmetries. Moreover, Q_{Dl} is Hermitian, contrary to Q_{eH}. We can now write the part of the SMEFT Lagrangian relevant for this example,

$$\begin{aligned}\mathcal{L}_{\mathrm{SMEFT}} \supset\ & i(\bar{\ell}_p \not{D} \ell_p) - \{[Y_e]_{pr}(\bar{\ell}^i_p e_r)H_i + \mathrm{H.c.}\} \\ & + \left(\frac{[C_{eH}]_{pr}}{\Lambda^2}[Q_{eH}]_{pr} + \mathrm{H.c.}\right) \\ & + \frac{[C_{Dl}]_{pr}}{\Lambda^2}[Q_{Dl}]_{pr} + \mathcal{O}(\Lambda^{-4}).\end{aligned} \tag{2.10}$$

We now apply the perturbative field redefinitions

$$\ell_{ip} \to \ell_{ip} + \frac{1}{\Lambda^2}F_{ip}(\ell, H), \quad \bar{\ell}^i_p \to \bar{\ell}^i_p + \frac{1}{\Lambda^2}\overline{F^i_p(\ell, H)}, \tag{2.11}$$

where F is an analytic function of the fields $\ell, \bar{\ell}, H$, and $H^\dagger$ and their derivatives. Since ℓ is a complex field, we also have to shift its charge conjugate or, equivalently, $\bar{\ell}$. Assuming that the field redefinition is perturbative in our EFT expansion, i.e., keeping a consistent truncation at mass dimension 6, we find that

$$\begin{aligned}\mathcal{L}_{\mathrm{SMEFT}} \to\ & i(\bar{\ell}_p \not{D} \ell_p) + \frac{i}{\Lambda^2}(\bar{F}_p \overleftrightarrow{\not{D}} \ell_p - \bar{\ell}_p \overleftrightarrow{\not{D}} F_p) \\ & - \left([Y_e]_{pr}(\bar{\ell}^i_p e_r)H_i + \frac{1}{\Lambda^2}[Y_e]_{pr}(\bar{F}^i_p e_r)H_i + \mathrm{H.c.}\right) \\ & + \frac{[C_{Dl}]_{pr}}{\Lambda^2}[\bar{\ell}_p(\overleftarrow{\not{D}} + \overrightarrow{\not{D}})\ell_r](H^\dagger H) \\ & + \left(\frac{[C_{eH}]_{pr}}{\Lambda^2}(\bar{\ell}^i_p e_r)H_i(H^\dagger H) + \mathrm{H.c.}\right) + \mathcal{O}(\Lambda^{-4}),\end{aligned} \tag{2.12}$$

where we use IBP for the last term of the first line to move the derivative away from the function F. We observe that, when $F_{ip} = -i[C_{Dl}]_{pr}\ell_{ir}(H^\dagger H)$ is chosen, the two terms originating from the shift of the kinetic term of the fermions exactly cancel the operator Q_{Dl}. The final result we thus obtain reads

$$\begin{aligned}\mathcal{L}_{\mathrm{SMEFT}} \supset\ & i(\bar{\ell}_p \not{D} \ell_p) - \{[Y_e]_{pr}(\bar{\ell}^i_p e_r)H_i + \mathrm{H.c.}\} \\ & + \left(\frac{[C'_{eH}]_{pr}}{\Lambda^2}[Q_{eH}]_{pr} + \mathrm{H.c.}\right) + \mathcal{O}(\Lambda^{-4}).\end{aligned} \tag{2.13}$$

We find that the operator Q_{Dl} is redundant and that it is sufficient to include only Q_{eH} in the Lagrangian. The effect of removing the redundant operator Q_{Dl} in our example is a shift of the Wilson coefficient of the remaining operator Q_{eH} given by $[C'_{eH}]_{pr} = [C_{eH}]_{pr} - i[C_{Dl}]_{ps}[Y_e]_{sr}$. Equally well we could also have removed Q_{eH} in favor of Q_{Dl} with the field redefinition $\ell_p \to \ell_p + [A]_{pr}\ell_r(H^\dagger H)/\Lambda^2$, where A is the matrix defined by $[A]_{ps}[Y_e]_{sr} = [C_{eH}]_{pr}$. However, it is often more convenient to remove operators with more derivatives instead of operators with fewer derivatives, which is also the strategy that we pursue in the following. The previously presented procedure can be used to eliminate any operator that is redundant due to field redefinitions. In the case where we remove an operator with derivatives, it is always the shift of the kinetic term that cancels the redundant effective operator.

In many cases, including the SMEFT, when one keeps effective operators of mass dimension 6 only, there is a simpler way to remove redundant operators than using field redefinitions. It can be shown that at leading power in the EFT expansion the use of equations of motion is equivalent to applying field redefinitions, which we now prove.

Consider a Lagrangian $\mathcal{L}$ depending on the fields ϕ, e.g., the SM Lagrangian depending on all of the SM fields. We then perform a perturbative field redefinition of the form $\phi \to \tilde{\phi} = \phi + \epsilon\delta\phi$ on the Lagrangian, where ϵ is again a small ($\epsilon \ll 1$) expansion parameter related to a power n of the EFT expansion $(E/\Lambda)^n$. Expanding the shifted action around the original field configuration ϕ, we find that

$$\begin{aligned}S[\phi] \to S[\tilde{\phi}] &= S[\tilde{\phi}]|_{\tilde{\phi}=\phi} + \epsilon\left.\frac{\delta S[\tilde{\phi}]}{\delta\tilde{\phi}}\right|_{\tilde{\phi}=\phi}\delta\phi + \mathcal{O}(\epsilon^2) \\ &= S[\phi] + \epsilon\int \mathrm{d}^4x\, E[\phi]\delta\phi + \mathcal{O}(\epsilon^2)\end{aligned} \tag{2.14}$$

at leading order in ϵ, where $E[\phi] = (\delta\mathcal{L}[\tilde{\phi}]/\delta\tilde{\phi})|_{\tilde{\phi}=\phi}$ symbolizes the equations of motion of the field ϕ. Therefore, instead

of performing a field redefinition, we can also add a term proportional to the equations of motion of a field to the Lagrangian, which at leading power has the same effect. Since we work up to the order $\mathcal{O}(\epsilon)$, it is also sufficient to use only the leading piece of the equations of motion. That means for the SM we can simply use the pure SM equations of motion, thereby dropping all contributions of higher-dimensional operators.

We now return to our example of Eq. (2.10) and find that the operator we removed before is indeed proportional to the equations of motion for the fields ℓ and $\overline{\ell}$. We already know that in this case $\epsilon = \Lambda^{-2}$. Thus, we can use the leading SM equations of motion

$$E[\overline{\ell}]_{ip} = i\vec{\not{D}}\ell_{ip} - [Y_e]_{pr} e_r H_i + \mathcal{O}(\Lambda^{-2}), \tag{2.15a}$$

$$E[\ell]^i_p = -i\overline{\ell}^i_p \overleftarrow{\not{D}} - [Y_e^*]_{pr} \bar{e}_r H^{*i} + \mathcal{O}(\Lambda^{-2}). \tag{2.15b}$$

Adding the term $\epsilon\overline{\delta\phi}^i_p E[\overline{\ell}]_{ip} + \epsilon E[\ell]^i_p \delta\phi_{ip}$ with $\delta\phi_p = F_p(\ell, H)$ to the Lagrangian in Eq. (2.10) then yields the same result as using field redefinitions. Note that since ℓ is a complex field we need to use the equations of motions for both the field and its charge conjugate. In practice it is easier to directly plug the equations of motion into the effective operators that we want to remove. In our example we could simply replace $\vec{\not{D}}\ell_{ip}$ and $\overline{\ell}^i_p\overleftarrow{\not{D}}$ in the operator Q_{Dl} by $-i[Y_e]_{pr}e_r H_i$ and $i[Y_e^*]_{pr}\bar{e}_r H^{*i}$, respectively, directly obtaining the result in Eq. (2.13).

In the literature it is often stated that some operators are removed by means of the equations of motion. This statement is not strictly correct in general, since the equations of motion can only be used at leading order in the EFT expansion. If we work at subleading power ϵ^2 (e.g., if we include dimension-8 operators in our previous example), we should add the term

$$\frac{1}{2}\epsilon^2 \frac{\delta^2 S[\tilde{\phi}]}{\delta\tilde{\phi}^2}\bigg|_{\tilde{\phi}=\phi} \delta\phi^2 \tag{2.16}$$

to Eq. (2.14) to obtain a consistent truncation of the EFT expansions up to the order $\mathcal{O}(\epsilon^2)$. It is immediately clear that in this case the use of equations of motion is no longer equivalent to applying field redefinitions, as the former do not capture the subleading shift of the fields in Eq. (2.16). Therefore, when considering a Lagrangian with effective operators of different powers, we must not use the equations of motion to remove redundancies, but we have to apply the field redefinitions to obtain the correct result. For more details on the failure of equations of motion, see Jenkins, Manohar, and Stoffer (2018a) and Criado and Pérez-Victoria (2019).

The common approach is thus to first use IBP, if necessary, to bring an operator into the form of the equations of motion, and then to use these to eliminate the operator in favor of other effective operators containing fewer derivatives. If we work at subleading power in the EFT, the equations of motion cannot be used and we have to apply field redefinitions instead. In this situation, we have to remove the redundant operators order by order, starting with the lowest-order operators, since a shift to eliminate an operator produces operators of the same or higher mass dimension when massless fields are shifted.[10]

c. Fierz identities

These identities follow from completeness relations on certain matrix spaces and provide additional relations among operators. We start by discussing Fierz identities of the Lorentz group (Fierz, 1937). These identities can be applied to four-fermion operators, allowing us to rearrange the ordering of the different spinors. For their derivation we follow the discussion of Nishi (2005). When working with a chiral theory such as the SMEFT, it is usually most convenient to derive the Fierz identities in the chiral basis $\{\Gamma^n\}$ for the Dirac algebra in four spacetime dimensions that we define as

$$\{\Gamma^n\} = \{P_L, P_R, \gamma^\mu P_L, \gamma^\mu P_R, \sigma^{\mu\nu}\}, \tag{2.17a}$$

$$\{\tilde{\Gamma}_n\} = \{P_L, P_R, \gamma_\mu P_R, \gamma_\mu P_L, \sigma_{\mu\nu}/2\}, \tag{2.17b}$$

where $P_{R/L} = (1/2)(\mathbb{1} \pm \gamma_5)$ are the chirality projectors and $\sigma^{\mu\nu} = (i/2)[\gamma^\mu, \gamma^\nu]$, with $\mu < \nu$. Moreover, we have also defined the dual basis $\{\tilde{\Gamma}_n\}$. With this definition the orthogonality condition $\mathrm{tr}\{\Gamma^n\tilde{\Gamma}_m\} = 2\delta^n_m$ is satisfied. Since $\{\Gamma^n\}$ forms a basis of all 4×4 matrices, we can write any such matrix X as $X = X_n\Gamma^n$, with $X_n = (1/2)\mathrm{tr}\{X\tilde{\Gamma}_n\}$, and thus $X = (1/2)\mathrm{tr}\{X\tilde{\Gamma}_n\}\Gamma^n$. Dividing the latter equation into its components and inserting the appropriate delta functions, we obtain

$$\delta_{ij}\delta_{kl} = \tfrac{1}{2}(\tilde{\Gamma}_n)_{kj}(\Gamma^n)_{il} \quad \text{or} \quad (\mathbb{1})\otimes[\mathbb{1}] = \tfrac{1}{2}(\tilde{\Gamma}_n]\otimes[\Gamma^n), \tag{2.18}$$

where in the second equation we schematically identify the indices with brackets as follows: $i \sim (, j\sim), k \sim [$, and $l\sim]$. Multiplying this equation by generic matrices X and Y, we find that

$$(X)\otimes[Y] = \tfrac{1}{4}\mathrm{tr}\{X\tilde{\Gamma}_n Y\tilde{\Gamma}_m\}(\Gamma^m]\otimes[\Gamma^n), \tag{2.19}$$

which allows us to project any tensor product of two matrices onto a product of matrices from the chosen Dirac basis. In particular, by choosing $X, Y \in \{\Gamma^n\}$ we can derive the Fierz identities

$$(P_A)\otimes[P_A] = \tfrac{1}{2}(P_A]\otimes[P_A) + \tfrac{1}{8}(\sigma^{\mu\nu}P_A]\otimes[\sigma_{\mu\nu}P_A), \tag{2.20a}$$

$$(P_A)\otimes[P_B] = \tfrac{1}{2}(\gamma^\mu P_B]\otimes[\gamma_\mu P_A), \tag{2.20b}$$

$$(\gamma^\mu P_A)\otimes[\gamma_\mu P_A] = -(\gamma^\mu P_A]\otimes[\gamma_\mu P_A), \tag{2.20c}$$

$$(\gamma^\mu P_A)\otimes[\gamma_\mu P_B] = 2(P_B]\otimes[P_A), \tag{2.20d}$$

[10] In the SMEFT, only the Higgs H has a mass term; thus, shifting it to remove a redundant operator can introduce lower-dimensional operators.

$$(\sigma^{\mu\nu}P_A)\otimes[\sigma^{\mu\nu}P_A] = 6(P_A]\otimes[P_A) - \tfrac{1}{2}(\sigma^{\mu\nu}P_A]\otimes[\sigma_{\mu\nu}P_A), \tag{2.20e}$$

$$(\sigma^{\mu\nu}P_A)\otimes[\sigma^{\mu\nu}P_B] = 0, \tag{2.20f}$$

where $A, B \in \{L, R\}$ but $A \neq B$. Equations (2.20) correspond only to relations among Dirac structures; however, when applying them to four-fermion operators we also anticommute two spinors, thus acquiring an additional minus sign with respect to the equations. For example, Eq. (2.20d) allows us to rewrite the operator as $(\bar{\ell}^i\gamma^\mu q_i)(\bar{d}\gamma_\mu e) = -2(\bar{\ell}^i e)(\bar{d}q_i)$, which has the quarks and leptons in separate currents. Note that we assumed the Dirac algebra in four spacetime dimensions to evaluate the traces in Eq. (2.19) and obtain Eqs. (2.20). However, when working at the loop level, we encounter divergent integrals that we regulate using dimensional regularization in $D = 4 - 2\epsilon$ dimensions, which is incompatible with the previously obtained results. At the loop level, using Eqs. (2.20) while working in D dimensions introduces so-called evanescent operators, i.e., operators that vanish in $D = 4$. We discuss these evanescent contributions in Sec. II.A.5.

Furthermore, we have the following Fierz identity for the generators T^a of the fundamental representation of SU(N) groups:

$$(T^a)_{ij}(T^a)_{kl} = \frac{1}{2}\left(\delta_{il}\delta_{kj} - \frac{1}{N}\delta_{ij}\delta_{kl}\right) \tag{2.21}$$

or, in our notation,

$$(T^a)\otimes[T^a] = \frac{1}{2}(\mathbb{1})\otimes[\mathbb{1}) - \frac{1}{2N}(\mathbb{1})\otimes[\mathbb{1}], \tag{2.22}$$

where the brackets now correspond to indices of the fundamental representation of SU(N). For example, for $\mathrm{SU}(2)_L$ this allows us to rewrite the Higgs operator as $(H^\dagger\tau^I H)(H^\dagger\tau^I H) = (H^\dagger H)^2$.

d. Dirac structure reduction

Equation (2.17a) constitutes a Dirac basis in $D = 4$ dimensions and is therefore enough to construct an EFT operator basis in the physical four-dimensional limit. Nevertheless, we can write operators with Dirac structures differing from those in Eq. (2.17a), which we then have to project onto our chosen basis $\{\Gamma^n\}$ using gamma-tensor reduction (Tracas and Vlachos, 1982; Buras and Weisz, 1990; Herrlich and Nierste, 1995). Following Fuentes-Martin *et al.* (2023b), we write this projection as

$$X\otimes Y = \sum_n b_n(X,Y)\Gamma^n\otimes\tilde{\Gamma}_n + E(X,Y). \tag{2.23}$$

Note that in D dimensions the Dirac algebra is infinite dimensional, and thus it is not possible to project a generic structure onto the finite four-dimensional basis $\{\Gamma^n\}$. As in the case of the Fierz identities, performing such a projection then introduces an evanescent operator $E(X,Y)$, which is implicitly defined by Eq. (2.23). Working at tree level, which we assume for the moment, we can take the four-dimensional limit; therefore, $E(X,Y)$ vanishes. However, at loop level this is not the case and the evanescent contributions can be treated as in the discussion in Sec. II.A.5 and in that of Fuentes-Martin *et al.* (2023b). The coefficients $b_n(X,Y)$ can be determined by contracting Eq. (2.23) with the basis elements Γ^k,

$$\mathrm{tr}\{\Gamma^k X\tilde{\Gamma}_k Y\} = \sum_n b_n(X,Y)\mathrm{tr}\{\Gamma^k\Gamma^n\tilde{\Gamma}_k\tilde{\Gamma}_n\} + \mathcal{O}(\epsilon^2), \tag{2.24}$$

which for $k = 1, \ldots, 10$ yields a system of equations that we can solve to find the coefficients $b_n(X,Y)$. To compute the aforementioned traces, we use naive dimensional regularization (NDR) (see Appendix A.2) to define our evanescent operator scheme. We find that

$$\gamma^\mu\gamma^\nu P_A\otimes\gamma_\nu\gamma_\mu P_A = (4-2\epsilon)P_A\otimes P_A + \sigma^{\mu\nu}P_A\otimes\sigma_{\mu\nu}P_A, \tag{2.25a}$$

$$\gamma^\mu\gamma^\nu P_A\otimes\gamma_\nu\gamma_\mu P_B = 4(1-2\epsilon)P_A\otimes P_B + E^{[2]}_{AB}, \tag{2.25b}$$

$$\gamma^\mu\gamma^\nu\gamma^\lambda P_A\otimes\gamma_\lambda\gamma_\nu\gamma_\mu P_A = 4(1-2\epsilon)\gamma^\mu P_A\otimes\gamma_\mu P_A + E^{[3]}_{AA}, \tag{2.25c}$$

$$\gamma^\mu\gamma^\nu\gamma^\lambda P_A\otimes\gamma_\lambda\gamma_\nu\gamma_\mu P_B = 16(1-\epsilon)\gamma^\mu P_A\otimes\gamma_\mu P_B + E^{[3]}_{AB}, \tag{2.25d}$$

$$\gamma^\mu\gamma^\nu\sigma^{\lambda\rho}P_A\otimes\sigma_{\lambda\rho}\gamma_\nu\gamma_\mu P_A = 16(3-5\epsilon)P_A\otimes P_A + 2(6-7\epsilon)\sigma^{\mu\nu}P_A\otimes\sigma_{\mu\nu}P_A + E^{[4]}_{AA}, \tag{2.25e}$$

implicitly defining the evanescent structures $E^{[2]}_{AB}$, $E^{[3]}_{AA}$, $E^{[3]}_{AB}$, and $E^{[4]}_{AA}$, where $A, B \in \{L, R\}$, with $A \neq B$. Other schemes, and hence alternative definitions of the evanescent operators differing from our choice by $\mathcal{O}(\epsilon)$ terms, are also possible; see Herrlich and Nierste (1995) and Dekens and Stoffer (2019).

2. The Warsaw basis

We can now apply the methods illustrated thus far in this section to the set of all effective operators that are compatible with the symmetries of the SM. By doing so, we can construct a basis, i.e., a minimal set of effective operators of the SMEFT.[11]

[11]Note that the term *basis* is not always appropriately used in the EFT literature. Keep in mind that sometimes it is also incorrectly used for overcomplete or even incomplete operator sets. Sometimes we refer here to complete operator sets without redundancies as *minimal bases*.

TABLE II. List of all baryon- and lepton-number-conserving SMEFT operators at mass dimension 6 in the Warsaw basis (Grzadkowski *et al.*, 2010). The division into classes 1–8 is adapted from Alonso, Jenkins *et al.* (2014) and further refined according to the chirality of the fields. It is also indicated which classes are *potentially tree generated* (PTG) and which are *loop generated* (LG) according to Arzt, Einhorn, and Wudka (1995) and Einhorn and Wudka (2013).

1–4: Bosonic operators

1: X^3 (LG)		2: H^6 (PTG)		3: H^4D^2 (PTG)		4: X^2H^2 (LG)			
Q_G	$f^{ABC}G^{A\nu}_{\mu}G^{B\rho}_{\nu}G^{C\mu}_{\rho}$	Q_H	$(H^\dagger H)^3$	$Q_{H\Box}$	$(H^\dagger H)\Box(H^\dagger H)$	Q_{HG}	$(H^\dagger H)G^A_{\mu\nu}G^{A\mu\nu}$	Q_{HB}	$(H^\dagger H)B_{\mu\nu}B^{\mu\nu}$
$Q_{\tilde{G}}$	$f^{ABC}\tilde{G}^{A\nu}_{\mu}G^{B\rho}_{\nu}G^{C\mu}_{\rho}$			Q_{HD}	$(H^\dagger D_\mu H)^*(H^\dagger D^\mu H)$	$Q_{H\tilde{G}}$	$(H^\dagger H)\tilde{G}^A_{\mu\nu}G^{A\mu\nu}$	$Q_{H\tilde{B}}$	$(H^\dagger H)\tilde{B}_{\mu\nu}B^{\mu\nu}$
Q_W	$\varepsilon^{IJK}W^{I\nu}_{\mu}W^{J\rho}_{\nu}W^{K\mu}_{\rho}$					Q_{HW}	$(H^\dagger H)W^I_{\mu\nu}W^{I\mu\nu}$	Q_{HWB}	$(H^\dagger\tau^I H)W^I_{\mu\nu}B^{\mu\nu}$
$Q_{\tilde{W}}$	$\varepsilon^{IJK}\tilde{W}^{I\nu}_{\mu}W^{J\rho}_{\nu}W^{K\mu}_{\rho}$					$Q_{H\tilde{W}}$	$(H^\dagger H)\tilde{W}^I_{\mu\nu}W^{I\mu\nu}$	$Q_{H\tilde{W}B}$	$(H^\dagger\tau^I H)\tilde{W}^I_{\mu\nu}B^{\mu\nu}$

5–6: Non-Hermitian fermion bilinears

5: $\psi^2H^3+\text{H.c.}$ (PTG)				6: $\psi^2XH+\text{H.c.}$ (LG)					
Q_{eH}	$(H^\dagger H)(\bar{\ell}_p e_r H)$	Q_{eW}	$(\bar{\ell}_p\sigma^{\mu\nu}e_r)\tau^I HW^I_{\mu\nu}$	Q_{uG}	$(\bar{q}_p\sigma^{\mu\nu}T^A u_r)\tilde{H}G^A_{\mu\nu}$	Q_{dG}	$(\bar{q}_p\sigma^{\mu\nu}T^A d_r)HG^A_{\mu\nu}$		
Q_{uH}	$(H^\dagger H)(\bar{q}_p u_r\tilde{H})$	Q_{eB}	$(\bar{\ell}_p\sigma^{\mu\nu}e_r)HB_{\mu\nu}$	Q_{uW}	$(\bar{q}_p\sigma^{\mu\nu}u_r)\tau^I\tilde{H}W^I_{\mu\nu}$	Q_{dW}	$(\bar{q}_p\sigma^{\mu\nu}d_r)\tau^I HW^I_{\mu\nu}$		
Q_{dH}	$(H^\dagger H)(\bar{q}_p d_r H)$			Q_{uB}	$(\bar{q}_p\sigma^{\mu\nu}u_r)\tilde{H}B_{\mu\nu}$	Q_{dB}	$(\bar{q}_p\sigma^{\mu\nu}d_r)HB_{\mu\nu}$		

7: Hermitian fermion bilinears $\psi^2H^2D+Q_{Hud}$ (PTG)

$(\bar{L}L)$		$(\bar{R}R)$		$(\bar{R}R')+\text{H.c.}$	
$Q^{(1)}_{H\ell}$	$(H^\dagger i\overleftrightarrow{D}_\mu H)(\bar{\ell}_p\gamma^\mu\ell_r)$	Q_{He}	$(H^\dagger i\overleftrightarrow{D}_\mu H)(\bar{e}_p\gamma^\mu e_r)$	Q_{Hud}	$i(\tilde{H}^\dagger D_\mu H)(\bar{u}_p\gamma^\mu d_r)$
$Q^{(3)}_{H\ell}$	$(H^\dagger i\overleftrightarrow{D}^I_\mu H)(\bar{\ell}_p\tau^I\gamma^\mu\ell_r)$	Q_{Hu}	$(H^\dagger i\overleftrightarrow{D}_\mu H)(\bar{u}_p\gamma^\mu u_r)$		
$Q^{(1)}_{Hq}$	$(H^\dagger i\overleftrightarrow{D}_\mu H)(\bar{q}_p\gamma^\mu q_r)$	Q_{Hd}	$(H^\dagger i\overleftrightarrow{D}_\mu H)(\bar{d}_p\gamma^\mu d_r)$		
$Q^{(3)}_{Hq}$	$(H^\dagger i\overleftrightarrow{D}^I_\mu H)(\bar{q}_p\tau^I\gamma^\mu q_r)$				

8: Fermion quadrilinears (ψ^4) (PTG)

Hermitian $(\bar{L}L)(\bar{L}L)$		Hermitian $(\bar{R}R)(\bar{R}R)$		Hermitian $(\bar{L}L)(\bar{R}R)$		Non-Hermitian $(\bar{L}R)(\bar{L}R)+\text{H.c.}$	
$Q_{\ell\ell}$	$(\bar{\ell}_p\gamma_\mu\ell_r)(\bar{\ell}_s\gamma^\mu\ell_t)$	Q_{ee}	$(\bar{e}_p\gamma_\mu e_r)(\bar{e}_s\gamma^\mu e_t)$	$Q_{\ell e}$	$(\bar{\ell}_p\gamma_\mu\ell_r)(\bar{e}_s\gamma^\mu e_t)$	$Q^{(1)}_{quqd}$	$(\bar{q}^i_p u_r)\varepsilon_{ij}(\bar{q}^j_s d_t)$
$Q^{(1)}_{qq}$	$(\bar{q}_p\gamma_\mu q_r)(\bar{q}_s\gamma^\mu q_t)$	Q_{uu}	$(\bar{u}_p\gamma_\mu u_r)(\bar{u}_s\gamma^\mu u_t)$	$Q_{\ell u}$	$(\bar{\ell}_p\gamma_\mu\ell_r)(\bar{u}_s\gamma^\mu u_t)$	$Q^{(8)}_{quqd}$	$(\bar{q}^i_p T^A u_r)\varepsilon_{ij}(\bar{q}^j_s T^A d_t)$
$Q^{(3)}_{qq}$	$(\bar{q}_p\gamma_\mu\tau^I q_r)(\bar{q}_s\gamma^\mu\tau^I q_t)$	Q_{dd}	$(\bar{d}_p\gamma_\mu d_r)(\bar{d}_s\gamma^\mu d_t)$	$Q_{\ell d}$	$(\bar{\ell}_p\gamma_\mu\ell_r)(\bar{d}_s\gamma^\mu d_t)$	$Q^{(1)}_{\ell equ}$	$(\bar{\ell}^i_p e_r)\varepsilon_{ij}(\bar{q}^j_s u_t)$
$Q^{(1)}_{\ell q}$	$(\bar{\ell}_p\gamma_\mu\ell_r)(\bar{q}_s\gamma^\mu q_t)$	Q_{eu}	$(\bar{e}_p\gamma_\mu e_r)(\bar{u}_s\gamma^\mu u_t)$	Q_{qe}	$(\bar{q}_p\gamma_\mu q_r)(\bar{e}_s\gamma^\mu e_t)$	$Q^{(3)}_{\ell equ}$	$(\bar{\ell}^i_p\sigma_{\mu\nu}e_r)\varepsilon_{ij}(\bar{q}^j_s\sigma^{\mu\nu}u_t)$
$Q^{(3)}_{\ell q}$	$(\bar{\ell}_p\gamma_\mu\tau^I\ell_r)(\bar{q}_s\gamma^\mu\tau^I q_t)$	Q_{ed}	$(\bar{e}_p\gamma_\mu e_r)(\bar{d}_s\gamma^\mu d_t)$	$Q^{(1)}_{qu}$	$(\bar{q}_p\gamma_\mu q_r)(\bar{u}_s\gamma^\mu u_t)$		
		$Q^{(1)}_{ud}$	$(\bar{u}_p\gamma_\mu u_r)(\bar{d}_s\gamma^\mu d_t)$	$Q^{(8)}_{qu}$	$(\bar{q}_p\gamma_\mu T^A q_r)(\bar{u}_s\gamma^\mu T^A u_t)$		
		$Q^{(8)}_{ud}$	$(\bar{u}_p\gamma_\mu T^A u_r)(\bar{d}_s\gamma^\mu T^A d_t)$	$Q^{(1)}_{qd}$	$(\bar{q}_p\gamma_\mu q_r)(\bar{d}_s\gamma^\mu d_t)$	$(\bar{L}R)(\bar{R}L)+\text{H.c.}$	
				$Q^{(8)}_{qd}$	$(\bar{q}_p\gamma_\mu T^A q_r)(\bar{d}_s\gamma^\mu T^A d_t)$	$Q_{\ell edq}$	$(\bar{\ell}^i_p e_r)(\bar{d}_s q_{ti})$

As mentioned, a complete list of operators up to mass dimension 6 was first given by Buchmüller and Wyler (1986). Besides proving that at dimension 5 there is a single operator, namely, Q_{Weinberg} in Eq. (2.2), they identified 80 independent operators at dimension 6 (up to the flavor structure) that conserve baryon and lepton number. However, some redundancies still remained in this set of operators, as pointed out by Grzadkowski *et al.* (2004), Fox *et al.* (2008), and Aguilar-Saavedra (2009a, 2009b). Not until 2010 was the first minimal basis for dimension-6 operators in the SMEFT derived by Grzadkowski *et al.* (2010). It contains only 59 dimension-6 operators that conserve baryon and lepton number. Considering the flavor structure of the operators, this amounts to 2499 couplings, of which 1350 are CP even and 1149 are CP odd (Alonso, Jenkins *et al.*, 2014). The basis is known as the Warsaw basis and is the most commonly used basis for the $d=6$ SMEFT. Table II lists all baryon- and lepton-number-conserving $d=6$ operators of the Warsaw basis. For the non-Hermitian operators the Hermitian conjugate is understood to be included. The operators are divided into classes according to their field content and chirality in the manner taken by Grzadkowski *et al.* (2010) and Alonso, Jenkins *et al.* (2014), which we now follow in our classification of the operators. The underlying algorithm used to construct the Warsaw basis can be summarized as follows:

(1) Use IBP and equations of motion to remove operators with more derivatives in favor of operators with fewer derivatives.
(2) Use the Fierz identities (2.20) and (2.21) such that the following apply:
   (a) Leptons and quarks do not appear in the same fermion currents.

(b) The gauge indices of the largest gauge group are contracted within each bilinear.
(c) Each current is a hypercharge singlet.

The purely bosonic operators are built out of combinations of the field-strength tensors $X_{\mu\nu} \in \{G_{\mu\nu}, W_{\mu\nu}, B_{\mu\nu}\}$, the Higgs doublet H, and the covariant derivatives D_μ. Owing to $\mathrm{SU}(2)_L$ and Lorentz invariance, the Higgs fields and the covariant derivatives must both appear in even numbers in the operators. After all allowed operators are constructed and the redundant ones removed, the following four classes of bosonic operators remain:

- Four pure gauge operators containing three field-strength tensors (class 1: X^3).
- One pure scalar operator with six Higgs doublets (class 2: H^6).
- Two operators with four Higgs fields and two covariant derivatives (class 3: H^4D^2).
- Eight mixed operators with two Higgs fields and two field-strength tensors (class 4: X^2H^2).

For operators with two fermion fields, we have the following three types of fermion currents: scalar $(\bar{\psi}_{L/R}\psi_{R/L})$, vector $(\bar{\psi}_{L/R}\gamma^\mu\psi_{L/R})$, and tensor $(\bar{\psi}_{L/R}\sigma^{\mu\nu}\psi_{R/L})$. After removing the redundant operators, we obtain one class of operators for each following type of current:

- Three non-Hermitian Yukawa-like operators with a scalar fermion current and three Higgs fields (class 5: ψ^2H^3).
- Eight non-Hermitian dipole operators with a tensor current, one Higgs field, and one field-strength tensor (class 6: ψ^2XH).
- Eight operators (all Hermitian except for Q_{Hud}) with a vector current, two Higgs fields, and a covariant derivative (class 7: ψ^2H^2D).

Last, we have 25 four-fermion operators in class 8 subdivided according to their chiral structures $(\bar{L}L)(\bar{L}L)$, $(\bar{R}R)(\bar{R}R)$, $(\bar{L}L)(\bar{R}R)$, $(\bar{L}R)(\bar{L}R)$, and $(\bar{L}R)(\bar{R}L)$. To learn explicitly how other types of operator classes can be removed, see the discussion given by Grzadkowski *et al.* (2010).[12]

3. Other bases

The Warsaw basis is only one viable choice of basis, and other options are possible. Although the Warsaw basis is most commonly used, other bases can be advantageous when specific sets of observables are considered. A commonly adopted set of dimension-6 operators in phenomenological analyses is the so-called strongly interacting light Higgs (SILH) basis (Giudice *et al.*, 2007). However, although called a basis, it does not represent a complete set at dimension 6 (Brivio and Trott, 2017). The same is also true for the Hagiwara-Ishihara-Szalapski-Zeppenfeld basis (Hagiwara *et al.*, 1993). A full and minimal basis containing the operators of the original SILH set was constructed by Elias-Miró *et al.* (2014); see also Contino *et al.* (2013). An extensive discussion on the basis choice in the SMEFT was given by Passarino (2017).

The *Green's basis* (Gherardi, Marzocca, and Venturini, 2020) is another common set of SMEFT operators. Although constituting a complete set of operators, it is not a minimal basis, as it contains redundancies. The Green's basis is an extension of the Warsaw basis where all the operators that are removed from the latter by the equations of motion are kept. Therefore, the operators in the Green's basis are independent only under IBP, but not under field redefinitions. This basis is often convenient for SMEFT matching computations. In functional matching the effective Lagrangian obtained by integrating out some heavy particles is usually in the Green's basis (up to IBP). In addition, the diagrammatic off-shell matching procedure involves the operators of this basis; see Sec. VI.B for more details. The results from the matching computations in the Green's basis can then be converted to the minimal Warsaw basis using the basis reduction relations given in the appendix of Gherardi, Marzocca, and Venturini (2020). See also Ren and Yu (2022) for a derivation of a Green's basis of the SMEFT at dimension 8.

4. Higher-dimensional operators

As discussed, at mass dimension 5 there is only a single operator, i.e., the Weinberg operator (Weinberg, 1979a), and it violates lepton number. Higher-dimensional operators that also do not conserve baryon and lepton number were derived by Weinberg (1980b). The first full set of dimension-7 operators was given by Lehman (2014) finding a total of 20 independent operators. However, Liao and Ma (2016) showed that two of these operators are redundant, thus obtaining a basis of 18 operators. All of these contain either two or four fermions and do not conserve lepton number. Furthermore, seven of these operators violate baryon number as well. An important point to note is that all odd mass-dimension operators in the SMEFT violate either baryon or lepton numbers or both (Kobach, 2016; Helset and Kobach, 2020). Owing to the stringent experimental bounds on processes that do not conserve these symmetries, the scale generating such violating process must be very high; see Sec. III. Given that these are exact global symmetries of the SM Lagrangian, it is common to assume that they are also exact or almost-exact symmetries of the SMEFT, and operators that violate baryon or lepton number are often neglected except for specific analyses devoted to the corresponding symmetry-violating processes.

More recently the first complete bases of dimension-8 operators were derived (Li, Ren, Shu *et al.*, 2021; Murphy, 2020), with 1029 independent structures up to different flavor contractions found (Murphy, 2020).[13] Although these operators are suppressed by 4 powers of the new-physics scale Λ^{-4}, they can still be relevant for phenomenological studies. This is particularly the case for UV theories that do not generate dimension-6 operators contributing to a given set of observables and in which the leading contribution starts at dimension 8. More generally dimension-8 terms can be relevant for observables where the dimension-6 operators do not interfere (or have a suppressed interference) with the SM amplitude; see Sec. II.C.1. Furthermore, a basis for the

[12]The Feynman rules for the SMEFT in the Warsaw basis in the R_ξ gauges were given by Dedes *et al.* (2017).

[13]For earlier attempts at deriving dimension-8 operators, see Lehman and Martin (2016).

SMEFT at dimension 9 is also known (Liao and Ma, 2020; Li, Ren, Xiao *et al.*, 2021a). An all-order approach to constructing bases of EFTs was presented by Henning *et al.* (2017b). They also counted the number of independent effective operators for the SMEFT present at different higher dimensions using the Hilbert series discussed by Henning *et al.* (2017a). See also Fonseca (2017, 2020) and Li, Ren *et al.* (2022) for discussions about computer tools that help with the construction of higher-dimensional operator bases in generic EFTs.

5. Evanescent operators

Nearly all loop computations in the SMEFT are currently performed using dimensional regularization working in $D = 4 - 2\epsilon$ dimensions. This leads to another subtlety when redundant operators are reduced to a specific basis. As mentioned, in noninteger dimensions the Lorentz algebra is infinite dimensional, whereas in $D = 4$ dimensions it is finite. Now consider a D-dimensional BSM Lagrangian obtained through a one-loop matching computation; see Sec. VI.B. When we want to reduce it to a physical four-dimensional basis such as the Warsaw basis, we necessarily introduce additional operators called evanescent ones due to the mismatch of the dimensionality of the bases. Schematically we can write

$$R \xrightarrow{\mathcal{P}} Q + E, \tag{2.26}$$

where R denotes a redundant operator, Q is an operator part of the physical four-dimensional basis, and E is an evanescent operator. The projection $\mathcal{P}$ is performed using, for example, Fierz identities or Dirac algebra reduction identities (as previously discussed), which are intrinsically four dimensional. The evanescent operator can then be implicitly defined as $E \equiv R - Q$. It is formally of rank ϵ and thus vanishes in the four-dimensional limit. However, when an evanescent operator is inserted into a UV divergent one-loop diagram, the operator can combine with a $1/\epsilon$ pole, resulting in a finite contribution to a one-loop matrix element. Therefore, despite vanishing in four dimensions, evanescent operators still yield physical contributions. However, these contributions are local since the UV poles of any one-loop diagram are as well. Thus, the one-loop effect of evanescent operators can be interpreted as finite shifts of the Wilson coefficients of the physical basis. Therefore, their physical effects can be absorbed by introducing finite counterterms. The resulting renormalization scheme is free of evanescent operators, but notably does not agree with the modified minimal subtraction ($\overline{\text{MS}}$) scheme.

Evanescent contributions were first studied in the context of next-to-leading-order (NLO) computations of the anomalous dimension of the *weak effective Hamiltonian* (Buras and Weisz, 1990; Dugan and Grinstein, 1991; Herrlich and Nierste, 1995) and were recently extended to the low-energy effective field theory (LEFT) (Aebischer and Pesut, 2022; Aebischer, Buras, and Kumar, 2023; Aebischer, Pesut, and Polonsky, 2023)[14] and the SMEFT (Fuentes-Martin *et al.*, 2023b).

[14]See also Aebischer *et al.* (2020) and Aebischer, Bobeth *et al.* (2021) for previous work on evanescent operators in $\Delta F = 1, 2$ transitions.

Fuentes-Martin *et al.* (2023b) introduced an alternative but equivalent projection prescription to handle evanescent operators. Let S_{R} be the action of the EFT containing redundant operators. Reducing the operators in S_{R} to the Warsaw basis (or any other physical basis) using four-dimensional identities (such as Fierz or Dirac structure reduction), we then obtain the action S'_{W}. As previously discussed, S_{R} and S'_{W} do not reproduce the same physics, and the difference is given by evanescent operators. However, we have seen that their effects can be absorbed by finite one-loop shifts of the Wilson coefficients in S'_{W}. Thus, take the action S_{W}, which contains the same operators as S'_{W}, and we fix the Wilson coefficients of S_{W} by requiring that it describes the same physics as S_{R}. We can achieve this by requiring the corresponding quantum effective actions to agree $\Gamma_{\text{W}} = \Gamma_{\text{R}}$. We can express the effective action as

$$\Gamma_{\text{X}} = S_{\text{X}}^{(0)} + S_{\text{X}}^{(1)} + \bar{\Gamma}_{\text{X}}^{(1)} + \cdots, \tag{2.27}$$

where $S_{\text{X}}^{(0,1)}$ contains only local operators and their corresponding tree-level or one-loop Wilson coefficients, respectively. Furthermore, $S_{\text{X}}^{(1)}$ contains the counterterms, and the ellipsis denotes higher-loop contributions. The term $\bar{\Gamma}_{\text{X}}^{(1)}$ represents the contributions by all one-loop diagrams built with insertions of operators from $S_{\text{X}}^{(0)}$. We then find that the physical evanescent-free action describing the same physics as S_{R} is given by

$$S_{\text{W}}^{(0)} = \mathcal{P} S_{\text{R}}^{(0)}, \tag{2.28}$$

$$S_{\text{W}}^{(1)} = \mathcal{P} S_{\text{R}}^{(1)} + \underbrace{\mathcal{P}[\bar{\Gamma}_{\text{R}}^{(1)} - \bar{\Gamma}_{\text{W}}^{(1)}]}_{\equiv \Delta S^{(1)}}, \tag{2.29}$$

where $\bar{\Gamma}_{\text{R}}^{(1)} - \bar{\Gamma}_{\text{W}}^{(1)}$ is the sum of all one-loop diagrams containing an evanescent operator. Since this term is already of one-loop order, we can simply apply the four-dimensional identities to project ($\mathcal{P}$) back to the Warsaw basis.[15] Any effect of evanescent operators in this projection would yield a two-loop effect and can be neglected at the desired order.[16] The action S_{W} thus obtained is free of evanescent operators and reproduces the same physics as the original action with redundant operators S_{R}.

[15]Different definitions of the projection operator $\mathcal{P}$ differing by their $\mathcal{O}(\epsilon)$ terms are possible. These define different prescriptions for the evanescent operators, and we have to follow one prescription consistently. For more details, see Fuentes-Martin *et al.* (2023b).

[16]Note that physical operators can flow into evanescent operators at two-loop order. Thus, leading to a nonvanishing coefficient for the latter even if we started with zero coupling for the evanescent operators, which could then possibly flow back into the physical coefficients. However, as observed by Dugan and Grinstein (1991) and Herrlich and Nierste (1995), the running of the physical coefficients can be made independent of the evanescent ones through an appropriate finite compensation of the evanescent couplings.

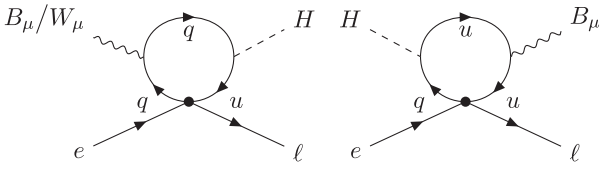

FIG. 2. One-loop SMEFT diagrams allowing for the insertion of the evanescent operator $E_{u^c elq^c}$ and contributing to the leptonic dipole operators.

For example, consider the redundant operator

$$[R_{u^c elq^c}]_{prst} = (\bar{u}^c_p e_r)\varepsilon_{ij}(\overline{\ell}^i_s q^{c\,j}_t), \tag{2.30}$$

which, as we see in Sec. VI.B, is generated at tree level by integrating out an S_1 leptoquark. It can be projected onto the Warsaw basis by applying the four-dimensional Fierz identity (2.20a),

$$[R_{u^c elq^c}]_{prst} \overset{(d=4)}{=} -\tfrac{1}{2}[Q^{(1)}_{lequ}]_{srtp} + \tfrac{1}{8}[Q^{(3)}_{lequ}]_{srtp}. \tag{2.31}$$

The evanescent operator introduced by Eq. (2.31) can be written as $E_{u^c elq^c} \equiv R_{u^c elq^c} - [-(1/2)Q^{(1)}_{lequ} + (1/8)Q^{(3)}_{lequ}]$ schematically. The tree-level action can be directly obtained from Eq. (2.31). However, this introduces the finite shift $\Delta S^{(1)}$ in the one-loop action of the evanescent-free scheme. To determine it, we have to compute all one-loop diagrams with the insertion of the operator $R_{u^c elq^c}$ or $Q^{(1,3)}_{lequ}$. For simplicity, we consider only the leptonic dipole contributions here, which are due to the diagrams shown in Fig. 2. Computing the corresponding amplitudes, we find

$$\begin{aligned}\Delta S^{(1)} = &-\frac{1}{16\pi^2}\frac{5}{8} g_1 [Y^*_u]_{pr}(1-\xi_{\rm rp})[C^{(R)}_{u^c elq^c}]_{rtsp}[Q_{eB}]_{st} \\ &+ \frac{1}{16\pi^2}\frac{3}{8} g_2 [Y^*_u]_{pr}(1-\xi_{\rm rp})[C^{(R)}_{u^c elq^c}]_{rtsp}[Q_{eW}]_{st} \\ &+ \cdots,\end{aligned} \tag{2.32}$$

where $C^{(R)}_{u^c elq^c}$ is the Wilson coefficient of $R_{u^c elq^c}$ and the ellipsis denotes other operators than the leptonic dipoles. The diagrams involving the $Q^{(3)}_{lequ}$ operator are particularly complicated since they involve closed fermion loops giving a Dirac trace of the form

$$\mathrm{tr}[\gamma^\mu\gamma^\nu\gamma^\rho\gamma_\mu\gamma^\sigma\gamma^\delta\gamma^5], \tag{2.33}$$

which is not well defined in dimensional regularization. This is attributed to the commonly known problem of extending γ^5, which is an intrinsically four-dimensional object, to D dimensions. Here we choose to work in NDR, where the cyclicity of Dirac traces of the type given in Eq. (2.33) is lost. Therefore, these traces exhibit a so-called reading point ambiguity: the results of these Dirac traces depend on where we start reading the closed fermion loops, i.e., on which vertex or propagator comes first in the trace. This reading point ambiguity is parametrized by $\xi_{\rm rp}$ in Eq. (2.32), which takes on different values depending on where we start the trace. In our case, we have $\xi_{\rm rp} = 0$ when the Dirac trace is read starting from the Higgs interaction vertex (or the propagator coming after it). For all other reading points we find that $\xi_{\rm rp} = 1$, therefore leading to a vanishing of this particular evanescent contribution. Nevertheless, removing $R_{u^c elq^c}$ in favor of $Q^{(1,3)}_{lequ}$ will still yield nonvanishing evanescent contributions to operators other than the dipoles, but we do not consider those here. We can use any prescription for choosing the reading point of this Dirac trace to compute the evanescent contribution in this basis change, given that we apply this prescription consistently in all subsequent computations within the EFT, i.e., for calculating all one-loop matrix elements involving $Q^{(3)}_{lequ}$. More details were provided by Fuentes-Martin *et al.* (2023b) and in Appendix A.2.

B. How large are the Wilson coefficients?

The value of the Wilson coefficients in an EFT is determined by the matching condition to the corresponding UV theory. However, in the bottom-up approach of SMEFT, the underlying BSM model is unknown. In this case the operator coefficients can be determined only by experiment. Nevertheless, it is still possible to derive some information about the size of the Wilson coefficients from general theoretical arguments.

One way of estimating the coefficients is to use more elaborate versions of dimensional analysis. A second option is understanding whether an operator can be generated at tree level, or only through loops by the full BSM theory. A third possibility is using global (approximate) symmetries of the underlying theory. We now discuss the first two options, while the case of global symmetries is discussed in Sec. III.

1. Power counting and dimensional analysis

Thus far we have merely estimated the size of the coefficient of an effective operator using its energy dimension. As is well known, in $D = 4$ spacetime dimensions each Lagrangian term must be of mass dimension 4. Thus, a mass dimension d operator must be suppressed by a factor of Λ^{4-d}, yielding its approximate size. There is, however, an alternative option for estimating the size of coefficients called naive dimensional analysis (NDA) that was first developed in the context of chiral perturbation theory by Manohar and Georgi (1984). It combines the EFT expansion in the new-physics scale Λ with an expansion in factors of 4π or, equivalently, in $\hbar$ coming from the loop-expansion factor $\hbar/(4\pi)^2$. It was later applied to general EFTs, and the NDA master formula for a term in the SMEFT Lagrangian is (Gavela *et al.*, 2016)

$$\frac{\Lambda^4}{(4\pi)^2}\left[\frac{\partial}{\Lambda}\right]^{N_p}\left[\frac{4\pi H}{\Lambda}\right]^{N_H}\left[\frac{4\pi A}{\Lambda}\right]^{N_A}\left[\frac{4\pi\psi}{\Lambda^{3/2}}\right]^{N_\psi}\left[\frac{g}{4\pi}\right]^{N_g}\left[\frac{y}{4\pi}\right]^{N_y}\left[\frac{\lambda}{(4\pi)^2}\right]^{N_\lambda}, \tag{2.34}$$

TABLE III. NDA scaling of the operator classes in the Warsaw basis.

1: X^3	2: H^6	3: H^4D^2	4: X^2H^2	5: ψ^2H^3	6: ψ^2XH	7: ψ^2H^2D	8: ψ^4
$\frac{4\pi}{\Lambda^2}X^3$	$\frac{(4\pi)^4}{\Lambda^2}H^6$	$\frac{(4\pi)^2}{\Lambda^2}H^4D^2$	$\frac{(4\pi)^2}{\Lambda^2}X^2H^2$	$\frac{(4\pi)^3}{\Lambda^2}\psi^2H^3$	$\frac{(4\pi)^2}{\Lambda^2}\psi^2XH$	$\frac{(4\pi)^2}{\Lambda^2}\psi^2H^2D$	$\frac{(4\pi)^2}{\Lambda^2}\psi^4$

where ∂ is a derivative, H is the Higgs doublet, $A \in \{G, W, B\}$ is a vector field, ψ is one of the SM fermion fields, $g \in \{g_3, g_2, g_1\}$, y is a Yukawa coupling, and λ is the quartic Higgs coupling. The numbers N_i give the power for each factor that is included in the Lagrangian term. The NDA scaling of all operator classes in the Warsaw basis is shown in Table III. We can now compare the SMEFT Lagrangian with the conventional normalization

$$\mathcal{L} \supset (D_\mu H)^\dagger (D^\mu H) + m^2 H^\dagger H - \frac{\lambda}{2}(H^\dagger H)^2 + \frac{C_H}{\Lambda^2}(H^\dagger H)^3 + \cdots \tag{2.35}$$

to the Lagrangian rewritten using NDA

$$\hat{\mathcal{L}} \supset (D_\mu H)^\dagger (D^\mu H) + \hat{m}^2 \Lambda^2 H^\dagger H - \frac{\hat{\lambda}}{2}(4\pi)^2 (H^\dagger H)^2 + \frac{(4\pi)^4 \hat{C}_H}{\Lambda^2}(H^\dagger H)^3 + \cdots, \tag{2.36}$$

and we refrain from writing out all of the other terms explicitly for simplicity. Since NDA does not modify the Lagrangian (i.e., we have $\hat{\mathcal{L}} = \mathcal{L}$), we can identify the coefficients as follows:

$$\hat{m} = \frac{m}{\Lambda}, \quad \hat{\lambda} = \frac{\lambda}{(4\pi)^2}, \quad \hat{C}_H = \frac{1}{(4\pi)^4} C_H. \tag{2.37}$$

Following the discussion provided by Gavela *et al.* (2016), we can now consider the one-loop contribution to C_H,

$$\Delta C_H \sim \sim \frac{\lambda}{(4\pi)^2} C_H\,, \tag{2.38}$$

where we assume that the loop comes with a suppression factor of $1/16\pi^2$. Using NDA instead, we find

$$\Delta \hat{C}_H \sim \sim \hat{\lambda} \hat{C}_H \tag{2.39}$$

without any factors of 4π. The form of Eq. (2.39) is universal and holds in general, regardless of the loop order, for NDA (Gavela *et al.*, 2016),

$$\Delta \hat{C}_i \sim \prod_k \hat{C}_{i_k}. \tag{2.40}$$

This holds for both strongly and weakly coupled theories. For strongly coupled theories we have $\Delta \hat{C} \lesssim 1$ (Manohar and Georgi, 1984), whereas for weakly coupled theories we can have $\Delta \hat{C} \ll 1$. Only $\Delta \hat{C} \gg 1$ is not allowed, as in this case the higher-order correction $\Delta \hat{C}$ would be larger than $\hat{C}$ itself. Thus, interactions become strongly coupled if $\hat{C} \sim 1$. Therefore, the Wilson coefficients $\hat{C}$ in the NDA formalism directly indicate how close a theory is to the strong coupling regime without any factors of 4π. In the usual normalization, which does not use NDA, the strong coupling regime is reached for $C_H \sim (4\pi)^4$ in the previous example or for the SM gauge couplings at $g \sim 4\pi$, as can be seen in Eq. (2.34).

Note that the NDA master formula (2.34) dictates only the maximally allowed size of an operator. Smaller or even vanishing coefficients are always possible. For example, this happens in the case where certain operators are forbidden or suppressed by a global symmetry, as we discuss in Sec. III.

2. Loop- versus tree-level-generated operators

In principle, BSM theories, when matched to the SMEFT, can generate effective operators at different orders in their loop expansion. If the UV theory contains a tree-level process that produces a specific effective operator after integrating out the heavy states this operator is called tree generated. Conversely, if there is no tree-level contribution but instead a contribution at the loop level, then we call the operator loop generated. Different UV theories can generate certain operators at different orders in the loop expansion. Even though the SMEFT is constructed to allow for a description of generic UV completions of the SM, it is impossible to generate certain effective operators at tree level, simply because no possible UV extension exists for producing these operators at leading order. The only assumption for the proof of this statement made by Arzt, Einhorn, and Wudka (1995) is that the underlying UV extension of the SM is a weakly coupled gauge theory built out of a finite (small) number of scalars, vectors, and fermions. For example, all four-fermion operators can in principle be generated by the exchange of either a heavy scalar or a heavy vector boson coupling to both fermion currents in the UV, as shown in Fig. 3. Therefore, we call them potentially tree generated (PTG), as it is still possible to find

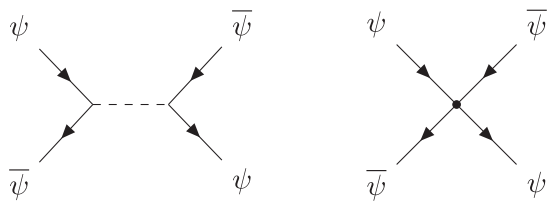

FIG. 3. The Feynman diagram on the left-hand side shows a process in the UV theory generating the effective four-fermion operator shown on the right-hand side. The solid lines represent SM fermions, whereas the dashed line denotes a heavy boson (either vector or scalar).

specific models in which they are produced at the loop level and not by tree graphs.

A counterexample are operators of the type X^3 with three field-strength tensors. It is impossible to generate them in any gauge theory at tree level. These operators are therefore called loop generated (LG), and their coefficients come with an additional suppression factor of $(16\pi^2)^{-n}$, where n is the loop order, if they are produced by a weakly coupled UV theory. The classification of the SMEFT operators according to tree and loop generation was worked out by Arzt, Einhorn, and Wudka (1995) and later adapted to the Warsaw basis by Einhorn and Wudka (2013). Einhorn and Wudka (2013) argued that, when constructing a basis of effective operators for an EFT and having a set of equivalent operators where some are PTG and others are LG, it is always preferable to remove the LG operators since the PTG operators potentially come with larger coefficients and are therefore phenomenologically more relevant. If on the contrary one removes a PTG operator in favor of a LG operator, the coefficient of the latter could potentially gain a tree-level contribution through the corresponding field redefinition (Arzt, Einhorn, and Wudka, 1995), depending on the specific UV model. This condition of removing LG operators in favor of PTG operators whenever possible is also satisfied by the Warsaw basis (Einhorn and Wudka, 2013). As an example, the application of the tree or loop classification to the dimension-6 operators of the SMEFT contributing to the renormalization of $h \to \gamma\gamma$ and $h \to \gamma Z$ was presented by Elias-Miró *et al.* (2013b). The role of the strong coupling assumption was illustrated by a model discussed by Manohar (2013): in the limit of infinitely many heavy particles, which is equivalent to the strong coupling limit, the leading terms are in fact loop generated. For further discussion of the tree or loop classification, see Jenkins, Manohar, and Trott (2013a) and Boggia, Gomez-Ambrosio, and Passarino (2016).

All UV completions of the SM containing general heavy scalar, spinor, and vector fields with arbitrary interactions that contribute to the dimension-6 SMEFT Wilson coefficients at tree level were classified by de Blas *et al.* (2018) and references therein. This work also reports all tree-level matching conditions for these models. Therefore, it presents a complete tree-level UV/IR dictionary for the $d = 6$ SMEFT, allowing one to figure out which SMEFT operator is generated by which UV model at tree level, and consequently to determine all other operators induced in this UV scenario at leading order. This greatly simplifies phenomenological analyses when a deviation in the experimental data is observed and the possibly contributing SMEFT operators have been identified. Generalizations of this dictionary to higher dimensions were discussed by Craig *et al.* (2020) and Li, Ni *et al.* (2022), while generalizations to the one-loop level were addressed by Guedes, Olgoso, and Santiago (2023).

C. Constraints and validity

We saw in Sec. II.B that the scaling of Wilson coefficients can be constrained by purely theoretical arguments. Further constraints on the entire structure of the theory and its validity can be derived from additional general theoretical considerations. A powerful constraint follows from unitarity: operators with arbitrary coefficients can lead to an uncontrolled growth of scattering amplitudes with energy, violating unitarity and hinting at possible inconsistencies in the UV or a breakdown of the EFT expansion. More general constraints on the EFT coefficients follow from the combined requirement of analyticity and unitarity of the S matrix. In this section, we review these arguments, together with some general considerations about the convergence of the operator expansion and the validity of the SMEFT.

1. Convergence of the $1/\Lambda$ expansion and validity range

The EFT expansion can be performed on two different levels, the amplitude (or Lagrangian) level and the level of the observables, which is proportional to the square of a given transition amplitude. To obtain results that have a consistent expansion in powers of the UV cutoff, it is necessary to consistently truncate the expansion of the observables. For example, if we want to work up to dimension 8, we can write the Lagrangian as

$$\mathcal{L} = \mathcal{L}_{\mathrm{SM}} + \frac{1}{\Lambda^2} C_6 Q_6 + \frac{1}{\Lambda^4} C_8 Q_8 + \mathcal{O}(\Lambda^{-6}), \tag{2.41}$$

where $Q_{6(8)}$ represents a generic dimension-6 (dimension-8) operator with the corresponding Wilson coefficient $C_{6(8)}$. Using this Lagrangian to compute an observable O, we schematically find

$$O \sim \mathrm{SM}^2 + \frac{1}{\Lambda^2} C_6 \times \mathrm{SM} + \frac{1}{\Lambda^4} C_6^2 + \frac{1}{\Lambda^4} C_8 \times \mathrm{SM} + \mathcal{O}(\Lambda^{-6}), \tag{2.42}$$

where SM denotes the standard model contribution. The first term is the pure SM contribution to the observable of interest. The second term is the interference of dimension-6 terms with the SM and the only term of the order of Λ^{-2}. Thus, if we would have chosen to work up to dimension 6 instead, these first two terms would be the only ones contributing. However, note that working to Λ^{-2} at an observable level can in principle lead to negative cross sections if the interference term is sizable and negative. To ensure a positive cross section, one includes the third term in Eq. (2.42) which is a "new-physics-squared" contribution of a combination of two dimension-6 operators and thus is of the order of Λ^{-4}. In principle, the last term, which is the interference of a dimension-8 operator with the SM, is also of the order of Λ^{-4}. In many phenomenological applications these contributions are neglected, which is consistent with the truncation of the EFT series at the amplitude level. Only this truncation ensures positive cross sections.

Besides the pure scaling with inverse powers of Λ, care must be taken on the size of the interference terms with the SM amplitude, which can easily be suppressed with respect to the formally leading terms. As pointed out by Azatov *et al.* (2017), helicity selection rules imply that, in a large fraction of $2 \to 2$ scattering processes at high energy, the $1/\Lambda^2$ terms in Eq. (2.42) vanish, and the contribution from dimension-8 operators can be relevant. More generally dimension-8 operators as well as dimension-6 squared terms can become

relevant for searches at high p_T due to the energy growth of the corresponding contribution to the cross section; see Sec. II.C.2.

Studies on the impact of dimension-8 operators in the SMEFT were conducted by Corbett *et al.* (2021), who analyzed their effect on electroweak precision data, and Hays *et al.* (2019), who investigated the operators' impact on Higgs measurements. A comparison of the effect of dimension-6 and dimension-8 operators in more general terms was made by Hays *et al.* (2020).

The issue regarding convergence of the $1/\Lambda$ expansion and the growth with energy of the cross section is closely related to the applicability range of the EFT approach. On the one hand, it is clear that the momentum expansion cannot be trusted if $E/\Lambda = \mathcal{O}(1)$, such that all terms in the operator-product expansion become of the same order. On the other hand, in a bottom-up approach, it is not clear how to determine the precise validity range of the EFT given the intrinsic ambiguity in determining the value of Λ. More precisely the new-physics scale Λ is not an independent parameter in the EFT. Only ratios of Wilson coefficients over the new-physics scale can be determined, i.e., $C^{(d)}/\Lambda^{d-4}$ for a dimension-d operator. Therefore, Wilson coefficients are often defined as dimensionful quantities in the literature ($\mathbf{C}^{(d)} = C^{(d)}/\Lambda^{d-4}$, such that $[\mathbf{C}^{(d)}] = M^{4-d}$). However, throughout this review we use dimensionless coefficients for the benefit of having an explicit EFT power counting. Consistency conditions for specific classes of reactions, ensuring that data are analyzed in a kinematical range where the SMEFT approach is valid, were discussed by Contino *et al.* (2016), Baglio *et al.* (2020), Boughezal, Mereghetti, and Petriello (2021), and Lang *et al.* (2021); see also Brivio *et al.* (2022).

2. Unitarity violation and positivity constraints

The high-energy behavior of scattering amplitudes in the SM is governed by a subtle set of cancellations among different contributions. These protect the theory from unitarity violations due to the unbounded growth of amplitudes with energy. When working with the low-energy degrees of freedom, i.e., the massive physical states after electroweak symmetry breaking, the gauge symmetries responsible for these cancellations are obscured, although they still guarantee the same protection at high energies. A well-known example in the SM is the scattering of longitudinally polarized W bosons $W_L W_L \to W_L W_L$ (Llewellyn Smith, 1973; Lee, Quigg, and Thacker, 1977a, 1977b). If one does not include the quartic self-interaction of the gauge bosons required by the non-Abelian nature of the gauge symmetry, the corresponding amplitude grows with the energy E as E^4. Including the quartic contact interaction dampens the energy growth to E^2 but still leads to unitarity violation. Only after also considering the contribution from the Higgs and Goldstone bosons, and in that way restoring the relations imposed by a linear realization of the $\mathrm{SU}(2)_L$ symmetry breaking via the VEV of the Higgs field, do we find the correct energy behavior of the amplitude, which no longer grows with the energy.

The additional effective operators in the SMEFT can modify the SM interactions or generate new Lorentz structures after electroweak symmetry breaking. Both can alter the energy growth of scattering amplitudes and potentially lead to unitarity-violating effects, despite the SMEFT still respecting the same gauge symmetry as the SM (Distler *et al.*, 2007; Corbett, Éboli, and Gonzalez-Garcia, 2015, 2017; Maltoni, Mantani, and Mimasu, 2019, 2020). To this purpose, we note that all SMEFT operators except for the four-fermion operators contain more than one interaction vertex. An operator containing a certain number of Higgs doublets can have different multiplicities of VEV insertions, and operators with field-strength tensors can lead to interactions with different numbers of gauge fields. Therefore, as in the SM, much different scattering processes can be related by the underlying gauge symmetry.

A contact interaction Q_d of mass dimension d must have a coupling of dimension $4-d$ in four spacetime dimensions $\mathcal{L} \supset Q_d/\Lambda^{d-4}$. The scattering amplitude for a $2 \to N$ process has the mass dimension $2-N$. The contact interaction Q_d thus leads to a contribution to the $2 \to N$ amplitude with the maximum energy scaling

$$\delta\mathcal{A} = \frac{1}{\Lambda^{d-4}} E^{d-N-2}. \tag{2.43}$$

Equation (2.43) implies that at $d = 6$ the maximal energy growth is E^2, as expected from general dimensional considerations, and it occurs in $2 \to 2$ scattering. The amplitude with the maximal energy growth induced by a specific operator originates from the highest-point contact interaction that the operator includes. Lower-point interactions, such as those obtained through VEV insertions or by picking the Abelian part of a field-strength tensor instead of the non-Abelian piece, usually come with lower energy scaling.[17] The energy scaling of amplitudes contributing to various scattering processes measurable at the LHC, including SMEFT contributions at $d = 6$, and corresponding constraints imposed by avoiding perturbative violations of unitarity were discussed by Corbett, Éboli, and Gonzalez-Garcia (2015, 2017) and Maltoni, Mantani, and Mimasu (2019).

A more general class of constraints on the SMEFT coefficients follows from the general requirement of analyticity and unitarity of the S matrix (Adams *et al.*, 2006). The corresponding bounds, which appear in the form of constraints on the sign of certain combinations of Wilson coefficients, are commonly known as positivity bounds. The basic idea behind these constraints is the following: cross sections, which are necessarily positive, can be related to the imaginary part of a forward scattering amplitude using the optical theorem (i.e., exploiting unitarity). The imaginary part of the scattering amplitude is in turn determined by the analytical structure of the amplitude containing isolated poles and branch cuts. We can then use Cauchy's integration formula to relate the amplitude to the Lagrangian parameters, allowing us to determine certain combinations of Wilson coefficients to be positive.

[17]However, a longitudinally polarized gauge boson can compensate a VEV insertion and bring an additional scaling with the energy E.

For concreteness, consider a $2 \to 2$ scattering process, for which the optical theorem reads

$$\mathrm{Im}\mathcal{A}(s) = s\sigma(s), \tag{2.44}$$

where $s = (p_1 + p_2)^2$ is the Mandelstam variable, $\mathcal{A}$ is the corresponding forward scattering amplitude, and σ is the $2 \to N$ cross section ($\sigma \geq 0$). After analytically continuing s to the complex plane, the analytic structure of $\mathcal{A}(s)$ is determined by isolated poles, due to intermediate single-particle on-shell production, and branch cuts, due to multiparticle on-shell production. This allows for a power expansion of the amplitude $\mathcal{A}(s) = \sum_k \lambda_k s^k$. To isolate individual expansion coefficients, we can then apply Cauchy's integral formula

$$\lambda_n = \frac{1}{2\pi i} \oint_\gamma \frac{\mathrm{d}s}{s^{n+1}} \mathcal{A}(s), \tag{2.45}$$

where we integrate along a suitable contour γ, as indicated by the green (inner) dashed line in Fig. 4. For simplicity, we consider only a branch cut on the real axis for $|s| > s_0$ (the gray shaded regions). Enlarging the radius of our contour γ [the green (inner) dashed line], we can deform it into a new contour containing a circle γ' [the blue (outer) dashed line] and an integration around the branch cuts (the orange dashed lines marked "Disc"). We find that

$$\lambda_n = \frac{1}{2\pi i} \oint_{\gamma'} \frac{\mathrm{d}s}{s^{n+1}} \mathcal{A}(s) + \frac{1}{2\pi i} \left(\int_{-\infty}^{-s_0} + \int_{s_0}^{\infty} \right) \frac{\mathrm{d}s}{s^{n+1}} \mathrm{Disc}\mathcal{A}(s), \tag{2.46}$$

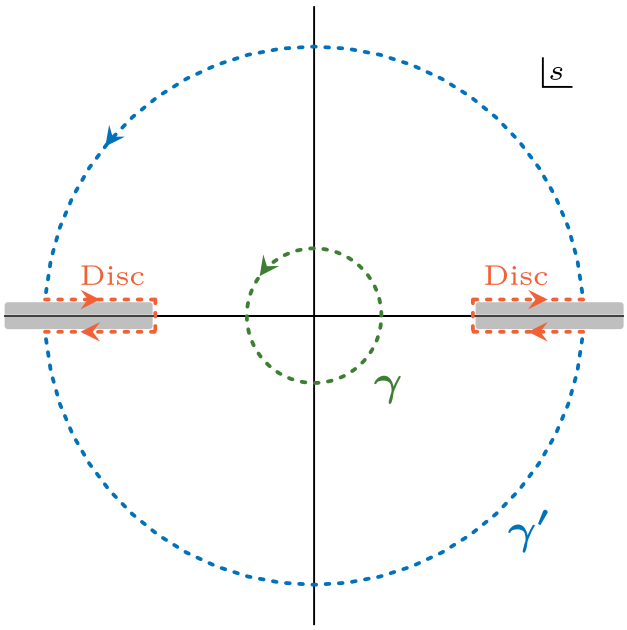

FIG. 4. Analytical structure of a scattering amplitude containing a branch cut (the gray shaded regions) on the real s axis. We also show certain integration contours that we use to determine positivity constraints on the coefficients entering the amplitude. See the text for more details.

where we defined the discontinuity on the real axis by $\mathrm{Disc}\mathcal{A}(s) = \lim_{\epsilon \to 0}[\mathcal{A}(s + i\epsilon) - \mathcal{A}(s - i\epsilon)] = 2i\mathrm{Im}\mathcal{A}(s)$ using the Schwarz reflection principle $[\mathcal{A}(s^*) = \mathcal{A}(s)^*]$. Assuming that $\mathcal{A}(s)$ falls off sufficiently rapidly at infinity, such that the integral along γ' vanishes when the radius of the circle is taken to infinity, we obtain

$$\begin{aligned} \lambda_n &= \frac{1}{\pi}[1 + (-1)^n] \int_{s_0}^{\infty} \frac{\mathrm{d}s}{s^{n+1}} \mathrm{Im}\mathcal{A}(s) \\ &= \frac{1}{\pi}[1 + (-1)^n] \int_{s_0}^{\infty} \frac{\mathrm{d}s}{s^n} \sigma(s), \end{aligned} \tag{2.47}$$

where we changed variables $s \to -s$ in the first integral of the second line in Eq. (2.46) and used $\mathcal{A}(-s) = \mathcal{A}(s)$, which holds due to the crossing symmetry of the forward scattering amplitude, from which we can deduce $\mathrm{Disc}\mathcal{A}(-s) = -\mathrm{Disc}\mathcal{A}(s)$. Furthermore, we directly applied the optical theorem (2.44) in the second equality. We thus find that $\lambda_n = 0$ for odd n, whereas

$$\lambda_n = \frac{2}{\pi} \int_{s_0}^{\infty} \frac{\mathrm{d}s}{s^n} \sigma(s) \geq 0 \tag{2.48}$$

holds for even n. The latter condition provides a positivity constraint on a combination of Wilson coefficients. For more on this topic, see Adams *et al.* (2006).

As a concrete but simple example, consider an EFT of a real massless scalar ϕ whose Lagrangian contains a single $d = 8$ interaction term,

$$\mathcal{L} = \frac{1}{2}(\partial_\mu \phi)(\partial^\mu \phi) + \frac{C_8}{2\Lambda^4}[(\partial_\mu \phi)(\partial^\mu \phi)]^2. \tag{2.49}$$

The $2 \to 2$ scattering amplitude $\mathcal{M}$ for this theory reads $\mathcal{M}(s,t) = 2(C_8/\Lambda^4)(s^2 + t^2 + st)$, where we use $s + t + u = 0$. Thus, we obtain the forward amplitude

$$\mathcal{A}(s) = \lim_{t \to 0} \mathcal{M}(s,t) = 2\frac{C_8}{\Lambda^4} s^2. \tag{2.50}$$

Realizing that $\lambda_2 = 2C_8/\Lambda^4$ and using our previous result from Eq. (2.48), we find that $C_8 > 0$. Therefore, we find that the Wilson coefficient C_8 must be positive based only on unitarity and analyticity. More details on this specific example were given by Remmen and Rodd (2019).

This type of bound can also be exploited for more complicated theories, such as the SMEFT. In general λ_n depend on several different coefficients, and we can thus determine only certain combinations of Wilson coefficients that must be positive. In fact, there has been substantial progress on this front recently (Dvali, Franca, and Gomez, 2012; Remmen and Rodd, 2019; Zhang and Zhou, 2019; Bellazzini *et al.*, 2021; Yamashita, Zhang, and Zhou, 2021; Chala and Santiago, 2022; Remmen and Rodd, 2022). The possible range of SMEFT coefficients has been narrowed down at both dimensions 6 and 8.

3. Gauge anomalies and reparametrization invariance

To conclude this section, we mention two additional aspects of the SMEFT coefficients related to the symmetry properties of the underlying theory. The first aspect deals with gauge anomalies. As is well known, in classically renormalizable theories the criterion for the absence of gauge anomalies relies entirely on the charges of the fermion fields under the local symmetry (Georgi and Glashow, 1972). When moving from the renormalizable case to the nonrenormalizable one, this property is less obvious. In particular, doubts have been raised if the request of anomaly cancellations does impose any additional constraint on the SMEFT Wilson coefficients. This issue was recently clarified by Feruglio (2021), who showed that the dependence of the anomaly on the nonrenormalizable part of the Lagrangian can be removed by adding a local counterterm to the theory. As a result, the condition for gauge anomaly cancellation is controlled only by the charge assignment of the fermion sector, exactly as in the renormalizable theory. In other words, no additional constraints can be derived on the SMEFT by requesting anomaly cancellations.

The second aspect is the so-called reparametrization invariance of the dimension-6 coefficients appearing in $\bar{\psi}\psi \to \bar{\psi}\psi$ scattering amplitudes (Brivio and Trott, 2017). In the Warsaw basis, the operators contributing to $\bar{\psi}\psi \to \bar{\psi}\psi$ scattering give rise to a flat direction. For some time, this created confusion in global SMEFT fits, given the central role played by $\bar{\psi}\psi \to \bar{\psi}\psi$ data in constraining the parameter space. As pointed out by Brivio and Trott (2017), this fact is a consequence of the combined action of a field redefinition (for the vector fields) together with a shift of the vector-fermion couplings. This transformation leaves all of the physical $\bar{\psi}\psi \to \bar{\psi}\psi$ amplitudes unchanged. However, this is not a complete degeneracy of the theory, and indeed it is lifted when considering other amplitudes, such as $\bar{\psi}\psi \to \bar{\psi}\psi\bar{\psi}\psi$. This property illustrates well the importance of considering complete sets of data and a complete operator basis when performing bottom-up analyses of the SMEFT parameter space.

III. GLOBAL SYMMETRIES

A. The role of accidental symmetries

A key concept in any EFT is that of *accidental symmetries*, i.e., symmetries that arise in the lowest-dimensional operators as indirect consequences of the field content and the symmetries explicitly imposed on the theory. Within the SMEFT, two well-known examples are baryon number (B) and lepton number (L). These are exact accidental global symmetries of the $d = 4$ part of the Lagrangian or the SM: they do not need to be imposed in the SM because gauge invariance forbids any $d = 4$ operator violating B or L.

If the accidental symmetries are not respected by the underlying UV completion, we expect them to be violated by the higher-dimensional operators. The strong bounds on B-violating terms from proton stability, as well as the small coefficient of the L-violating Weinberg operator in Eq. (2.2) from neutrino masses, indicate that such symmetries remain almost unbroken in the SMEFT. This observation can be interpreted in a natural way, assuming that the fundamental interactions responsible for B and L violation appear at high energy scales, therefore assuming a high cutoff scale for these operators. This does not contradict the possibility of having a lower cutoff scale for the $d = 6$ SMEFT operators preserving B and L, since the symmetry-preserving sector cannot induce violations of the global symmetries. In other words, accidental global symmetries allow us to define a stable partition of the tower of effective operators in different sectors characterized by different cutoff scales, reflecting a possible multiscale structure of the underlying theory. The key point is that this partition is stable with respect to quantum corrections.

Besides B and L, the SM Lagrangian (or, better, the SMEFT at $d = 4$) has two additional exact accidental global symmetries related to the individual lepton flavor that we can conventionally choose as $L_{e-\mu}$ and $L_{\mu-\tau}$ (combined with L, these correspond to the conservation of each individual lepton flavor). However, a much larger number of approximate accidental symmetries appears in the limit in which we neglect the small Yukawa couplings of the light families and the small off-diagonal entries of the Cabibbo-Kobayashi-Maskawa matrix. These approximate flavor symmetries are responsible for the smallness of flavor-changing neutral-current (FCNC) processes such as B–$\bar{B}$ and K–$\bar{K}$ mixing, which are severely constrained by the data. Despite the precision and the energy scales involved being much different, the situation is similar to that of B and L: the experimental bounds on FCNC processes imply high cutoff scales for the $d = 6$ operators violating the approximate SM flavor symmetries. As in the case of exact accidental symmetries, approximate accidental symmetries allow us to conceive an underlying multiscale structure separating the symmetry-preserving and symmetry-breaking sectors of the theory (with the maximal scale separation limited by the size of the explicit symmetry-breaking terms). This implies that the scale of the symmetry-preserving sector of the SMEFT can be as low as a few TeV, if at that scale not only B and L but also the tightly constrained accidental flavor symmetries remain valid, or are broken only by small symmetry-breaking terms.

The technical implementation of the concept of small symmetry-breaking terms, in the presence of approximate (or exact) symmetries in the low-energy sector of the EFT, is obtained via the *spurion* technique, which is discussed in Sec. III.C. Generalizing the case of exact accidental symmetries, this technique can be viewed as a consistent partitioning of the tower of effective operators, reflecting a possible underlying multiscale structure. This classification is particularly important in the SMEFT given the large number of flavor-violating operators at $d = 6$, and the much different bounds on the symmetry-preserving and symmetry-breaking terms. If we do not conceive an underlying multiscale structure, we are unavoidably led to the conclusion that the cutoff scale of the SMEFT is extremely high, preventing the observation of any deviation from the SM except in rare B- or L-violating processes.

B. Baryon and lepton number

As discussed in Sec. II.A, the unique $d = 5$ operator of the SMEFT is the L-violating term in Eq. (2.2). This operator provides an illustration of the previously discussed general concept of accidental symmetries: it describes all phenomena

TABLE IV. Baryon-number-violating dimension-6 operators in the Warsaw basis (Grzadkowski *et al.*, 2010), with the operator labels adapted from Alonso, Chang *et al.* (2014). The color indices are labeled $\{a,b,c\}$, the indices of $\mathrm{SU}(2)_L$ are $\{i,j,k,l\}$, the flavor indices read $\{p,r,s,t\}$, the charge conjugation matrix is $C=i\gamma^2\gamma^0$, and ε denotes the totally antisymmetric rank-2 or rank-3 tensor.

Baryon-number-violating ψ^4 operators	
Q_{duql}	$\varepsilon^{abc}\varepsilon^{ij}[(d_{ap})^{\intercal}Cu_{br}][(q_{cis})^{\intercal}C\ell_{jt}]$
Q_{qque}	$\varepsilon^{abc}\varepsilon^{ij}[(q_{aip})^{\intercal}Cq_{bjr}][(u_{cs})^{\intercal}Ce_{t}]$
Q_{qqql}	$\varepsilon^{abc}\varepsilon^{il}\varepsilon^{jk}[(q_{aip})^{\intercal}Cq_{bjr}][(q_{cks})^{\intercal}C\ell_{lt}]$
Q_{duue}	$\varepsilon^{abc}[(d_{ap})^{\intercal}Cu_{br}][(u_{cs})^{\intercal}Ce_{t}]$

related to neutrino masses well; hence, it provides indirect evidence[18] that L is violated beyond $d=4$. However, its coupling inferred from neutrino masses points to a high effective scale: $10^{14}<\Lambda<10^{15}$ TeV for $\mathcal{O}(1)$ coefficients (following from $0.03<\sum m_\nu<0.3$ eV).

Possible baryon-number-violating terms first appear at $d=6$. The complete list of B (and L) violating $d=6$ operators is shown in Table IV. These operators satisfy the SM gauge symmetries because of the $\mathrm{SU}(3)_c$ property $\mathbf{3}\otimes\mathbf{3}\otimes\mathbf{3}\sim\mathbf{1}$. This is also the reason why there are no baryon- or lepton-number-violating operators of dimension 6 with three leptons and one quark, and why $B-L$ is conserved at this order. The strong bound from proton decay implies severe bounds on some of these operators: $\Lambda>10^{16}$ GeV for $\mathcal{O}(1)$ coefficients for terms involving only first-generation fermions. The constraints are significantly weaker for operators involving heavy fermions that cannot contribute to proton decay at tree level (Nikolidakis and Smith, 2008).

C. Flavor symmetries

After imposing exact B and L conservation, the number of independent electroweak structures at $d=6$ amounts to the 59 terms listed in Table II. The large proliferation in the number of independent coefficients in the SMEFT at $d=6$ occurs when all of the possible flavor structures for these terms are taken into account: in the absence of a flavor symmetry, they amount to 1350 CP-even and 1149 CP-odd independent coefficients for the dimension-6 operators (Alonso, Jenkins *et al.*, 2014).

Among these couplings, those contributing at tree level to flavor-violating observables, particularly meson-antimeson mixing and lepton-flavor-violating processes, are strongly constrained: these set bounds of $\mathcal{O}(10^5\ \mathrm{TeV})$ on Λ for $\mathcal{O}(1)$ coefficients (Isidori, Nir, and Perez, 2010). If this high scale were the overall cutoff scale of the SMEFT, it would imply that all the other $d=6$ operators play an irrelevant role in current experiments, making the entire construction uninteresting from a phenomenological point of view. However, from the known structure of the SM Yukawa couplings, we know that flavor is highly nongeneric, at least in the $d=4$ sector of the SMEFT. As anticipated, it is conceivable to assume this being the result of an underlying multiscale structure, leading to approximate flavor symmetries in the entire SMEFT also beyond $d=4$. This assumption allows us to reduce in a consistent way the number of relevant parameters, making the entire construction more consistent and more interesting from a phenomenological point of view, with competing constraints from flavor-conserving and flavor-violating processes on a given effective operator.

The price to pay to achieve this goal is the choice of the flavor symmetry and symmetry-breaking sector, which necessarily introduces some model dependence given that there is no exact flavor symmetry to start with (unlike the case of B and L). If we are interested in symmetries and symmetry-breaking patterns able to successfully reproduce the SM Yukawa couplings and, at the same time, suppress nonstandard contributions to flavor-violating observables, the choice is limited. Here we analyze in some detail two cases that are particularly inspired by this point of view: the flavor symmetries $\mathrm{U}(3)^5$ and $\mathrm{U}(2)^5$, with possible minor variations. In both cases the starting point is the flavor symmetry allowed by the SM gauge group.

The $\mathrm{U}(3)^5$ symmetry is the maximal flavor symmetry allowed by the SM gauge group, while $\mathrm{U}(2)^5$ is the corresponding subgroup acting only on the first two light generations. The $\mathrm{U}(3)^5$ symmetry allows us to implement the minimal flavor violation (MFV) hypothesis (Chivukula and Georgi, 1987; D'Ambrosio *et al.*, 2002), which is the most restrictive consistent hypothesis that we can utilize in the SMEFT to suppress nonstandard contributions to flavor-violating observables (D'Ambrosio *et al.*, 2002). The $\mathrm{U}(2)^5$ symmetry with minimal breaking (Barbieri *et al.*, 2011, 2012; Blankenburg, Isidori, and Jones-Perez, 2012) is interesting since it retains most of the MFV virtues, but it allows us to have a much richer structure as far as the third-generation dynamics is concerned.

1. $\mathrm{U}(3)^5$ and minimal flavor violation

The largest group of global symmetry transformations of the SM fermions compatible with the gauge symmetries of the SM Lagrangian is (Gerard, 1983; Chivukula and Georgi, 1987)

$$\begin{aligned}\mathcal{G}_f &= \mathrm{U}(3)_\ell\times\mathrm{U}(3)_q\times\mathrm{U}(3)_e\times\mathrm{U}(3)_u\times\mathrm{U}(3)_d\\ &\equiv \mathrm{U}(3)^5=\mathrm{SU}(3)^5\times\mathrm{U}(1)^5.\end{aligned}\tag{3.1}$$

Within the SM, the Yukawa couplings ($Y_{e,u,d}$) are the only source of breaking of $\mathcal{G}_f$. They break this global symmetry as follows:

$$\mathcal{G}_f=\begin{cases}\mathrm{SU}(3)^5\\ \mathrm{U}(1)^5\end{cases}\xrightarrow{Y_{e,u,d}\neq 0}\begin{matrix}\mathrm{U}(1)_{e-\mu}\times\mathrm{U}(1)_{\tau-\mu},\\ \mathrm{U}(1)_B\times\mathrm{U}(1)_L\times\mathrm{U}(1)_Y,\end{matrix}\tag{3.2}$$

where we explicitly separate the flavor-universal and flavor-nonuniversal subgroups. The three unbroken flavor-universal $\mathrm{U}(1)$ groups are baryon number, lepton number, and hypercharge.

[18]Alternative descriptions of neutrino masses not involving the Weinberg operator and preserving L are possible but require the enlargement of the field content or the inclusion of operators of even higher dimensions; see Gonzalez-Garcia and Maltoni (2008).

TABLE V. Number of independent $d = 6$ SMEFT operators without any symmetry for three or one generation (gen.), and when imposing a $U(3)^5$ or $U(2)^5$ flavor symmetry with different powers of symmetry-breaking terms (Faroughy *et al.*, 2020). In each column the left (right) number corresponds to the number of CP-even (CP-odd) coefficients. $\mathcal{O}(X^n)$ indicates that terms up to $\mathcal{O}(X^n)$ are included.

		No symmetry				$U(3)^5$						$U(2)^5$					
Class	operators	3 gen.		1 gen.		Exact		$\mathcal{O}(Y^1_{e,d,u})$		$\mathcal{O}(Y^1_e, Y^1_d Y^2_u)$		Exact		$\mathcal{O}(V^1)$		$\mathcal{O}(V^2, \Delta^1)$	
1–4	X^3, H^6, H^4D^2, X^2H^2	9	6	9	6	9	6	9	6	9	6	9	6	9	6	9	6
5	ψ^2H^3	27	27	3	3	0	0	3	3	4	4	3	3	6	6	9	9
6	ψ^2XH	72	72	8	8	0	0	8	8	11	11	8	8	16	16	24	24
7	ψ^2H^2D	51	30	8	1	7	0	7	0	11	1	15	1	19	5	23	5
8	$(\bar{L}L)(\bar{L}L)$	171	126	5	0	8	0	8	0	14	0	23	0	40	17	67	24
	$(\bar{R}R)(\bar{R}R)$	255	195	7	0	9	0	9	0	14	0	29	0	29	0	29	0
	$(\bar{L}L)(\bar{R}R)$	360	288	8	0	8	0	8	0	18	0	32	0	48	16	69	21
	$(\bar{L}R)(\bar{R}L)$	81	81	1	1	0	0	0	0	0	0	1	1	3	3	6	6
	$(\bar{L}R)(\bar{L}R)$	324	324	4	4	0	0	0	0	4	4	4	4	12	12	28	28
Total		1350	1149	53	23	41	6	52	17	85	26	124	23	182	81	264	123

Most of the $d = 6$ SMEFT operators can be viewed as independent $\mathcal{G}_f$-breaking terms; hence, they can be classified according to their transformation properties under $\mathcal{G}_f$. To begin, we consider the limit of unbroken $\mathcal{G}_f$: retaining only the $\mathcal{G}_f$ invariant operators at $d = 6$ is not a fully consistent hypothesis, since $\mathcal{G}_f$ is broken in the $d = 4$ sector. However, it is a useful starting point for the classification of the operators, and it is a coherent hypothesis to be implemented in the SMEFT in the limit where we also neglect $\mathcal{G}_f$-breaking terms in the SM sector, i.e., in the limit where we neglect the SM Yukawa couplings.

The number of independent $d = 6$ terms respecting $\mathcal{G}_f$ is reported in Table V in the "Exact" $U(3)^5$ column: the left (right) value in each entry indicates the number of CP-even (CP-odd) coefficients. For comparison, the counting of independent coefficients if no symmetry is imposed, or if a single generation of fermions is considered, is also shown. As seen, the number of independent coefficients respecting the $\mathcal{G}_f$ symmetry is smaller than in the single-generation case: this is because $\mathcal{G}_f$ forbids bilinear couplings of fermions with different gauge quantum numbers, such as those appearing in the Yukawa couplings.

The MFV hypothesis is the assumption that the SM Yukawa couplings are the only sources of $U(3)^5$ breaking (Chivukula and Georgi, 1987; D'Ambrosio *et al.*, 2002). The exact $U(3)^5$ limit can be viewed as employing the MFV hypothesis and working to zeroth order in the symmetry-breaking terms. To go beyond the leading order, we promote the SM Yukawa couplings to become $U(3)^5$ spurions, i.e., nondynamical fields with well-defined transformation properties under $U(3)^5$. The latter are deduced by the structure of the SM Lagrangian (D'Ambrosio *et al.*, 2002),

$$Y_u = (\mathbf{1}, \mathbf{3}, \mathbf{1}, \bar{\mathbf{3}}, \mathbf{1}), \quad Y_d = (\mathbf{1}, \mathbf{3}, \mathbf{1}, \mathbf{1}, \bar{\mathbf{3}}), \quad Y_e = (\mathbf{3}, \mathbf{1}, \bar{\mathbf{3}}, \mathbf{1}, \mathbf{1}). \tag{3.3}$$

With these transformation properties, the $d = 4$ sector of the theory is formally invariant under $U(3)^5$. The MFV hypothesis consists in constructing the higher-dimensional operators using SM fields and spurions such that the EFT remains formally invariant under $U(3)^5$ to all orders, and the breaking occurs only via the appropriate insertions of the spurions $Y_{u,d,e}$.

In principle, the spurions can appear with arbitrary powers both in the renormalizable ($d = 4$) part of the Lagrangian and in the dimension-6 effective operators. However, via a suitable redefinition of both fermion fields and spurions, we can always set the $d = 4$ Lagrangian to its standard expression, identifying the spurions with the SM Yukawa couplings. This implies that we can always choose a flavor basis where the spurions are completely determined in terms of fermion masses and the Cabibbo-Kobayashi-Maskawa (CKM) matrix V_{CKM}. A representative example is the down-quark mass-eigenstate basis, where

$$Y_e = \mathrm{diag}(y_e, y_\mu, y_\tau), \qquad Y_d = \mathrm{diag}(y_d, y_s, y_b),$$
$$Y_u = V^\dagger_{\mathrm{CKM}} \times \mathrm{diag}(y_u, y_c, y_t). \tag{3.4}$$

The key point is that there are no free (observable) parameters in the structure of the MFV spurions. A related important point is the fact that, knowing the structure of the spurions, we know that they are all small except for the top Yukawa y_t. We can thus limit the spurion expansion to a few terms.

The overall number of independent terms allowed by the MFV hypothesis with at most one "small" Yukawa coupling, namely, Y_d or Y_e, and up to 2 powers of Y_u is shown in the last column of Table V (Faroughy *et al.*, 2020). This number is almost 2 orders of magnitude smaller than what is obtained in the absence of any symmetry (for three generations) and is close to the single-generation case. With the corresponding set of operators, we can describe the SM spectrum and possible deviations from the SM in a series of rare flavor-violating processes (D'Ambrosio *et al.*, 2002). A representative set of these operators is shown in Table VI.

The number of insertions of the leading Y_u spurions has been limited to two since, in the reference basis (3.4), one gets

$$[Y_u (Y_u)^\dagger]^n_{r \neq p} \approx y_t^{2n} V^*_{tr} V_{tp} \propto [Y_u (Y_u)^\dagger]_{r \neq p}. \tag{3.5}$$

TABLE VI. Representative set of SMEFT operators, with their flavor structure determined according to the MFV hypothesis. Each electroweak structure (first column) can admit different MFV implementations. In the second column we indicate the one more constrained by flavor-violating processes in the quark sector. The corresponding bounds on the effective scale set by B- and K-meson physics measurements is reported in the third column (95% C.L. bound, assuming an effective coupling $\sim \pm 1/\Lambda^2$, considering each operator separately).

EW type	Possible MFV form	Bound on Λ (TeV)
Q_{dB}	$[\bar{q}_r(Y_u Y_u^\dagger Y_d)_{rp}\sigma^{\mu\nu} d_p]H(g_1 B_{\mu\nu})$	6.1
Q_{dG}	$[\bar{q}_r(Y_u Y_u^\dagger Y_d)_{rp}\sigma^{\mu\nu} T^A d_p]H(g_3 G^A_{\mu\nu})$	3.4
$Q_{Hq}^{(1)}$	$(H^\dagger i\overleftrightarrow{D}_\mu H)[\bar{q}_r(Y_u Y_u^\dagger)_{rp}\gamma_\mu q_p]$	2.3
$Q_{qq}^{(1)}$	$[\bar{q}_r(Y_u Y_u^\dagger)_{rp}\gamma_\mu q_p][\bar{q}_r(Y_u Y_u^\dagger)_{rp}\gamma_\mu q_p]$	6.0
Q_{qe}	$[\bar{q}_r(Y_u Y_u^\dagger)_{rp}\gamma_\mu q_p][\bar{e}_s\gamma_\mu e_s]$	2.7
$Q_{\ell q}^{(1)}$	$[\bar{q}_r(Y_u Y_u^\dagger)_{rp}\gamma_\mu q_p][\bar{\ell}_s\gamma_\mu \ell_s]$	1.7

Equation (3.5) implies that within the MFV hypothesis rare FCNC processes that, within the SM, are not helicity suppressed and are dominated by virtual top-quark contributions (such as B^0–$\bar{B}^0$ and K^0–$\bar{K}^0$ mixing, $b \to s\gamma$, $b \to s\ell^+\ell^-$, …) receive exactly the same CKM suppression as in the SM,

$$\mathcal{A}(d^i \to d^j)_{\rm MFV} = (V_{ti}^* V_{tj})\mathcal{A}_{\rm SM}^{(\Delta F=1)}\left[1 + a_1 \frac{16\pi^2 M_W^2}{\Lambda^2}\right],$$
$$\mathcal{A}(M_{ij} - \bar{M}_{ij})_{\rm MFV} = (V_{ti}^* V_{tj})^2\mathcal{A}_{\rm SM}^{(\Delta F=2)}\left[1 + a_2 \frac{16\pi^2 M_W^2}{\Lambda^2}\right], \tag{3.6}$$

where $\mathcal{A}_{\rm SM}^{(i)}$ denote the SM loop amplitudes and a_i are the $\mathcal{O}(1)$ parameters. The a_i depend on different combinations of SMEFT coefficients but are flavor independent. Actually, Eq. (3.6) can be used to define in an operative way the MFV hypothesis for a large class of flavor-changing processes, as proposed by Buras (2003).

2. The U(2)^5 symmetry

The U(2)^5 flavor symmetry is the subgroup of the U(3)^5 global symmetry that, by construction, distinguishes the first two generations of fermions from the third one (Barbieri *et al.*, 2011, 2012; Blankenburg, Isidori, and Jones-Perez, 2012). For each set of SM fermions with the same gauge quantum numbers, the first two generations form a doublet of a given U(2) subgroup, whereas the third one transforms as a singlet. Denoting the five independent flavor doublets as L, Q, E, U, and D, the flavor symmetry decomposes as

$$\mathrm{U}(2)^5 = \mathrm{U}(2)_L \times \mathrm{U}(2)_Q \times \mathrm{U}(2)_E \times \mathrm{U}(2)_U \times \mathrm{U}(2)_D. \tag{3.7}$$

In the limit of unbroken U(2)^5, only third-generation fermions can have nonvanishing Yukawa couplings, which is an excellent first-order approximation for the SM Lagrangian. This is why, unlike in the MFV case, the U(2)^5 symmetry allows us to build an EFT where all the symmetry-breaking terms are small.

A U(2)^3 symmetry in the quark sector can be viewed as the result of a generalized MFV framework, taking into account arbitrary insertions of the third-generation Yukawa couplings without suppression [the so-called nonlinear representation of MFV (Feldmann and Mannel, 2008) or general MFV (Kagan *et al.*, 2009) hypothesis]. However, this interpretation is less motivated in the lepton sector and also implies a strict structure for the symmetry-breaking terms. Nevertheless, the symmetry group in Eq. (3.7) with the symmetry-breaking terms discussed next can be viewed as an effective way to describe in general terms the large class of SM extensions where the third generation of fermions plays a special role.

a. Yukawa couplings and spurion structures

A set of symmetry-breaking terms sufficient to reproduce the complete structure of the SM Yukawa couplings is (Barbieri *et al.*, 2011)

$$V_\ell \sim (\mathbf{2},\mathbf{1},\mathbf{1},\mathbf{1},\mathbf{1}), \qquad V_q \sim (\mathbf{1},\mathbf{2},\mathbf{1},\mathbf{1},\mathbf{1}),$$
$$\Delta_e \sim (\mathbf{2},\mathbf{1},\bar{\mathbf{2}},\mathbf{1},\mathbf{1}), \qquad \Delta_{u(d)} \sim (\mathbf{1},\mathbf{2},\mathbf{1},\bar{\mathbf{2}}(\mathbf{1}),\mathbf{1}(\bar{\mathbf{2}})). \tag{3.8}$$

By construction $V_{q,\ell}$ are complex two-vectors and $\Delta_{e,u,d}$ are complex 2×2 matrices. In terms of these spurions, we can express the Yukawa couplings as

$$Y_e = y_\tau \begin{pmatrix} \Delta_e & x_\tau V_\ell \\ 0 & 1 \end{pmatrix}, \quad Y_u = y_t \begin{pmatrix} \Delta_u & x_t V_q \\ 0 & 1 \end{pmatrix},$$
$$Y_d = y_b \begin{pmatrix} \Delta_d & x_b V_q \\ 0 & 1 \end{pmatrix}, \tag{3.9}$$

where $y_{\tau,t,b}$ and $x_{\tau,t,b}$ are free complex parameters expected to be of order unity.

The spurion set in Eq. (3.9) is minimal in terms of independent U(2)^5 structures (at least as far as the quark sector is concerned) and leads to spurions that are small and hierarchical in size. Unlike in the MFV framework, in this case we cannot completely determine the spurions in terms of the SM parameters. However, we can constrain their size while requiring no tuning in the $\mathcal{O}(1)$ parameters. In particular, from the $2 \leftrightarrow 3$ mixing in the CKM matrix we deduce $|V_q| = \mathcal{O}(|V_{cb}|)$, while light-quark and lepton masses imply $|\Delta_{u,d,e}|_{ij} \ll |V_q|$.

There are no unambiguous constraints about the size of V_ℓ. Actually, the SM lepton Yukawa coupling can be reproduced even when setting $V_\ell = 0$. However, assuming a common structure for the three Yukawa couplings, as suggested by the similar hierarchies observed in the eigenvalues, we also assume that $|V_\ell| \sim |V_q|$. The assumption that $V_{q,\ell}$ are the leading U(2)^5-breaking spurions ensures a suppression of flavor-violating terms in the quark sector, via higher-dimensional operators, that is as effective as the one implied by the MFV hypothesis.

It is convenient to define as reference (or interaction) basis the flavor basis in U(2)^5 space where $V_{q,\ell} = |V_{q,\ell}| \times \vec{n}$, with $\vec{n} = (0,1)^\intercal$, and where $\Delta_{u,d,e}^\dagger \Delta_{u,d,e}$ are diagonal. After the U(2)^5 symmetry is broken, the residual flavor symmetry implies that the Yukawa matrices in the interaction basis can

be written in the following form (Fuentes-Martin, Isidori *et al.*, 2020):

$$Y_u = |y_t| \begin{pmatrix} U_q^\dagger O_u^\intercal \hat{\Delta}_u & |V_q||x_t| e^{i\phi_q} \vec{n} \\ 0 & 1 \end{pmatrix}, \tag{3.10a}$$

$$Y_d = |y_b| \begin{pmatrix} U_q^\dagger \hat{\Delta}_d & |V_q||x_b| e^{i\phi_q} \vec{n} \\ 0 & 1 \end{pmatrix}, \tag{3.10b}$$

$$Y_e = |y_\tau| \begin{pmatrix} O_e^\intercal \hat{\Delta}_e & |V_\ell||x_\tau| \vec{n} \\ 0 & 1 \end{pmatrix}, \tag{3.10c}$$

where $\hat{\Delta}_{u,d,e}$ are 2×2 diagonal positive matrices, $O_{u,e}$ are 2×2 orthogonal matrices, and U_q is a complex unitary matrix. The unitary matrices that diagonalize the aforementioned Yukawa matrices were discussed by Fuentes-Martin, Isidori *et al.* (2020). After expressing the free parameters in terms of fermion masses and CKM elements, the residual terms that cannot be determined in terms of SM parameters are as follows:

- *Quark sector*: $2 \leftrightarrow 3$ mixing angle in the down sector, $s_b \approx |x_b||V_q|$, and *CP*-violating phase ϕ_q.
- *Lepton sector*: $2 \leftrightarrow 3$ mixing angle $s_\tau \approx |x_\tau||V_\ell|$ and $1 \leftrightarrow 2$ mixing angle s_e (which appears in O_e).

As pointed out by Greljo, Palavrić, and Thomsen (2022), the parametrization in Eq. (3.10) is redundant and all of the previously listed non-SM parameters can be eliminated via a suitable change of basis consistent within the $\mathrm{U}(2)^5$ framework. For instance, in the quark sector both s_b and ϕ_q can be eliminated by a transformation mixing the $\mathrm{U}(2)_Q$ singlet field with the $\mathrm{U}(2)_Q$ doublet appropriately contracted with spurions. While this is certainly correct, this change of basis implies a shift in the tower of higher-dimensional operators. In a pure bottom-up approach, this shift has no practical consequences; hence, the redundancy can safely be removed. However, keeping the redundant formulation in Eq. (3.10) is particularly useful when matching to a specific UV theory: it highlights the fact that the third generation, with a special role in the UV, is not unambiguously determined by the SM Yukawa couplings.

b. Higher-dimensional operators

The exact $\mathrm{U}(2)^5$ symmetry is the natural and unavoidable starting point to describe all processes where we can neglect light-fermion masses. This is why the SMEFT with unbroken $\mathrm{U}(2)^5$ is employed to describe top-quark physics and related processes at colliders (Barducci *et al.*, 2018). The numbers of relevant operators are listed in Table V.

In Table V the terms obtained with one V spurion, or two of them and one Δ spurion, are given. The higher-dimensional operators built in terms of a single $V_{q,\ell}$ spurion contribute to flavor-violating transitions that involve only left-handed fields and connect only the $2 \leftrightarrow 3$ sectors in the interaction basis. Considering terms with two V_q spurions is the analog of considering two Y_u insertions in MFV. Compared to the latter case, the $\mathrm{U}(2)^5$ hypothesis leads to more freedom (differentiating, for instance, effective operators contributing to the flavor-violating process in B- and K-meson physics), but also more terms. The latter statement can be understood by looking at the number of independent invariant $\bar{q}_r \gamma^\mu q_p$ bilinears in the two cases,[19]

$$\left.\begin{matrix} \bar{q}_r \gamma^\mu q_r \\ \bar{q}_r (Y_u Y_u^\dagger)_{rp} \gamma^\mu q_p \end{matrix}\right|_{\mathrm{U}(3)^5} \rightarrow \left.\begin{matrix} \bar{q}_3 \gamma^\mu q_3 \\ \bar{q}_i \gamma^\mu q_i \\ \bar{q}_i (V_q)_i \gamma^\mu q_3 + \mathrm{H.c.} \\ \bar{q}_i (V_q)_i \gamma^\mu (V_q^\dagger)_j q_j \end{matrix}\right|_{\mathrm{U}(2)^5}.$$

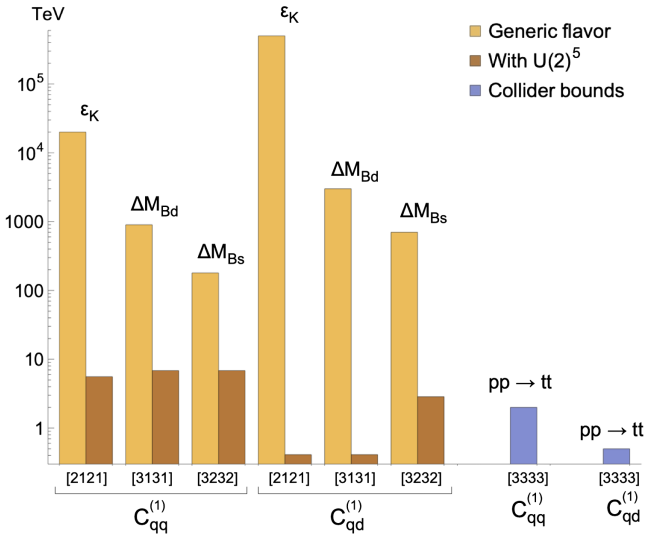

FIG. 5. Bounds on the effective scales of the SMEFT four-quark operators $Q_{qq}^{(1)}$ and $Q_{qd}^{(1)}$ for different flavor indices, as reported on the horizontal axis between square brackets (the bounds are 95% C.L. limits for effective scales defined as in Table VI). For left-handed fields, the flavor indices refer to the down-quark mass-eigenstate basis. The bounds "with $\mathrm{U}(2)^5$" (brown bars) are obtained while incorporating into the operators one or more $\mathrm{U}(2)^5$-breaking terms, according to the rules discussed in Sec. III.C.2. The observables used to derive the bounds are also indicated.

In Fig. 5 we illustrate more concretely some of the features showing bounds on two representative four-quark SMEFT operators $Q_{qq}^{(1)}$ and $Q_{qd}^{(1)}$ (see Table II) for different flavor indices. The strong bounds on the effective scales exceeding 100 TeV (the light yellow bars in Fig. 5) are those obtained without any symmetry hypothesis. They correspond to flavor combinations leading to unsuppressed tree-level contributions to specific meson-antimeson mixing amplitudes. By contrast, once the suppression due to the $\mathrm{U}(2)^5$-breaking spurions is taken into account, the same observables lead to bounds on the effective scales below 10 TeV. Note that these bounds are comparable to those obtained by direct searches for flavor-conserving combinations involving only third-generation fermions, which are the most severely constrained by high-energy LHC data.

[19]Here the flavor indices $\{r, p\}$ run from 1 to 3, whereas $\{i, j\}$ run only from 1 to 2.

We stress that the hypothesis of a $U(2)^5$ flavor symmetry broken by the minimal set of spurions in Eq. (3.9) implies lepton-flavor violation in the charged lepton sector. This is controlled by the size of V_ℓ and s_e, which are left unconstrained by the SM Yukawa couplings. This is one of the most evident differences between the genuine $U(2)^5$ approach and the nonlinear MFV hypothesis (Feldmann and Mannel, 2008; Kagan *et al.*, 2009).

3. Other options and running

The previously discussed $U(2)^5$ case is the prototype of a series of symmetry groups providing a suppression similar to MFV in the quark sector but allowing more general breaking terms. The common ground is the presence of the chiral non-Abelian group $U(2)^3$ acting in the quark sector. The variations come from obtaining this group as a subgroup of possible larger symmetries, such as $U(2)^2 \times U(3)_d$ or $U(2)^3 \times U(1)_d$ (Faroughy *et al.*, 2020; Greljo, Palavrić, and Thomsen, 2022). Given the smaller set of phenomenological constraints, a larger set of variations have been proposed in the lepton sector (Greljo, Palavrić, and Thomsen, 2022).

A somehow different approach is that of using only $U(1)$ groups, as originally proposed by Froggatt and Nielsen (1979). Recent analyses of this type were given by Smolkovič, Tammaro, and Zupan (2019) and Bordone, Catà, and Feldmann (2020).

To conclude the discussion about flavor symmetries, we mention that the approximate symmetries present in the SM are responsible for a series of powerful (approximate) selection rules in the renormalization group evolution of the SMEFT (Feldmann, Mannel, and Schwertfeger, 2015; Machado, Renner, and Sutherland, 2023). These are simply manifestations of the statement made in Sec. III.A, namely, that the partitioning of the EFT due to global symmetries is stable with respect to quantum corrections. These selection rules become manifest when one works in a basis of flavor invariants, where the apparently large anomalous-dimension matrix of dimension-6 current-current operators is reduced to a block-diagonal structure with several blocks of small dimension (Machado, Renner, and Sutherland, 2023).

D. Custodial symmetry

The large number of fermions in the SM implies that most of the exact or approximate global symmetries of the theory are related to the fermion sector, as discussed. However, there is one important symmetry that involves mainly (but not only) the scalar sector.

Custodial symmetry is an exact symmetry of the pure Higgs sector of the SM

$$\mathcal{L}_H = \partial_\mu H^\dagger \partial^\mu H - V(H), \tag{3.11}$$

with the scalar potential defined as in Eq. (1.6). The simplest way to realize the global symmetry of $\mathcal{L}_H$ is to write the complex Higgs doublet in terms of four independent real scalar components ϕ^i as in Eq. (1.7),

$$H = \frac{1}{\sqrt{2}} \begin{pmatrix} \phi^2 + i\phi^1 \\ \phi^4 - i\phi^3 \end{pmatrix}. \tag{3.12}$$

We find that

$$\mathcal{L}_\phi = \frac{1}{2}(\partial_\mu \boldsymbol{\phi}) \cdot (\partial^\mu \boldsymbol{\phi}) + \frac{m^2}{2} \boldsymbol{\phi} \cdot \boldsymbol{\phi} - \frac{\lambda}{8} (\boldsymbol{\phi} \cdot \boldsymbol{\phi})^2, \tag{3.13}$$

where we define

$$\boldsymbol{\phi} = \begin{pmatrix} \phi^1 \\ \phi^2 \\ \phi^3 \\ \phi^4 \end{pmatrix} = \begin{pmatrix} \varphi^1 \\ \varphi^2 \\ \varphi^3 \\ v + h \end{pmatrix}, \tag{3.14}$$

with the Higgs VEV v, the physical Higgs boson h, and the Goldstone bosons of electroweak symmetry breaking φ^a. One can verify that $\mathcal{L}_H$ and $\mathcal{L}_\phi$ depend only on $\boldsymbol{\phi} \cdot \boldsymbol{\phi} = 2H^\dagger H$ and are thus invariant under a global $O(4)$ symmetry, with the symmetry transformation $\boldsymbol{\phi} \to O\boldsymbol{\phi}$ for $O \in O(4)$. The minimum of the Higgs potential is the three-sphere S^3 with radius v defined by $\langle \boldsymbol{\phi} \cdot \boldsymbol{\phi} \rangle = v^2$. Hence, the $O(4)$ global symmetry of $\mathcal{L}_H$ is spontaneously broken by the Higgs VEV to its subgroup $O(3)$. The corresponding Goldstone bosons $\boldsymbol{\varphi} = (\varphi^1, \varphi^2, \varphi^3)^\intercal$ transform under this group as $\boldsymbol{\varphi} \to \tilde{O}\boldsymbol{\varphi}$, where $\tilde{O} \in O(3)$.

This $O(3)$ global symmetry of the Higgs sector after electroweak symmetry breaking is responsible for, among other things, the tree-level relation $\rho = 1$, where

$$\rho \equiv \frac{m_W^2}{m_Z^2} \frac{g_1^2 + g_2^2}{g_2^2}. \tag{3.15}$$

Equation (3.15) is tested to the per mill level, finding good agreement with the SM prediction after taking into account the small deviations generated beyond tree level. However, adding to $\mathcal{L}_H$ generic dimension-6 operators that are compatible only with the gauge symmetry of the SM, one would expect $\rho - 1 = \mathcal{O}(v^2/\Lambda^2)$.

Custodial symmetry is explicitly broken in the SM, both by the electroweak gauge symmetry, which acts differently on the different ϕ^i components, and by the Yukawa interactions. These breaking terms are responsible for the deviation from $\rho = 1$ generated beyond tree level. In particular, the leading contribution induced by the top Yukawa coupling reads

$$(\rho - 1)^{y_t}_{\mathrm{SM}} = \frac{3y_t^2}{32\pi^2} \approx 1\%. \tag{3.16}$$

Given the strong constraints on the SMEFT imposed by the ρ parameter, one can conceive of the case of new-physics models where the breaking of custodial symmetry is small, as in the SM, originating only from the gauge and the Yukawa sector. In other words, in close analogy to the previously discussed flavor symmetries, one can treat custodial symmetry as an approximate global symmetry of the SMEFT broken by a well-defined set of spurion terms.

To describe the explicit breaking of custodial symmetry occurring in the SM, it is more convenient to express the

symmetry in a different way, taking into account the local equivalence of the SO(4) group with the product of two SU(2) groups,

$$\mathrm{O}(4) \simeq \mathrm{SU}(2)_L \times \mathrm{SU}(2)_R. \tag{3.17}$$

To see how the SU(2) groups in Eq. (3.17) act on the Higgs field, we can combine H and its conjugate $\tilde{H} = \varepsilon H^*$, where $\varepsilon = i\tau^2$ is the totally antisymmetric SU(2) tensor, to form the 2×2 matrix field Σ, which transforms as $(\mathbf{2}_L, \bar{\mathbf{2}}_R)$ under Eq. (3.17), namely,

$$\Sigma \equiv (\tilde{H}, H) \to V_L \Sigma V_R^\dagger, \tag{3.18}$$

with $V_{L(R)} \in \mathrm{SU}(2)_{L(R)}$. We find that $\mathrm{tr}[\Sigma^\dagger \Sigma] = 2H^\dagger H = \boldsymbol{\phi} \cdot \boldsymbol{\phi}$, which allows us to write the Higgs Lagrangian $\mathcal{L}_H$ as

$$\mathcal{L}_\Sigma = \frac{1}{2}\mathrm{tr}[(\partial_\mu \Sigma)^\dagger (\partial^\mu \Sigma)] + \frac{m^2}{2}\mathrm{tr}[\Sigma^\dagger \Sigma] - \frac{\lambda}{8}(\mathrm{tr}[\Sigma^\dagger \Sigma])^2. \tag{3.19}$$

With this notation one can verify that $\mathcal{L}_H$ and $\mathcal{L}_\Sigma$ are invariant under $\mathrm{SU}(2)_L \times \mathrm{SU}(2)_R$ global transformations, and that the spontaneous symmetry breaking due to the Higgs VEV corresponds to $\mathrm{O}(4) \simeq \mathrm{SU}(2)_L \times \mathrm{SU}(2)_R \to \mathrm{SU}(2)_{L+R} \simeq \mathrm{O}(3)$. While the $\mathrm{SU}(2)_L$ group is fully gauged in the SM, only a part of the $\mathrm{SU}(2)_R$ group is gauged, leading to an explicit breaking of custodial symmetry. To be more precise, gauging the hypercharge in the Higgs sector is equivalent to gauging only the U(1) subgroup of $\mathrm{SU}(2)_R$ corresponding to the diagonal generator T_R^3.

Up to this level, i.e., when only the gauge sector is considered, the identification of the explicit breaking of custodial symmetry from a general EFT point of view is unambiguous. An ambiguity arises when the fermion sector is also considered, given that the action of T_R^3 is not sufficient to describe fermion hypercharges. On general grounds, we can extend the symmetry to (Elias-Miró *et al.*, 2013a)

$$\mathcal{G}_{\mathrm{cust}} = \mathrm{SU}(2)_L \times \mathrm{SU}(2)_R \times \mathrm{U}(1)_X \tag{3.20}$$

such that the hypercharge reads

$$Y = T_R^3 + X. \tag{3.21}$$

However, different embeddings of the SM fermions in $\mathcal{G}_{\mathrm{cust}}$ are possible. The simplest one corresponds to the choice of $X = (B - L)/2$. In such a case, all right-handed fermions belong to doublets of $\mathrm{SU}(2)_R$, with an incomplete doublet in the lepton sector due to the absence of right-handed neutrinos, while all left-handed fermions are assumed to be singlets of $\mathrm{SU}(2)_R$. But other options are also possible (Elias-Miró *et al.*, 2013a).

Once a representation of the SM fermions under $\mathcal{G}_{\mathrm{cust}}$ is chosen, we have all the ingredients to define a consistent EFT based on the hypothesis of minimal breaking of custodial symmetry that is able to reproduce all SM properties. First, all representations of $\mathcal{G}_{\mathrm{cust}}$ including some SM fermions are promoted to be complete representations by introducing appropriate spurion (unphysical) fields that are set to zero in physical processes (Elias-Miró *et al.*, 2013a). Second, $\mathrm{SU}(2)_R$-breaking terms in the Yukawa couplings, such as the one responsible for the top-bottom splitting when t_R and b_R are embedded in the same $\mathrm{SU}(2)_R$ multiplet, are also promoted as spurion fields (Isidori, 2010). Finally, spurion gauge bosons are also introduced so that the entire group $\mathcal{G}_{\mathrm{cust}}$ is formally gauged, and the SM is recovered as the limit obtained by setting the spurion fields to zero (Gonzalez-Alonso *et al.*, 2015). The consequences of these hypotheses for various subsets of SMEFT operators (or physical amplitudes evaluated at $d = 6$ in the SMEFT) were discussed by Contino *et al.* (2013), Elias-Miró *et al.* (2013a), and Gonzalez-Alonso *et al.* (2015).

IV. NONLINEAR REALIZATION OF ELECTROWEAK SYMMETRY BREAKING

Within the SM, the spontaneous breaking of electroweak symmetry occurs through the nonvanishing vacuum expectation value of the $\mathrm{SU}(2)_L$-doublet scalar H. Expanding around the minimum of H as in Eq. (1.7), one identifies the massive field with h and the three Goldstone bosons with $\varphi_{1,2,3}$. From measurements of various electroweak observables and high-energy processes, the existence of the three Goldstone bosons and the massive scalar h is well established. However, it is not yet evident that they are necessarily embedded in the four components of a single $\mathrm{SU}(2)_L$-doublet H, as in Eq. (1.7). We refer to this embedding as the linear realization of the electroweak symmetry-breaking mechanism. As we soon discuss, in principle other embeddings are still viable.

The inclusion of the scalar state h in the theory and the relations among the different couplings provided by embedding h and the three $\varphi_{1,2,3}$ in the doublet H are essential to ensuring the unitarity of scattering amplitudes for longitudinally polarized electroweak gauge bosons at high energies. However, within an EFT approach the loss of unitarity is not a problem as long as it happens above the cutoff scale of the theory; see Brivio and Trott (2019). As a consequence, in a general EFT approach to physics beyond the SM we are allowed to relax the strict constraints following from the linear embedding of h and the three $\varphi_{1,2,3}$ in H and consider a more general structure.

To this end, we employ the Callan-Coleman-Wess-Zumino (CCWZ) formalism (Callan *et al.*, 1969; Coleman, Wess, and Zumino, 1969) and proceed as with the construction of chiral perturbation theory. In other words, we construct an EFT with a nonlinear realization of the electroweak symmetry-breaking mechanism. To make contact with the SM Lagrangian, we can decompose the matrix field Σ introduced in Eq. (3.18) as

$$\Sigma(x) = \frac{v + \hat{h}(x)}{\sqrt{2}} U(x), \quad \text{with } U(x) = \exp\left(i \frac{\boldsymbol{\tau} \cdot \boldsymbol{\pi}(x)}{v}\right), \tag{4.1}$$

where we introduce the unitary dimensionless field $U(x)$ and $\boldsymbol{\tau}$ denotes the three-vector of the Pauli matrices. The new fields $\hat{h}$ and $\boldsymbol{\pi} = (\pi_1, \pi_2, \pi_3)^\intercal$, where the latter are the counterpart of the pions in two-flavor QCD, are related to the original fields h and $\boldsymbol{\varphi}$ via a nonlinear field redefinition. We can still interpret

$\hat{h}$ as the physical Higgs boson and $\boldsymbol{\pi}$ as the vector containing the three Goldstone bosons. The fields transform under the custodial symmetry group (3.17) as

$$\hat{h}(x) \to \hat{h}(x), \qquad U(x) \to V_L U(x) V_R^\dagger. \tag{4.2}$$

Following the discussion of Appelquist and Bernard (1980), Longhitano (1980, 1981), Appelquist and Bernard (1981), Feruglio (1993), Grinstein and Trott (2007), and Stoffer (2023) and substituting Eq. (4.1) into Eq. (3.19), we can express the scalar part of the SM Lagrangian, including the interactions with the weak gauge bosons, as

$$\begin{aligned}\mathcal{L}_{p^2}^{\text{scalar}} &= \tfrac{1}{2}(\partial_\mu \hat{h})(\partial^\mu \hat{h}) - \tfrac{1}{2} m_h^2 \hat{h}^2 \\ &\quad + \frac{v^2}{4} \mathcal{F}\left(\frac{\hat{h}}{v}\right) \mathrm{tr}[(D_\mu U)^\dagger (D^\mu U)] - V\left(\frac{\hat{h}}{v}\right),\end{aligned} \tag{4.3}$$

with the mass $m_h^2 = 2m^2 = \lambda v^2$ of the physical Higgs boson $\hat{h}$ and where we define

$$\mathcal{F}\left(\frac{\hat{h}}{v}\right) = \left(1 + \frac{\hat{h}}{v}\right)^2, \tag{4.4}$$

$$V\left(\frac{\hat{h}}{v}\right) = v^4 \left[\frac{m_h^2}{2v^2}\left(\frac{\hat{h}}{v}\right)^3 + \frac{m_h^2}{8v^2}\left(\frac{\hat{h}}{v}\right)^4\right]. \tag{4.5}$$

We now have a nonlinear formulation of the custodial symmetry breaking that is in close analogy to chiral perturbation theory, with the only difference being the presence of the additional singlet state $\hat{h}$. To write Eq. (4.3), we promoted the global custodial symmetry to a local one by introducing two 2×2 matrix spurion fields $\hat{W}_\mu$ and $\hat{B}_\mu$ as the gauge bosons of the chiral $\mathrm{SU}(2)_L$ and $\mathrm{SU}(2)_R$ groups, respectively. These fields must transform in the adjoint representation of the chiral groups[20] to make Eq. (4.3) formally invariant. The covariant derivative then reads

$$D_\mu U = \partial_\mu U - i\hat{W}_\mu U + iU\hat{B}_\mu, \tag{4.6}$$

and we obtain the SM case by fixing the spurions to

$$\hat{W}_\mu \to g_2 \frac{\tau^I}{2} W_\mu^I, \qquad \hat{B}_\mu \to g_1 \frac{\tau^3}{2} B_\mu, \tag{4.7}$$

where W_μ and B_μ are the weak gauge bosons of the SM. This breaks the chiral symmetry down to its gauged SM subgroup

$$\mathrm{SU}(2)_L \times \mathrm{SU}(2)_R \to \mathrm{SU}(2)_L \times \mathrm{U}(1)_Y. \tag{4.8}$$

A. The Higgs effective field theory

After the fermion and gauge sectors are added to the chiral Lagrangian (Longhitano, 1980; Feruglio, 1993) as given in Eqs. (4.3)–(4.5), it is equivalent to the usual SM Lagrangian written in terms of the Higgs doublet H shown in Eq. (1.3). The two Lagrangians are related via the nonlinear field redefinition (4.1), which leaves the physical observables invariant.

However, going beyond the SM, i.e., considering the EFT extension of Eq. (4.3), the equivalence between the linear and nonlinear realizations can be broken, as we soon discuss. Amending the Lagrangian (4.3) to an EFT, we can express the functions $\mathcal{F}$ and V as generic power series in their argument $\hat{h}/v$,

$$\mathcal{F}\left(\frac{\hat{h}}{v}\right) = 1 + \sum_{n=1}^{\infty} a_n \left(\frac{\hat{h}}{v}\right)^n, \tag{4.9}$$

$$V\left(\frac{\hat{h}}{v}\right) = v^4 \sum_{n=3}^{\infty} b_n \left(\frac{\hat{h}}{v}\right)^n, \tag{4.10}$$

where we reproduce the SM by choosing $a_1 = 2$, $a_2 = 1$, $b_3 = \lambda/2$, and $b_4 = \lambda/8$, with all other coefficients vanishing. Given that $\hat{h}$ is a singlet, in this generic EFT approach the coefficients a_n and b_n are free parameters that are not fixed by the symmetries of the theory and have to be determined experimentally. Since their determination requires the measurement of multi-Higgs processes, the current experimental constraints on these parameters are rather imprecise. Allowing for generic coefficients a_n and b_n is incompatible with the field redefinition (4.1) that we used to relate the chiral SM Lagrangian (4.3) to the linear one. In general, it is not possible to find a field redefinition that brings the generic nonlinear EFT case back to the linear one, while the reverse processes is always possible.

This statement implies that the EFT constructed from the chiral Lagrangian (4.3) is more general than the SMEFT, which is built under the assumption of a linear realization of the electroweak symmetry-breaking mechanism. This effective theory is known as the HEFT (Feruglio, 1993; Alonso *et al.*, 2013; Buchalla, Catà, and Krause, 2014; Pich *et al.*, 2017). The HEFT contains the SMEFT as the special case where a nonlinear field redefinition can be found to map the scalar components ($\hat{h}$ and $\pi_{1,2,3}$) into a single $\mathrm{SU}(2)_L$ doublet (H). For more details on distinguishing the SMEFT and the HEFT, see the discussion in Sec. IV.B, Falkowski and Rattazzi (2019), and Cohen *et al.* (2021). When the Yukawa interactions are added to the EFT, these can also be multiplied by an arbitrary power of $\hat{h}/v$, leading to an expansion of these similar to Eqs. (4.4) and (4.5). The NLO Lagrangian can be constructed in close analogy to chiral perturbation theory, with the only difference being the presence of the additional singlet $\hat{h}$, which allows every operator to be multiplied by a generic function of $\hat{h}/v$.

The HEFT is therefore a combination of the fermionic and gauge sectors of the SMEFT, with their power counting in the canonical mass dimension, and the scalar sector of chiral perturbation theory with a chiral power counting. The HEFT is based on the same gauge symmetry as the SMEFT and contains the same degrees of freedom apart from the Higgs doublet H, which is replaced by the scalar singlet $\hat{h}$ and the

[20]The transformation rules read $\hat{W}_\mu \to V_L \hat{W}_\mu V_L^\dagger + iV_L(\partial_\mu V_L)^\dagger$ and $\hat{B}_\mu \to V_R \hat{B}_\mu V_R^\dagger + iV_R(\partial_\mu V_R)^\dagger$.

Goldstone boson matrix U. This decorrelates the interactions of one or more $\hat{h}$ and the Goldstone bosons, therefore allowing more general BSM scenarios to be covered. A complication in the HEFT is that the matrix field U and $\hat{h}/v$ are adimensional: $[U] = [\hat{h}/v] = 1$. Therefore, the EFT series cannot be truncated according only to the canonical mass dimension as in the SMEFT case, but we also need to consider a chiral power counting, i.e., an expansion in the number of derivatives. This is possible since $U^\dagger U = \mathbb{1}$, and thus the field U must always be derivatively coupled, as is generically expected for Goldstone bosons. Owing to the mixture of the different countings, there is no unique way to define a consistent power counting for the HEFT, but a commonly used counting (Gavela *et al.*, 2016) is NDA; see Sec. II.B.1. This counting was employed for the construction of the NLO HEFT basis given by Brivio *et al.* (2016); see also Sun, Xiao, and Yu (2023a, 2023b). A discussion of the counting of the HEFT operators using the Hilbert series technique was given by Sun, Wang, and Yu (2022) and Gráf *et al.* (2023).

B. Geometric interpretation for the scalar sector

An interesting approach to better appreciate the difference between the SMEFT and the HEFT is the geometric interpretations of the scalar sectors of these EFTs, which we review in this section. This technique, initially developed in the context of nonlinear sigma models, has been extensively applied to analyzing the scalar sectors of the SMEFT and the HEFT (Alonso, Jenkins, and Manohar, 2016a, 2016b, 2016c; Helset, Paraskevas, and Trott, 2018; Helset, Martin, and Trott, 2020; Corbett, Helset, and Trott, 2020).

The starting point of the geometric formulation is the observation that, after spontaneous symmetry breaking, a tower of higher-dimensional operators collapses into a single composite operator form (Helset, Martin, and Trott, 2020). Consider the SMEFT[21] with the Higgs VEV defined by $v_T \equiv \sqrt{2\langle H^\dagger H\rangle}$. An example of the breakdown of a tower of higher-dimensional operators can be observed in the effective Yukawa interactions. The operators of interest are of the form $(H^\dagger H)^n(\bar{\psi}_L H\psi_R)$ for $n \in \mathbb{N}$. When the Higgs field acquires a VEV $\langle H^\dagger H\rangle \to v_T^2/2$, these higher-dimensional operators collapse into a number multiplying the effective SM Yukawa operator, as illustrated in Fig. 6. A similar breakdown of higher-dimensional operators is perceptible for other interactions as well. Thus, the interactions of all of the particles, including the physical Higgs h itself, can be thought of as taking place in a Higgs medium (Helset, Martin, and Trott, 2020). This medium can be described by a scalar field manifold $\mathcal{M}$ with coordinates defined by the scalar fields. The S matrix of the theory is invariant under scalar field redefinitions that in this case are equivalent to coordinate transformations on $\mathcal{M}$. These coordinate redefinitions also leave the geometry of the scalar manifold $\mathcal{M}$ invariant. Therefore, the S matrix (and thus all of the physical observables) depends only on the geometric properties of $\mathcal{M}$, but not on the choice of coordinates (Alonso, Jenkins, and Manohar, 2016c).

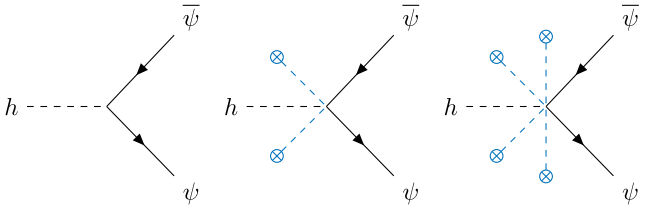

FIG. 6. Feynman diagrams contributing to the effective Yukawa interactions in the SMEFT after one takes the vacuum expectation value v_T, which is symbolized by the crossed dot $\otimes$ in the diagrams, by replacing $\langle H^\dagger H\rangle = v_T^2/2$.

The geometric formulation leads to a factorization of the EFT power counting expansions. In the SMEFT there are two distinct expansions that are often not properly distinguished. The first expansion (i) is in the ratio of the electroweak scale v_T to the new-physics scale Λ, whereas the second expansion (ii) is in the ratio of the kinematical scale p for the process of interest relative to the new-physics scale,

$$\text{(i)}: \frac{v_T}{\Lambda}, \qquad \text{(ii)}: \frac{p^2}{\Lambda^2},$$

where p^2 is a kinematic Lorentz invariant. In the geometric formulation, expansion (i) is largely factorized out, as it can be linked to the curvature of the scalar manifold, whereas (ii) is determined by the derivative expansion (Alonso, Jenkins, and Manohar, 2016c). This factorization of the power counting allows one to define the SM Lagrangian parameters to all orders in the SMEFT power counting, as shown by Helset, Martin, and Trott (2020).

The geometric interpretation of the SM is particularly simple. As seen in Sec. III.D, the scalar sector of the SM is invariant under a global O(4) symmetry, and the minimum of the scalar potential $V(\boldsymbol{\phi})$ defines a three-sphere S^3 with radius $v = \sqrt{\langle \boldsymbol{\phi}\cdot\boldsymbol{\phi}\rangle}$. Conventionally we align the VEV of $\boldsymbol{\phi}$ to its fourth component, i.e., $\langle\boldsymbol{\phi}\rangle = (0,0,0,v)^\intercal$. This triggers the breaking of the custodial symmetry group $\mathcal{G} = \mathrm{O}(4)$ down to the subgroup $\mathcal{H} = \mathrm{O}(3)$ acting on the first three components of $\boldsymbol{\phi}$. Expressing $\boldsymbol{\phi}$ in terms of the radial component h and the three Goldstone bosons as in Eq. (3.14), the scalar Lagrangian (3.13) assumes the form

$$\mathcal{L}_\varphi = \frac{1}{2}(D_\mu\boldsymbol{\varphi})\cdot(D_\mu\boldsymbol{\varphi}) + \frac{1}{2}(\partial_\mu h)^2 - \frac{\lambda}{8}(h^2 + 2hv + \boldsymbol{\varphi}\cdot\boldsymbol{\varphi})^2. \tag{4.11}$$

The real scalar fields φ^a with $a \in \{1,2,3\}$ transform in the vector representation of $\mathcal{H}$, whereas the physical Higgs h transforms as a singlet under $\mathcal{H}$. Together these four real scalar fields constitute coordinates in the scalar field space of the SM.

1. Geometric formulation of the SMEFT

The generic kinetic term for a scalar field Φ^i in a general scalar field space is

[21]Note that in general we have $v \neq v_T$ due to the presence of higher-dimensional operators in the scalar potential of the SMEFT, as we discuss in Sec. V.

$$\mathcal{L}_{\text{kin}} = \tfrac{1}{2} g_{ij}(\Phi)(D_\mu \Phi)^i (D_\mu \Phi)^j, \tag{4.12}$$

where $g_{ij}(\Phi)$ is the metric of the scalar field space. Comparing Eqs. (3.13) and (4.12) by choosing $\Phi^i = \phi^i$ and promoting partial to covariant derivatives, we find that $g_{ij}(\boldsymbol{\phi}) = \delta_{ij}$. Therefore, the scalar field manifold of the standard model is $\mathcal{M}_{\text{SM}} = \mathbb{R}^4$, i.e., the scalar field space is flat four-dimensional Euclidean space and the fields ϕ^i (with $i \in \{1,2,3,4\}$) or, equivalently, φ^a and h (with $a \in \{1,2,3\}$) define a Cartesian coordinate system on $\mathcal{M}_{\text{SM}}$, as shown at the top of Fig. 7. The black dot in the center represents $\boldsymbol{\phi} = \mathbf{0}$ or, equivalently, $H = 0$. The blue circle symbolizes the Goldstone boson vacuum manifold S^3 given by the coset space $\mathcal{G}/\mathcal{H}$. The dashed blue arrow points to the physical vacuum denoted by the green dot, where the Cartesian coordinate system is centered. The direction h is orthogonal to S^3 and φ^a are the remaining three directions orthogonal to h.

We have seen that the SM corresponds to the simple case of a flat four-dimensional scalar manifold. In the following we generalize our previous considerations by extending the SM by higher-dimensional operators and analyzing the geometric properties of the SMEFT. The scalar kinetic term in the SMEFT consists of all terms containing only Higgs doublets and exactly two derivatives acting on them. At dimension 6 in the Warsaw basis (Grzadkowski *et al.*, 2010), the term reads

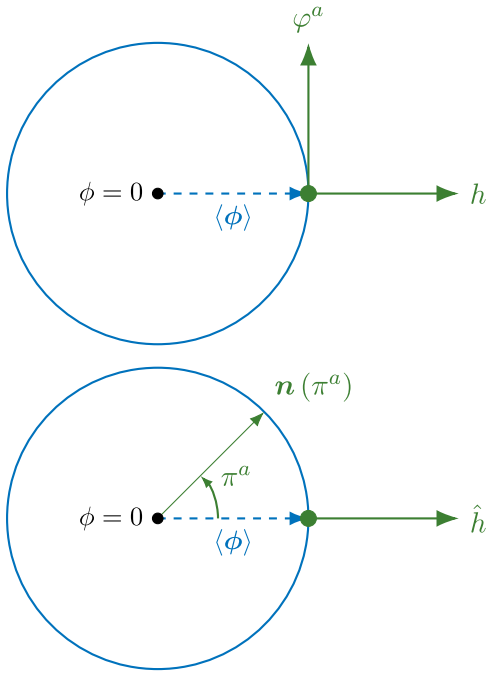

FIG. 7. Illustration of the SM flat scalar field manifold $\mathcal{M}_{\text{SM}} = \mathbb{R}^4$. The vacuum manifold $S^3 = \mathcal{G}/\mathcal{H}$ is represented by the blue circle with radius $\langle\phi\rangle = v$, the green dot on this circle represents the physical vacuum, and the solid green axes symbolize the scalar field coordinate system. In the top graphic the Cartesian coordinates $\{\varphi^1, \varphi^2, \varphi^3, h\}$ centered at the physical vacuum are chosen, whereas in the the bottom graphic polar coordinates $\{\pi^1, \pi^2, \pi^3, \hat{h}\}$ are used, where $\hat{h}$ is the radial coordinate and the three π^a form a vector $\boldsymbol{n}(\pi^a) \in S^3$. Adapted from Alonso, Jenkins, and Manohar, 2016c.

$$\begin{aligned}\mathcal{L}^{H,\text{kin}}_{\text{SMEFT}} &= (D_\mu H)^\dagger (D^\mu H) \\ &\quad + \frac{C_{HD}}{\Lambda^2}(H^\dagger D_\mu H)^*(H^\dagger D^\mu H) \\ &\quad + \frac{C_{H\Box}}{\Lambda^2}(H^\dagger H)\Box(H^\dagger H) + \mathcal{O}(\Lambda^{-4}).\end{aligned} \tag{4.13}$$

Using only $\text{SU}(2)_L \times \text{U}(1)_Y$ gauge invariance and the SU(2) Fierz identity in Eq. (2.21), it is straightforward to show that at higher powers only two different, independent operator structures can appear at each mass dimension,[22]

$$Q^{(8+2n)}_{H,\text{kin}} = (H^\dagger H)^{n+2}(D_\mu H)^\dagger (D^\mu H), \tag{4.14}$$

$$Q^{(8+2n)}_{HD} = (H^\dagger H)^{n+1}(H^\dagger D_\mu H)^*(H^\dagger D^\mu H). \tag{4.15}$$

Using Eq. (3.12), we can express $\mathcal{L}^{H,\text{kin}}_{\text{SMEFT}}$ (and these operators) in terms of the real scalar coordinates ϕ^i. The general expression for the kinetic term of the SMEFT in terms of the coordinates ϕ^i is given by[23]

$$\begin{aligned}\mathcal{L}^{\text{kin}}_{\text{SMEFT}} = \frac{1}{2}\Bigg[&A\left(\frac{\boldsymbol{\phi}\cdot\boldsymbol{\phi}}{\Lambda^2}\right)(D_\mu\boldsymbol{\phi})\cdot(D^\mu\boldsymbol{\phi}) \\ &+ B\left(\frac{\boldsymbol{\phi}\cdot\boldsymbol{\phi}}{\Lambda^2}\right)\frac{(D_\mu\phi)^i \mathfrak{f}_{ij}(\phi)(D_\mu\phi)^j}{\Lambda^2}\Bigg],\end{aligned} \tag{4.16}$$

where we have defined

$$\mathfrak{f}^{ij}(\phi) = \begin{pmatrix} a & 0 & b & c \\ 0 & a & c & -b \\ b & c & d & 0 \\ c & -b & 0 & d \end{pmatrix}, \qquad \begin{pmatrix} a \\ b \\ c \\ d \end{pmatrix} = \begin{pmatrix} (\phi^1)^2 + (\phi^2)^2 \\ \phi^1\phi^3 - \phi^2\phi^4 \\ \phi^1\phi^4 + \phi^2\phi^3 \\ (\phi^3)^2 + (\phi^4)^2 \end{pmatrix}. \tag{4.17}$$

Equation (4.17) is valid only for a specific choice of the operator basis. In Eq. (4.16) A and B are defined through a power series expansion in their argument $z \equiv (\boldsymbol{\phi}\cdot\boldsymbol{\phi})/\Lambda^2$, which simplifies to the usual EFT expansion in v_T^2/Λ^2 after spontaneous symmetry breaking. Since Eq. (4.17) has to reduce to the SM case in the limit $\Lambda \to \infty$, we must have $A(0) = 1$ and $B(0) = 0$. Making a comparison again to the general scalar kinetic term on a curved manifold in Eq. (4.12), we find the SMEFT scalar field-space metric

$$g_{ij}(\phi) = A\left(\frac{\boldsymbol{\phi}\cdot\boldsymbol{\phi}}{\Lambda^2}\right)\delta_{ij} + B\left(\frac{\boldsymbol{\phi}\cdot\boldsymbol{\phi}}{\Lambda^2}\right)\frac{\mathfrak{f}_{ij}(\phi)}{\Lambda^2}. \tag{4.18}$$

[22] See also Helset, Martin, and Trott (2020) and references therein. Note, however, that we use a different operator definition, and thus a different basis. The two bases differ only by a Fierz redefinition and thus reproduce the same metric.

[23] Similar expressions were given by Alonso, Jenkins, and Manohar (2016c) for the SMEFT in the custodial limit. Note, however, that the operator Q_{HD} breaks custodial symmetry. Therefore, the formulas presented here are more general.

Equation (4.18) describes in general a curved manifold $\mathcal{M}_{\text{SMEFT}}$, and only for $B = 0$ is the manifold flat. In the limit $\Lambda \to \infty$ we find that the SMEFT metric reduces to the SM metric in Cartesian coordinates

$$g_{ij}^{\text{SMEFT}}(\phi) \overset{\Lambda\to\infty}{\longrightarrow} \delta_{ij} = g_{ij}^{\text{SM}}. \tag{4.19}$$

Therefore, the curvature of $\mathcal{M}_{\text{SMEFT}}$ is determined entirely by the EFT expansion parameter v_T^2/Λ^2. Furthermore, we can deduce all kinds of geometric quantities, such as Christoffel symbols and Riemann curvature tensors.

Taking Eq. (4.13) we find the scalar metric of the SMEFT up to dimension 6 (Helset, Paraskevas, and Trott, 2018),

$$g_{ij}(\phi) = \delta_{ij} + \frac{C_{HD}}{2\Lambda^2}\mathfrak{f}_{ij}(\phi) - 2\frac{C_{H\Box}}{\Lambda^2}\phi_i\phi_j. \tag{4.20}$$

Note that the last term in Eq. (4.20) does not match the general form of the metric in Eq. (4.18). This is because the operator $Q_{H\Box}$ of the Warsaw basis does not agree with the definitions in Eqs. (4.14) and (4.15). It could be rewritten in that form using integration by parts identities. Apart from $Q_{H,\text{kin}}^{(6)}$, this would introduce further operators that have to be removed using field redefinitions.[24] The latter, however, change the scalar field-space metric. Thus, the last term in Eq. (4.20) could be removed in favor of a term proportional to δ_{ij}, but for consistency we stick with the Warsaw basis at dimension 6. In this example we see that the explicit form of the metric is basis dependent. However, a geometric formulation of the SMEFT exists in every basis (Helset, Martin, and Trott, 2020).

We can now use Eqs. (4.14) and (4.15) and our previous results to define the scalar field metric to all orders in the EFT power counting

$$\begin{aligned} g_{ij} = &\left[1 + \sum_{n=0}^{\infty}\left(\frac{\boldsymbol{\phi}\cdot\boldsymbol{\phi}}{2}\right)^{n+2}\frac{C_{H,\text{kin}}^{(8+2n)}}{\Lambda^{4+2n}}\right]\delta_{ij} \\ &+ \frac{1}{2}\left[C_{HD}^{(6)} + \sum_{n=0}^{\infty}\left(\frac{\boldsymbol{\phi}\cdot\boldsymbol{\phi}}{2}\right)^{n+1}\frac{C_{HD}^{(8+2n)}}{\Lambda^{4+2n}}\right]\mathfrak{f}_{ij}(\phi) \\ &- 2\frac{C_{H\Box}}{\Lambda^2}\phi_i\phi_j. \end{aligned} \tag{4.21}$$

This entails a choice of basis; nevertheless, it is noteworthy that we are able to define this geometric quantity to all orders in the EFT power counting.

The ideas discussed thus far in this section apply to the Higgs two-point function leading to the scalar field-space metric. Following Helset, Martin, and Trott (2020), we can generalize the concepts to higher n-point functions and other types of field connections by factorizing the operators in the SMEFT Lagrangian,

$$\mathcal{L}_{\text{SMEFT}} = \sum_n f_n(\mu, \alpha, \ldots)G_n(I, A, \ldots). \tag{4.22}$$

The factors f_n are composite operator forms containing all nonscalar fields and all dependence on spacetime indices, i.e., Lorentz $(\mu, \ldots)$ and spinor $(\alpha, \ldots)$ indices. The f_n can only depend on the scalar field coordinates through derivatives acting on the scalars, for example, $(D_\mu H)$. The factors G_n, however, depend on the nonspacetime group indices $(I, A, \ldots)$ and contain only scalar field coordinates and symmetry generators acting on them, i.e., expressions built only out of $H^{(\dagger)}$ and τ^I. It is evident that after electroweak symmetry breaking the G_n collapse to a number and an appropriate power of Higgs h emissions, largely factoring out the expansion in v_T^2/Λ^2 from the remaining composite operator form f_n, whereas the latter (f_n) contain the derivative expansion in p^2/Λ^2 and retain only a minimal dependence on the scalar coordinates and v_T mixing the two expansions (Helset, Martin, and Trott, 2020).

This allows us to define the scalar field metric

$$g_{ij}(\phi) = \frac{g^{\mu\nu}}{D}\frac{\delta^2\mathcal{L}_{\text{SMEFT}}}{\delta(D^\mu\phi)^i\delta(D^\nu\phi)^j}\bigg|_{f_n\to 0}. \tag{4.23}$$

Similarly, we can now define all sorts of field-space connections, for example, the Yukawa-type connection (Helset, Martin, and Trott, 2020) that we already encountered,

$$[\Upsilon_\psi]_{pr}(\phi_i) = \frac{\delta\mathcal{L}_{\text{SMEFT}}}{\delta(\bar\psi_p^{L,i}\psi_r^R)}\bigg|_{f_n\to 0}. \tag{4.24}$$

For this case we find $f_n = \bar\psi_p^{L,i}\psi_r^R$ containing the fermion bilinear and the factor $G_n \sim \sum_k (H^\dagger H)^k H_i$. Making a comparison to Fig. 6, we see that f_n corresponds to the fermion current, whereas the G_n corresponds to the emission of h and the VEV (marked by $\otimes$). The operators contributing to G_n at all orders in this case are (Helset, Martin, and Trott, 2020)

$$[Q_{\psi H}^{(6+2n)}]_{pr} = (H^\dagger H)^{n+1}(\bar\psi_p^{L,i}\psi_r^R H_i), \tag{4.25}$$

leading to the all-order Yukawa connection

$$\begin{aligned} [\Upsilon_\psi]_{pr}(\phi) = &-H(\phi)[Y_\psi]_{pr} \\ &+ H(\phi)\sum_{n=0}^{\infty}\frac{[C_{\psi H}^{(6+2n)}]_{pr}}{\Lambda^{2+2n}}\left(\frac{\boldsymbol{\phi}\cdot\boldsymbol{\phi}}{2}\right)^{n+1}. \end{aligned} \tag{4.26}$$

For more details and the definition of other field-space connections, as well as for more all-order results, see Helset, Martin, and Trott (2020). The key advantage of this formulation is the reduction of the number of relevant structures, especially when one goes beyond dimension 6 and obtains all-order results (or, better, results independent of the operator power counting) for a series of relevant quantities, such as the physical fermion masses.

[24]The replacement reads $Q_{H\Box} = 2Q_{H,\text{kin}}^{(6)} + \cdots$, where the ellipsis denotes terms that do not contribute to the metric after the appropriate redefinition of the Higgs field H is applied.

2. Geometric formulation of the HEFT

Thus far we have used Cartesian coordinates to describe the scalar field manifold $\mathcal{M}$. We could alternatively choose polar coordinates on $\mathcal{M}$ since any given measurable quantity does not depend on the choice of the coordinate system. Following Alonso, Jenkins, and Manohar (2016c), we can use polar coordinates to write the real scalar fields as

$$\boldsymbol{\phi} = (v + \hat{h})\boldsymbol{n}(\pi), \tag{4.27}$$

where $\boldsymbol{n}(\pi) \in S^3 \sim \mathcal{G}/\mathcal{H}$, with the radial coordinate $\hat{h}$ and the three angular coordinates π^a/v associated with the Goldstone bosons of the broken generators. The three angular coordinates π^a form a four-dimensional unit vector $\boldsymbol{n}(\pi^a) \in S^3$. The polar coordinate system is shown in the bottom graphic of Fig. 7. In the polar coordinate parametrization (4.27), there is no obvious relation between the physical Higgs field $\hat{h}$ and the Goldstone bosons in $\boldsymbol{n}$, unlike in the case of Cartesian coordinates in Eq. (3.14), where such a relation is implicit as h and φ^a transform together in the vector representation of $\mathcal{G} = \mathrm{O}(4)$ as $\boldsymbol{\phi} \to O\boldsymbol{\phi}$, with $O \in \mathcal{G}$.

The transformation properties of the coordinates under the chiral symmetry group $\mathcal{G}$ are

$$\hat{h} \xrightarrow{\mathcal{G}} \hat{h}, \qquad \boldsymbol{n} \xrightarrow{\mathcal{G}} O\boldsymbol{n}, \quad \text{with } O \in \mathcal{G}. \tag{4.28}$$

The field $\hat{h}$ is a singlet, whereas $\boldsymbol{n}$ transforms linearly under $\mathcal{G}$. However, owing to the constraint $\boldsymbol{n} \cdot \boldsymbol{n} = 1$, this four-component vector has only the three independent components π^a with $a \in \{1, 2, 3\}$. Therefore, π^a do not transform linearly under $\mathcal{G}$, which is why this choice of coordinates is called the nonlinear representation.[25] Possible parametrizations are the square root parametrization $\boldsymbol{n}(\pi) = (\pi^1, \pi^2, \pi^3, \sqrt{v^2 - \boldsymbol{\pi}\cdot\boldsymbol{\pi}})^{\mathsf{T}}/v$ and the exponential representation

$$\begin{aligned}\boldsymbol{n}(\pi) &= \exp\left(\frac{1}{v}\begin{bmatrix} 0 & 0 & 0 & \pi^1 \\ 0 & 0 & 0 & \pi^2 \\ 0 & 0 & 0 & \pi^3 \\ -\pi^1 & -\pi^2 & -\pi^3 & 0 \end{bmatrix}\right)\begin{pmatrix} 0 \\ 0 \\ 0 \\ 1 \end{pmatrix} \\ &= \begin{pmatrix} \sin\left(\frac{|\boldsymbol{\pi}|}{v}\right)\frac{\pi^1}{|\boldsymbol{\pi}|} \\ \sin\left(\frac{|\boldsymbol{\pi}|}{v}\right)\frac{\pi^2}{|\boldsymbol{\pi}|} \\ \sin\left(\frac{|\boldsymbol{\pi}|}{v}\right)\frac{\pi^3}{|\boldsymbol{\pi}|} \\ \cos\left(\frac{|\boldsymbol{\pi}|}{v}\right) \end{pmatrix},\end{aligned} \tag{4.29}$$

where $|\boldsymbol{\pi}| = \sqrt{\boldsymbol{\pi}\cdot\boldsymbol{\pi}}$. The latter corresponds to the standard coordinates of CCWZ (Alonso, Jenkins, and Manohar, 2016c). However, we do not pick any explicit parametrizations here.

[25]Unlike in Eq. (4.1), we use the vector notation with the field $\boldsymbol{n}$ here rather than the matrix notation with the field U. Nevertheless, the two formulations are completely equivalent.

Using Eq. (4.27) to express the scalar part of the SM Lagrangian (3.13) in polar coordinates yields

$$\mathcal{L} = \tfrac{1}{2}(v + \hat{h})^2 (D_\mu \boldsymbol{n}) \cdot (D^\mu \boldsymbol{n}) + \tfrac{1}{2}(\partial_\mu \hat{h})(\partial^\mu \hat{h}) - \frac{\lambda}{8}(\hat{h}^2 + 2v\hat{h})^2, \tag{4.30}$$

where the Goldstone bosons of $\boldsymbol{n}$ are only derivatively coupled and the potential is independent of the angular coordinates π^a, unlike in the case of Cartesian coordinates in Eq. (4.11). Instead of changing the coordinate system on the scalar field manifold $\mathcal{M}$, we could alternatively compose a field redefinition. Using Eqs. (3.14) and (4.27), we find that $(v + h)^2 + \boldsymbol{\varphi}\cdot\boldsymbol{\varphi} = (v + \hat{h})^2$, which yields

$$\hat{h} = h + \frac{\boldsymbol{\varphi}\cdot\boldsymbol{\varphi}}{2v} - \frac{h}{2}\frac{\boldsymbol{\varphi}\cdot\boldsymbol{\varphi}}{v^2} + \mathcal{O}(v^{-3}), \tag{4.31}$$

where h and $\hat{h}$ are the Higgs fields in Cartesian and polar coordinates, respectively.

As discussed, in the Cartesian coordinate system the Higgs field in Eq. (3.12) or the corresponding real scalar fields $\boldsymbol{\phi}$ in Eq. (3.14) transform linearly under $\mathcal{G}$ or the electroweak symmetry group. On the contrary, in the polar coordinate system the scalar fields $\boldsymbol{\pi}$ do not transform linearly. However, physical observables must be independent of the choice of coordinates and, therefore, the SM Lagrangians in Eqs. (4.30) and (4.11) are equivalent, as they differ only by a coordinate redefinition. The question as to whether the Higgs transforms linearly or nonlinearly under the electroweak symmetry group thus depends on the choice of coordinate system and is therefore unphysical (Alonso, Jenkins, and Manohar, 2016c). The appropriate question is whether it is always possible to pick a coordinate system in which the Higgs field transforms linearly. As we have seen, this is true for the SM, but as we later discuss this is not possible in general for all EFT extensions of the SM.

In fact, it is possible if and only if the scalar field manifold $\mathcal{M}$ has a $\mathcal{G}$ invariant fixed point (Alonso, Jenkins, and Manohar, 2016c). In a neighborhood of this fixed point, it is then possible to pick a coordinate system in which the Higgs field transforms linearly under O(4). For the SM, this fixed point is the origin $\boldsymbol{\phi} = \boldsymbol{0}$ (black central dot), as can be seen in both parts of Fig. 7.

We saw in Sec. IV.B.1 that the SMEFT is the extension of the SM with higher-dimensional operators using Cartesian coordinates on $\mathcal{M}$. The Higgs field H transforms linearly under $\mathcal{G}$ or the electroweak gauge group and the SMEFT has a $\mathcal{G} = \mathrm{O}(4)$ fixed point at the origin $\boldsymbol{\phi} = \boldsymbol{0}$. On the contrary, the HEFT is the EFT extension of the SM using polar coordinates on the scalar field manifold $\mathcal{M}_{\mathrm{HEFT}}$. The corresponding scalar part of the HEFT Lagrangian is a generalization of Eq. (4.30) that is given by

$$\mathcal{L}_{\mathrm{HEFT}} = \tfrac{1}{2}v^2 F(\hat{h})^2 (D_\mu \boldsymbol{n}) \cdot (D^\mu \boldsymbol{n}) + \tfrac{1}{2}(\partial_\mu \hat{h})(\partial^\mu \hat{h}) - V(\hat{h}), \tag{4.32}$$

where $V(\hat{h})$ is the scalar potential that depends only on the radial coordinate $\hat{h}$ and $F(\hat{h})$ is a generic dimensionless

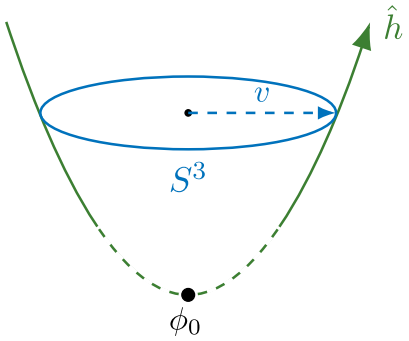

FIG. 8. The scalar field manifold $\mathcal{M}_{\rm HEFT}$ of the HEFT is fibered with a three-sphere S^3 of radius $vF(\hat{h})$ for every $\hat{h}$. An O(4) fixed point ϕ_0 does only exist if there is a value $\hat{h}_*$ such that the radius of the three-sphere vanishes $[F(\hat{h}_*)=0]$. If no fixed point ϕ_0 exists, the green dashed region does not exist and the manifold might either be smoothly connected without a fixed point or extend to infinity. The SMEFT corresponds to the theories with an O(4) fixed point at $\phi_0=0$. For this type of theory it is possible to change from polar coordinates to Cartesian coordinates, and vice versa, in a neighborhood of the fixed point. Adapted from Alonso, Jenkins, and Manohar, 2016c.

function that is defined by a power expansion in $\hat{h}/v$ with $F(0)=1$, such that the radius of the vacuum manifold is fixed by v (Alonso, Jenkins, and Manohar, 2016c). The $\mathcal{G}$ transformation rules for the fields $\hat{h}$ and $\boldsymbol{n}$ are the same as in Eq. (4.28). We can write

$$F(\hat{h}) = 1 + c_1\left(\frac{\hat{h}}{v}\right) + c_2\left(\frac{\hat{h}}{v}\right)^2 + \cdots \tag{4.33}$$

and, as stated in Sec. IV.A, we recover the SM case $F_{\rm SM}(\hat{h}) = 1+\hat{h}/v$ for $c_1=1$ and $c_{n\geq 2}=0$.

Defining the HEFT scalar field-space metric as in Eq. (4.12) by choosing $\Phi=(\pi^1,\pi^2,\pi^3,\hat{h})^\intercal$, we find that (Alonso, Jenkins, and Manohar, 2016a)

$$g_{ij}^{\rm HEFT}(\phi) = \begin{pmatrix} F(\hat{h})g_{ab}(\pi) & 0 \\ 0 & 1 \end{pmatrix}_{ij}, \tag{4.34}$$

where g_{ab} is the $\mathcal{H}=\mathrm{O}(3)$ invariant metric on the coset space $S^3=\mathcal{G}/\mathcal{H}$ for the angular coordinates $\boldsymbol{\pi}$.

The scalar field manifold $\mathcal{M}_{\rm HEFT}$ for HEFT is shown in Fig. 8. The manifold consists of $\hat{h}$ (green arrow) and a sequence of three-spheres (S^3) of radius $vF(\hat{h})$ fibered over any value of $\hat{h}$ (the blue circle symbolizes the sphere for a specific value of $\hat{h}$). From Eq. (4.28) we know that $\mathcal{G}$ acts on any point $\boldsymbol{n}\in S^3$ by rotations on the surface of S^3, i.e., rotations along the blue circle. Therefore, it is possible to have a $\mathcal{G}=\mathrm{O}(4)$ invariant fixed point only if the radius of the vacuum sphere is vanishing, meaning that there is an $\hat{h}_*$ for which we have $F(\hat{h}_*)=0$. In the SM this is the case for $\hat{h}_*^{\rm SM}=-v$. However, such a value $\hat{h}_*$ does not exist in general, as can be seen in the example $F(\hat{h})=e^{\hat{h}/v}\cosh(1+\hat{h}/v)$, which is nonvanishing for all $\hat{h}$ (Alonso, Jenkins, and Manohar, 2016c). In this case the green dashed range of $\hat{h}$ in Fig. 8 does not exist.

In summary, we found that the most general EFT extension of the SM is the HEFT using polar coordinates on the scalar field manifold. In this framework the Goldstone bosons transform nonlinearly under the electroweak symmetry group or the larger custodial symmetry group $\mathcal{G}=\mathrm{O}(4)$. The subcategory of EFTs that have a $\mathcal{G}$ fixed point at the origin belong to the SMEFT class. For these theories it is possible to pick coordinates around this fixed point in which the Higgs field transforms linearly. Eventually the SM becomes a subcategory of SMEFT with a flat scalar field manifold $\mathcal{M}_{\rm SM}=\mathbb{R}^4$. We can therefore schematically write

$$\text{SM} \subseteq \text{SMEFT} \subseteq \text{HEFT}. \tag{4.35}$$

Given Eq. (4.35), the past few years have seen intense activity in identifying concrete examples of UV models that cannot be well described by the SMEFT. As pointed out by Cohen *et al.* (2021), this can happen under the following two conditions: (i) when non-SM particles that acquire mass via electroweak symmetry breaking are integrated out, introducing nonanalytic dependence from the Higgs field in the corresponding EFT (Falkowski and Rattazzi, 2019) and (ii) when additional sources of electroweak symmetry breaking besides a single scalar doublet are present.[26] These two conditions signal that the O(4) fixed point in the scalar manifold is not the most convergent choice as origin for a Taylor expansion and that the cutoff of the effective theory is necessarily low, in fact below $4\pi v$ (Alonso and West, 2022; Banta *et al.*, 2022). Depending on how these two conditions are realized (in terms of masses and couplings of the new states), the SMEFT represents a good or bad description of the underlying theory. An instructive comparison of the SMEFT and the HEFT for a concrete UV model was given by Buchalla *et al.* (2017).

On general grounds, a breakdown of the SMEFT description happens only if the non-SM states that have been integrated out, which are connected to the mechanism of electroweak symmetry breaking (either as sources of the breaking or because they acquire mass via this breaking), are sufficiently close to the electroweak scale (Banta *et al.*, 2022). No indication of such states is present in current high-energy data.

At low energies, a pragmatic way to distinguish the two EFTs is by looking at transition amplitudes with identical electroweak and flavor structures that differ only by the number of massive Higgs fields (Brivio *et al.*, 2014; Isidori, Manohar, and Trott, 2014; Isidori and Trott, 2014). In the SMEFT, the linear realization implies a well-defined relation among all these processes at a given order in the EFT expansion. This relation can be broken at higher orders; however, the effect is expected to be small based upon power counting. On the contrary, in the HEFT the $F(\hat{h})$ function and its analog for other electroweak structures lead to a potentially complete decoupling among processes with different numbers of Higgs fields. A particularly interesting study case is provided by nonuniversal corrections to the $Z\to f\bar{f}$

[26] An example was mentioned previously (Manohar, 2018).

couplings (Isidori and Trott, 2014). Measurements at the Z pole imply small deviations from the SM, implying strong bounds on several operators in class 7 of Table II that control these effects. Within the SMEFT, this implies in turn small deviations from the SM in the related processes $h \to Zf\bar{f}$ and $f\bar{f} \to Zh$. A large deviation from the SM in the latter processes could occur naturally in the HEFT, while it would imply a breakdown of the SMEFT power counting.

V. LOW-ENERGY EFFECTIVE FIELD THEORY

A. Introduction and overview

The success of the SM rests to a large degree on tests in low-energy processes such as decays of kaons and D mesons, and even more on B physics, because these processes can be calculated with high precision.[27] The tool for this is the so-called LEFT,[28] which is derived from the SM by integrating out the Higgs boson (h), the weak gauge bosons ($\mathcal{Z}$ and $\mathcal{W}$), and the top quark (t_L and t_R). This is a generalization of the original Fermi theory with the four-fermion interaction

$$-\frac{4G_F}{\sqrt{2}}(\bar{\psi}\gamma_\mu\psi)(\bar{\psi}\gamma^\mu\psi), \tag{5.1}$$

where the Fermi constant G_F is related to the vacuum expectation value v by $G_F = 1/\sqrt{2}v^2$. The method works so well because the relevant energies E are much smaller than v or m_W (and thus smaller than Λ) and the asymptotic freedom of the strong interactions. Since the pioneering work in the mid 1970s, this theory has been developed to an astonishing degree of precision by including all kinds of strong and electromagnetic corrections; see Buras (2020) for a recent review.

The LEFT is thus an $\mathrm{SU}(3)_c \times \mathrm{U}(1)_e$ invariant effective theory valid below the electroweak symmetry-breaking scale containing five quark flavors (u, d, s, c, b), three charged leptons (e, μ, τ), three left-handed neutrinos $(\nu_e, \nu_\mu, \nu_\tau)$, the gluons, and the photon. The LEFT Lagrangian is the sum of the Lagrangians of QCD and QED of these particles and the mass terms of the fermions

$$\begin{aligned}\mathcal{L}_{\mathrm{SM}}^{\mathrm{broken}} = &-\frac{1}{4}F_{\mu\nu}F^{\mu\nu} - \frac{1}{4}G^A_{\mu\nu}G^{A\mu\nu} - \theta_3\frac{g_3^2}{32\pi^2}G^A_{\mu\nu}\tilde{G}^{A\mu\nu} \\ &+ \sum_{\psi=u,d,e,\nu_L}\sum_{X=L,R}(\bar{\psi}^X_p i\not{D}\psi^X_p) \\ &- \left[\sum_{\psi=u,d,e}[\mathcal{M}_\psi]_{pr}(\bar{\psi}^L_p\psi^R_r) + \mathrm{H.c.}\right]\end{aligned} \tag{5.2}$$

and a series of higher-dimensional operators $(\mathcal{Q})$ that is made precise later,

$$\mathcal{L}_{\mathrm{LEFT}} = \mathcal{L}_{\mathrm{SM}}^{\mathrm{broken}} + \mathcal{L}_{\mathrm{EFT}}, \tag{5.3}$$

$$\mathcal{L}_{\mathrm{EFT}} = \sum_{n=-1}^{\infty}\sum_i \frac{\mathcal{C}_i^{(n)}(\mu)}{v^n}\mathcal{Q}_i^{(n)}(\mu), \tag{5.4}$$

arising from the interactions with the heavy particles that were integrated out. The best-known operator is the four-fermion operator in Eq. (5.1). In Eq. (5.2) the flavor indices p and r run over the values 1, 2, and 3 for $\psi = d$, e, and ν and over 1 and 2 for $\psi = u$. These operators are organized by their dimension, starting with terms of dimension 3, and increasing powers of $1/v$ (often expressed using the Fermi constant G_F). Sometimes $m_W = \mathcal{O}(1) \times v$ is instead used as expansion parameter. In a SMEFT theory, there is an additional expansion in powers of $1/\Lambda = 1/v \times (v/\Lambda)$, and therefore more operators than in the SM. The LEFT Wilson coefficients $\mathcal{C}(\mu)$ multiplying the operators depend on the renormalization scale μ. As a rule, the renormalization scale should be chosen near the physically relevant energy in order to avoid additional large corrections in matrix elements of the operators. However, the Wilson coefficients $\mathcal{C}(v)$ from the matching to the underlying model, be it the SM or the SMEFT, are given at the weak scale $\mu \approx m_W$. The connection between the two scales is realized by the renormalization group and the running of the $\mathcal{C}(\mu)$ described by the renormalization group equation

$$\dot{\mathcal{C}} = 16\pi^2\mu\frac{\mathrm{d}}{\mathrm{d}\mu}\mathcal{C} = \beta_{\mathcal{C}}, \tag{5.5}$$

where $\beta_{\mathcal{C}}$ is the beta function of the coefficient $\mathcal{C}$. This implies that the Wilson coefficients can pick up large logarithmic correction of the form $\log(m_b/m_W)$. Furthermore, the running of the Wilson coefficients of lower-dimensional operators can be proportional to the coefficients of higher-dimensional operators due to the presence of light scales and masses in the theory.

As mentioned, much work has been done in developing the LEFT from the SM. If the underlying theory is the SMEFT rather than the SM, we need to match the Wilson coefficients of the LEFT to the coefficients in the SMEFT. We have to do this matching in the broken phase of the SMEFT, in the same way that we do for the SM. This implies that additional terms suppressed by appropriate powers of $1/\Lambda$ must be added in the matching equations for the LEFT coefficients at the scale m_W.

B. Electroweak symmetry breaking in the SMEFT

The Lagrangian for the SMEFT in the *unbroken phase*, i.e., above the electroweak symmetry-breaking (EWSB) scale $\sim v$, was discussed in Sec. I.D. We now consider EWSB in the SMEFT by determining the Lagrangian in the *broken phase*. We especially emphasize how EWSB is altered compared to the SM due to the presence of additional higher-dimensional operators, which modify the definition of several SM parameters at tree level. For this, we follow the discussions presented by Alonso, Jenkins *et al.* (2014) and Jenkins, Manohar, and Stoffer (2018b).

1. The Higgs sector

In the scalar sector both the Higgs kinetic term and the scalar potential are modified in the SMEFT and read

[27] See Buchalla, Buras, and Lautenbacher (1996) for an early review.

[28] Sometimes this theory is also called the weak effective theory.

$$\mathcal{L}_H = (D_\mu H)^\dagger (D^\mu H) + m^2 H^\dagger H - \frac{\lambda}{2}(H^\dagger H)^2 + \frac{C_{H\Box}}{\Lambda^2}(H^\dagger H)\Box(H^\dagger H) + \frac{C_{HD}}{\Lambda^2}(H^\dagger D_\mu H)^*(H^\dagger D_\mu H) + \frac{C_H}{\Lambda^2}(H^\dagger H)^3 + \mathcal{O}(\Lambda^{-4}). \tag{5.6}$$

In unitary gauge we can write the Higgs doublet as

$$H = \frac{1}{\sqrt{2}}\begin{pmatrix} 0 \\ [1 + c_{H,\mathrm{kin}}]h + v_T \end{pmatrix}, \tag{5.7}$$

where

$$c_{H,\mathrm{kin}} \equiv \left(C_{H\Box} - \frac{1}{4}C_{HD}\right)\frac{v^2}{\Lambda^2}, \quad v_T \equiv \left(1 + \frac{3C_H}{4\lambda}\frac{v^2}{\Lambda^2}\right)v. \tag{5.8}$$

In Eqs. (5.7) and (5.8) $c_{H,\mathrm{kin}}$ guarantees a canonical normalization of the kinetic term of the physical real Higgs h and v_T is the vacuum expectation value of the complex Higgs doublet H in the SMEFT, whereas $v = \sqrt{2m^2/\lambda}$ is the VEV of H in the SM.[29] Substituting Eqs. (5.7) and (5.8) into Eq. (5.6) we find all self-interactions of the physical Higgs h. For example, its mass term m_h, which is defined by $\mathcal{L}_h \supset \frac{1}{2}m_h^2 h^2$, reads

$$m_h^2 = \lambda v_T^2\left(1 - \frac{3C_H}{\lambda}\frac{v^2}{\Lambda^2} + 2c_{H,\mathrm{kin}}\right). \tag{5.9}$$

All masses and couplings of the particles are modified in a similar manner. This concerns the fermions and their Yukawa couplings as well as the masses and couplings of the gauge bosons, which are modified by similar shifts.

2. The Yukawa sector

The fermion masses and Yukawa couplings in the broken phase

$$\mathcal{L}_{\mathrm{Yukawa}}^{\mathrm{broken}} = -[\mathcal{M}_\psi]_{pr}(\bar\psi_p^L \psi_r^R) - [\mathcal{Y}_{\psi h}]_{pr}(\bar\psi_p^L \psi_r^R)h + \mathrm{H.c.} \tag{5.10}$$

are determined by the parameters Y_ψ and $C_{\psi H}$ through

$$[\mathcal{M}_\psi]_{pr} = \frac{v_T}{\sqrt{2}}\left([Y_\psi]_{pr} - \frac{1}{2}\frac{v^2}{\Lambda^2}[C_{\psi H}]_{pr}\right), \tag{5.11}$$

$$[\mathcal{Y}_{\psi h}]_{pr} = \frac{1}{\sqrt{2}}\left((1 + c_{H,\mathrm{kin}})[Y_\psi]_{pr} - \frac{3}{2}\frac{v^2}{\Lambda^2}[C_{\psi H}]_{pr}\right) \tag{5.12}$$

for $\psi \in \{u, d, e\}$. Note that unlike in the SM the Yukawa matrices $\mathcal{Y}_{\psi h}$ are no longer proportional to the mass matrices $\mathcal{M}_\psi$. Therefore, the two cannot be diagonalized simultaneously in general,[30] and hence, when working in the mass basis, the Higgs boson h will have flavor-violating couplings starting at $\mathcal{O}(\Lambda^{-2})$ (Alonso, Jenkins *et al.*, 2014).

Similarly, the $d = 5$ Weinberg operator (2.2) of the SMEFT yields a neutrino Majorana-mass matrix in the LEFT

$$\mathcal{L} \supset -\tfrac{1}{2}[\mathcal{M}_\nu]_{pr}(\bar\nu_p^{L\,c}\nu_r^L) + \mathrm{H.c.}, \tag{5.13}$$

where $[\mathcal{M}_\nu]_{pr} = -[C_{\mathrm{Weinberg}}]_{pr}v_T^2/\Lambda_{\not L}$. Here $\Lambda_{\not L}$ denotes the new-physics scale of the Weinberg operator, where lepton number is violated by $\Delta L = 2$. As mentioned, this scale is not necessarily related to the new-physics scale Λ of other operators and is known to be high [$\Lambda_{\not L} \gtrsim 10^{13}$ GeV for an $\mathcal{O}(1)$ coefficient C_{Weinberg}], which explains the small neutrino masses being of the order of $\sim$1 eV. Note that $[\mathcal{M}_\nu]_{pr}$ is symmetric in the flavor indices p and r, and that this is the only dimension-3 operator present in the LEFT.

In general, the mass matrices $\mathcal{M}_\psi$ for $\psi \in \{\nu, e, u, d\}$ are nondiagonal. To go to the mass basis we need to diagonalize them by unitary rotations $U_{\psi_{L/R}}$ of the fermion fields $\psi_{L/R} \to U_{\psi_{L/R}}\psi_{L/R}$, such that

$$U_{\psi_L}^\dagger \mathcal{M}_\psi U_{\psi_R} \equiv \mathrm{diag}(m_{\psi_1}, m_{\psi_2}, m_{\psi_3}). \tag{5.14}$$

In general we have $U_{d_L} \neq U_{u_L}$ and $U_{e_L} \neq U_{\nu_L}$ leading to the CKM and Pontecorvo-Maki-Nakagawa-Sakata (PMNS) matrices, respectively,

$$V_{\mathrm{CKM}} = U_{u_L}^\dagger U_{d_L}, \qquad V_{\mathrm{PMNS}} = U_{e_L}^\dagger U_{\nu_L}, \tag{5.15}$$

which contribute to charged-current interactions. In the SM it is conventional to align the mass- and weak-eigenstate bases in either the up sector ($U_{u_L} = \mathbb{1}$) or the down sector ($U_{d_L} = \mathbb{1}$). In the SM these two choices, and any other arbitrary alignment choices, are equivalent since the CKM matrix is the only source of flavor violation in the SM, and it is determined experimentally. On the contrary, in the SMEFT there are potentially other sources of flavor violation due to the higher-dimensional operators. Therefore, the alignment of mass and weak eigenstates is crucial, as different choices lead to different physics results for a given set of Wilson coefficients. For example, for a four-fermion operator we find that

$$[C]_{prst}(\bar\psi_{1,p}\Gamma\psi_{2,r})(\bar\psi_{3,s}\Gamma\psi_{4,t}) \downarrow [C]_{prst}[U_1^\dagger]_{p'p}[U_2]_{rr'}[U_3^\dagger]_{s's}[U_4]_{tt'}(\bar\psi_{1,p'}\Gamma\psi_{2,r'})(\bar\psi_{3,s'}\Gamma\psi_{4,t'}), \tag{5.16}$$

where Γ denotes a Dirac structure, possibly in combination with generators. We see that different alignment choices, i.e., different choices for the U_n matrices, lead to different results for the operators in the mass basis.

3. The gauge sector

The kinetic terms for the gauge bosons in the broken phase receive additional contributions from the operators Q_{HG}, Q_{HW}, Q_{HB}, and Q_{HWB}. To properly normalize the kinetic terms, we redefine the gauge fields and couplings as (Alonso, Jenkins *et al.*, 2014)

[29] Note that we have $v_T^2 = v^2 + \mathcal{O}(v^2/\Lambda^2)$, and thus, when working at dimension-6 level, we can always replace v_T with v when it is multiplied by a $d = 6$ operator.

[30] The two matrices also have different RG equations.

$$G_\mu^A = \mathcal{G}_\mu^A\left(1+\frac{v_T^2}{\Lambda^2}C_{HG}\right), \quad \bar{g}_3 = g_3\left(1+\frac{v_T^2}{\Lambda^2}C_{HG}\right), \tag{5.17}$$

$$W_\mu^I = \mathcal{W}_\mu^I\left(1+\frac{v_T^2}{\Lambda^2}C_{HW}\right), \quad \bar{g}_2 = g_2\left(1+\frac{v_T^2}{\Lambda^2}C_{HW}\right), \tag{5.18}$$

$$B_\mu = \mathcal{B}_\mu\left(1+\frac{v_T^2}{\Lambda^2}C_{HB}\right), \quad \bar{g}_1 = g_1\left(1+\frac{v_T^2}{\Lambda^2}C_{HB}\right) \tag{5.19}$$

such that their products are left invariant (for example, $g_2 W_\mu^I = \bar{g}_2 \mathcal{W}_\mu^I$). This leads to canonically normalized kinetic terms for the gluons $\mathcal{G}_\mu^A$, but not for the weak gauge bosons $\mathcal{W}_\mu^I$ and $\mathcal{B}_\mu$ due to the kinetic mixing induced by Q_{HWB}, which mixes the $\mathcal{W}_\mu^3$ state with the $\mathcal{B}_\mu$ state. For the kinetic and mass terms we find that

$$\begin{aligned}\mathcal{L}_{\text{gauge}}^{\text{broken}} = &-\tfrac{1}{2}\mathcal{W}_{\mu\nu}^+\mathcal{W}_-^{\mu\nu} - \tfrac{1}{4}\mathcal{W}_{\mu\nu}^3\mathcal{W}_3^{\mu\nu} + \tfrac{1}{4}\bar{g}_2^2 v_T^2 \mathcal{W}_\mu^+\mathcal{W}_-^\mu \\ &-\frac{1}{4}\mathcal{B}_{\mu\nu}\mathcal{B}^{\mu\nu} - \frac{1}{2}\frac{v_T^2}{\Lambda^2}C_{HWB}\mathcal{W}_{\mu\nu}^3\mathcal{B}^{\mu\nu} \\ &+\frac{1}{8}v_T^2\left(1+\frac{1}{2}\frac{v_T^2}{\Lambda^2}C_{HD}\right)(\bar{g}_2\mathcal{W}_\mu^3 - \bar{g}_1\mathcal{B}_\mu)\Big)^2,\end{aligned} \tag{5.20}$$

where $\mathcal{W}_\mu^\pm = (\mathcal{W}_\mu^1 \mp i\mathcal{W}_\mu^2)/\sqrt{2}$, and a similar definition is adopted for the field-strength tensors. We can apply two rotations (Grinstein and Wise, 1991)

$$\begin{pmatrix}\mathcal{W}_\mu^3 \\ \mathcal{B}_\mu\end{pmatrix} = \begin{pmatrix}1 & \epsilon \\ \epsilon & 1\end{pmatrix}\begin{pmatrix}\bar{c}_\theta & \bar{s}_\theta \\ -\bar{s}_\theta & \bar{c}_\theta\end{pmatrix}\begin{pmatrix}\mathcal{Z}_\mu \\ \mathcal{A}_\mu\end{pmatrix}, \tag{5.21}$$

where $\epsilon = -v_T^2 C_{HWB}/2\Lambda^2$, to diagonalize the kinetic terms and go to the mass-eigenstate basis containing the photon $\mathcal{A}_\mu$ and the $\mathcal{Z}_\mu$ boson. The rotation angles are

$$\bar{s}_\theta \equiv \sin\bar{\theta} = \frac{\bar{g}_1}{\sqrt{\bar{g}_1^2+\bar{g}_2^2}}\left[1+\epsilon\frac{\bar{g}_2}{\bar{g}_1}\frac{\bar{g}_1^2-\bar{g}_2^2}{\bar{g}_1^2+\bar{g}_2^2}\right], \tag{5.22}$$

$$\bar{c}_\theta \equiv \cos\bar{\theta} = \frac{\bar{g}_2}{\sqrt{\bar{g}_1^2+\bar{g}_2^2}}\left[1-\epsilon\frac{\bar{g}_1}{\bar{g}_2}\frac{\bar{g}_1^2-\bar{g}_2^2}{\bar{g}_1^2+\bar{g}_2^2}\right]. \tag{5.23}$$

The photon $\mathcal{A}_\mu$ remains massless due to $\mathrm{U}(1)_e$ gauge invariance, whereas the $\mathcal{W}_\mu^\pm$ and $\mathcal{Z}_\mu$ bosons acquire the masses

$$m_W^2 = \frac{\bar{g}_2^2 v_T^2}{4}, \tag{5.24}$$

$$m_Z^2 = \frac{v_T^2}{4}\left[(\bar{g}_1^2+\bar{g}_2^2)\left(1+\frac{1}{2}\frac{v_T^2}{\Lambda^2}C_{HD}\right) - 4\bar{g}_1\bar{g}_2\epsilon\right]. \tag{5.25}$$

We can then define the gauge couplings

$$\bar{e} = \bar{g}_2(\bar{s}_\theta + \epsilon\bar{c}_\theta), \qquad \bar{g}_Z = \frac{\bar{e}}{\bar{s}_\theta\bar{c}_\theta}\left(1-\frac{\epsilon}{\bar{s}_\theta\bar{c}_\theta}\right) \tag{5.26}$$

and the covariant derivative of the broken phase

$$\begin{aligned}D_\mu = &\,\partial_\mu - i\bar{g}_2(\mathcal{W}_\mu^+ t^+ + \mathcal{W}_\mu^- t^-) \\ &- i\bar{g}_Z(T_3 - \bar{s}_\theta^2 Q)\mathcal{Z}_\mu - i\bar{e}Q\mathcal{A}_\mu,\end{aligned} \tag{5.27}$$

where the electric charge is $Q = T_3 + Y$ with the hypercharge Y and the third component of weak isospin T_3. Furthermore, we define $t^\pm = (t^1 \pm it^2)/\sqrt{2}$, where t^I are the $\mathrm{SU}(2)_L$ generators. In addition, the couplings of the $\mathcal{W}$ and $\mathcal{Z}$ bosons to fermions are modified by operators of the class $\psi^2 H^2 D$. For example, in the broken phase the operator $[Q_{Hl}^{(3)}]_{pr}$ yields an interaction term of the form

$$\begin{aligned}[Q_{Hl}^{(3)}]_{pr} \to v_T^2\Big\{&\frac{\bar{g}_Z}{2}(\bar{\nu}_p^L\gamma^\mu\nu_r^L - \bar{e}_p^L\gamma^\mu e_r^L)\mathcal{Z}_\mu \\ &+\frac{\bar{g}_2}{\sqrt{2}}[(\bar{\nu}_p^L\gamma^\mu e_r^L)\mathcal{W}_\mu^+ + (\bar{e}_p^L\gamma^\mu\nu_r^L)\mathcal{W}_\mu^-]\Big\} + \mathcal{O}(h),\end{aligned} \tag{5.28}$$

in addition to the SM interactions. For more details, see Jenkins, Manohar, and Stoffer (2018b).[31]

C. Integrating out the weak-scale particles in the SMEFT

After having derived the SMEFT Lagrangian in the broken phase, we can construct the LEFT Lagrangian by removing the heaviest particles from the theory, i.e., the Higgs h, the W and Z bosons, and the top quark t. This procedure is discussed in general in Sec. VI.B; here we only anticipate the determination of the Fermi interaction (5.1) as an example.

For illustration consider the four-fermion interaction

$$-\frac{4\mathcal{G}_F}{\sqrt{2}}(\bar{\nu}_\mu^L\gamma^\mu\mu^L)(\bar{e}^L\gamma_\mu\nu_e^L) \tag{5.29}$$

in the LEFT mediating the muon decay $\mu^- \to e^- + \nu_\mu + \bar{\nu}_e$, whose measurement allows the value of the coupling constant $\mathcal{G}_F$ to be determined. In the SMEFT this decay is mediated through the exchange of a $\mathcal{W}_\mu^-$ boson, either with its SM couplings or with the modified coupling due to $Q_{Hl}^{(3)}$, as shown in Eq. (5.28), or through the four-fermion SMEFT operator Q_{ll}. The corresponding tree-level Feynman diagrams are shown in Fig. 9.

We can now compute the tree-level amplitudes in the LEFT and the SMEFT, expanding the $\mathcal{W}$ propagators as $1/(p^2 - m_W^2) = -1/m_W^2 + \mathcal{O}(p^2/m_W^2)$, where p is the momentum carried by the $\mathcal{W}$ boson, which in the range of validity of the LEFT is small $p^2 \ll m_W^2$. Equating our results, we find that (Alonso, Jenkins *et al.*, 2014)

$$\begin{aligned}-\frac{4\mathcal{G}_F}{\sqrt{2}} = &-\frac{2}{v_T^2} - \frac{2}{\Lambda^2}([C_{Hl}^{(3)}]_{11} + [C_{Hl}^{(3)}]_{22}) \\ &+\frac{2}{\Lambda^2}\mathrm{Re}([C_{ll}]_{1221}),\end{aligned} \tag{5.30}$$

[31] Note also that in the SMEFT the $\mathcal{W}$ boson can couple to right-handed fermions through the Q_{Hud} operator.

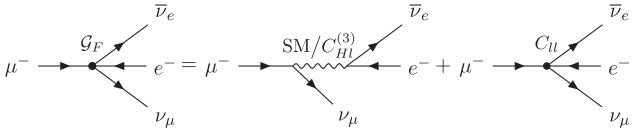

FIG. 9. Tree-level diagrams contributing to the SMEFT-to-LEFT matching for the Fermi constant. The $\mathcal{W}$-boson propagators in the SMEFT diagrams are understood to be expanded in p^2/m_W^2, thus generating local contributions.

where we use $[C_{ll}]_{2112} = [C_{ll}^*]_{1221}$. Equation (5.30) is called a matching condition and determines the LEFT coefficient $\mathcal{G}_F$ in terms of the SMEFT parameters. We see that the LEFT and SMEFT power expansions get mixed up in this case. In general LEFT operators of dimension d are suppressed by

$$\frac{1}{\Lambda^a}\frac{1}{v^b}, \qquad a+b=d-4, \quad a \geq 0, \tag{5.31}$$

where a is always positive since the SMEFT contains Λ only as a multiplicative prefactor with negative powers and b can be negative due to Higgs VEV insertions.

From Eq. (5.30) we see that what is actually extracted from experimental data on the muon decay is $\mathcal{G}_F$, not the SM value $G_F = (\sqrt{2}v^2)^{-1}$. The modification of the tree-level relations of SM parameters like the aforementioned one in the SMEFT requires extra care in extracting these from experiments. For more details on the determination of the SM parameters and a discussion of appropriate input schemes for SMEFT computations, see Brivio and Trott (2017) and Brivio *et al.* (2021).

The construction of a complete basis of the LEFT up to dimension 6 and the derivation of all tree-level relations of the LEFT Wilson coefficients to the SMEFT Wilson coefficients was presented by Jenkins, Manohar, and Stoffer (2018b). Subsequently LEFT operator bases of dimensions 7 (Liao, Ma, and Wang, 2020), 8 (Li, Ren, Xiao *et al.*, 2021b; Murphy, 2021), and 9 (Li, Ren, Xiao *et al.*, 2021b) were also derived in the literature. At the one-loop level, the matching requires the calculation of a large number of loop diagrams. This monumental program was taken up by Dekens and Stoffer (2019). These are lengthy expressions and are most convenient and usable given directly in digital form as in Appendix G and the Supplemental Material of Dekens and Stoffer (2019).[32] Therein the SMEFT coefficients appearing in the matching conditions were understood to be renormalized in the $\overline{\text{MS}}$ scheme and implicitly dependent on the matching scale $\mu \sim m_W$. When using these one-loop matching results it is important to also strictly follow all of the conventions used in their derivation in all subsequent computations with the resulting LEFT Lagrangian to avoid any inconsistencies. The one-loop anomalous dimensions of all $d \leq 6$ LEFT coefficients were eventually derived by Jenkins, Manohar, and Stoffer (2018a), so the toolbox for LEFT computations has been augmented.

[32]The SMEFT-to-LEFT one-loop matching is also implemented in codes such as `Wilson` (Aebischer, Kumar, and Straub, 2018) and `DsixTools` (Celis *et al.*, 2017; Fuentes-Martin, Ruiz-Femenia *et al.*, 2021).

VI. BEYOND THE STANDARD MODEL PHENOMENOLOGY WITH THE SMEFT

In this section we showcase the practical application of effective field theory, particularly of the SMEFT, in the search for new physics. Since the standard model predictions to date have agreed well with experiments, a detailed treatment is important. The uneven history of some of the precision results shows the importance of a systematic treatment. Here we discuss the different EFTs involved, and how they are linked. We comment on existing work and consider in detail two explicit examples to illustrate all of the steps needed in order to reliably constrain the possible BSM scenarios.

A. The SMEFT analysis workflow

We start by discussing the general EFT workflow for new-physics searches; detailed information on the various steps involved is discussed in Secs. VI.B–VI.E. For a typical BSM analysis, we consider a tower of effective theories, as illustrated in Fig. 10. Each of these EFTs provides an accurate description of nature at a given energy scale. The EFTs

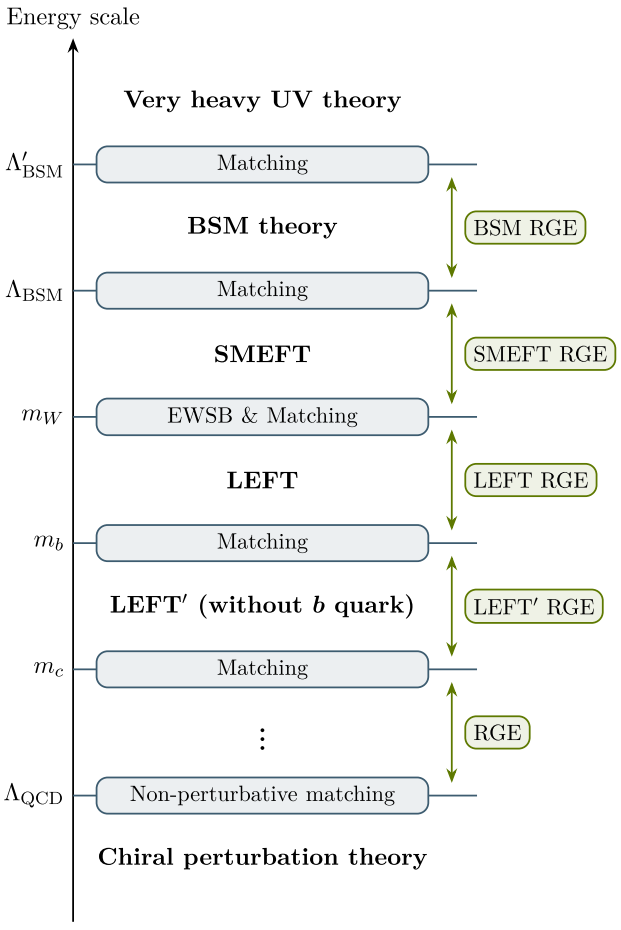

FIG. 10. Tower of effective field theories ranging from far UV scales to the low energies at which the experiments are performed. Depending on the observable, different EFTs might be appropriate. The various EFTs can be connected through matching and RG evolution. Moreover, spontaneous symmetry breaking may occur at intermediate steps.

contain only the relevant degrees of freedom at that energy and incorporate the effects of heavier states through higher-dimensional effective operators. To connect theories at different energy scales, matching computations are performed that allow one to integrate out the heavy particles from one theory to obtain the corresponding low-energy EFT. We encountered a matching computation for the Fermi constant in Eq. (5.30); further details on the procedure are given in Sec. VI.B. Within each EFT, the corresponding RG equations can then be used to evolve all couplings from the high-energy scale, where the matching was performed, to the low-energy scale of the heaviest particles remaining in the EFT; see Sec. VI.C. These can then be integrated out in the next matching computation to obtain yet another EFT, one that is valid at even lower energies. This procedure has to be repeated until the desired energy scale (usually the energy range of experimental observables) is reached. Using such a multistep procedure of alternate matching and running, we can ensure a proper description of physics at all involved scales, as the RG evolution allows one to resum large logarithms that would appear if only a single matching would be performed at the lowest scale, or if we would even use only the full theory. As one can easily imagine, such a multiscale computation can become highly involved, which would require automation of all of the steps involved. There are already several computer tools available that automate some of these steps; for an overview, see Aebischer, Fael *et al.* (2019) and Aebischer *et al.* (2023). However, complete automation is still a goal to be achieved in the future.

To be concrete, we can take a BSM theory containing some heavy particles with masses of the order of $\Lambda_{\rm BSM}$ that are not accessible at the energies of current experiments. We can then match such a theory to the SMEFT, where the effect of these heavy states is encoded in the effective operators. In general not all of the SMEFT operators will be generated by the matching, but instead only a certain subset. For example, a list of all operators that are generated at tree level in all possible BSM scenarios was worked out in the UV-IR dictionary provided by de Blas *et al.* (2018). Consequently the SMEFT RG equations (Jenkins, Manohar, and Trott, 2013b; Alonso, Jenkins *et al.*, 2014; Jenkins, Manohar, and Trott, 2014) are used to evolve the couplings from the matching scale $\Lambda_{\rm BSM}$ down to the electroweak scale $\sim m_W$. Through this RG mixing further operators can be generated that were absent from the matching. At the electroweak scale spontaneous symmetry breaking then takes place, as discussed in Sec. V.B. After expanding the Higgs field around its vacuum expectation value, we end up with the SMEFT Lagrangian in the broken phase, which is invariant under the $\mathrm{SU}(3)_c \times \mathrm{U}(1)_e$ gauge symmetry and contains only the physical Higgs h, not the full Higgs doublet H, which is present only in the unbroken phase above the electroweak scale. One can now integrate out the heaviest SM particles, i.e., the top quark t and the Higgs h, Z, and W bosons, to arrive at the LEFT (Jenkins, Manohar, and Stoffer, 2018b; Dekens and Stoffer, 2019). Usually EWSB and the matching is performed at the single scale $\sim m_W$. Since the masses of all particles that are integrated out here are similar, no large logarithms arise, even though we choose only a single matching scale. Afterward the known LEFT RG equations (Jenkins, Manohar, and Stoffer, 2018a) can be used to evolve the theory down to the bottom-quark mass scale m_b. If necessary, the b quark can then be integrated out, etc., until one reaches the energy scale of the experimental observables of interest. For example, for B physics experiments it is sufficient to stop the procedure here, but for processes at even lower energies one might also require integrating out the charm quark. See Buchalla, Buras, and Lautenbacher (1996) for a review of the EFTs at the b scale.

Ultimately one could end up at the QCD confinement scale $\Lambda_{\rm QCD}$, where one matches onto ChPT. However, owing to confinement, in this case the IR degrees of freedom of ChPT, i.e., the pions, are not the same as in the EFT above $\Lambda_{\rm QCD}$, where we have quarks. Because of the growth of the strong coupling constant, perturbativity is lost and the matching has to be performed nonperturbatively. The discussion of this process, however, is beyond the scope of this review; see Bernard (2008) for further details.

The BSM theory that we started with could well be simply an EFT itself, originating from integrating out even heavier particles in some more fundamental theory that is valid at even higher scales $\Lambda'_{\rm BSM}$. In this EFT picture we can simply consider any theory as an effective description at a given energy containing only the relevant degrees of freedom at these energies and incorporating our agnosticism about the laws of nature being valid at higher energies in terms of higher-dimensional effective operators. Relating the different EFTs through matching and running as previously discussed, we can express the couplings in a UV theory through the couplings or Wilson coefficients of a low-energy EFT that is valid at the scale of experiments, therefore allowing us to constrain these UV parameters from low-energy data.

Describing nature by a chain of EFTs is, by construction, always an approximation. However, it can be systematically improved by including higher orders in the EFT power counting, i.e., higher-dimensional operators, thereby allowing one in principle to describe physical laws up to arbitrary precision. In practice, usually only the leading contributions given by the dimension-6 operators and their interference with the SM are relevant. Nevertheless, higher orders, such as dimension-6-squared or $d \geq 8$ operators, can be relevant when they introduce new interactions that are not generated by the leading order (Hays *et al.*, 2019; Corbett *et al.*, 2021) or when they exhibit some energy enhancement, as in the case of high-p_T Drell-Yan tails that we discuss in Sec. VI.E.1. For a discussion of higher-order operators and the EFT validity, see Secs. II.A.4 and II.C.

Any SMEFT computation always involves a double expansion in the EFT power-counting order and the loop order, and the truncation of both has to be chosen individually according to the desired precision and the process of interest.[33] Going to the one-loop level in the matching computation might be especially required in cases where the operators of interest are not generated at tree level, i.e., for all loop-generated operators; see Sec. II.B.2. In principle consistency in the

[33]Conversely, in the HEFT the two expansions are linked together and cannot be truncated individually.

expansion parameters should be obeyed. For instance, a one-loop matching computation would require two-loop running to obtain scheme independent results. However, in practice nearly always the one-loop RG equations are considered only, as the full two-loop SMEFT RG equations are not yet known and only partial results are available. In addition, one-loop running suffices for the required precision and one-loop matching computations are usually required only for operators that cannot be generated at tree level.

Depending on the question that we ask, the EFT analysis starts at the top or bottom of the tower of EFTs shown in Fig. 10, which we have already denoted as top-down or bottom-up studies. In the top-down approach one starts with a given BSM theory and matches it to the SMEFT and consecutively to the LEFT, etc., to determine the implications of this given theory at low energies. The ultimate goal is to constrain specific parameters of the BSM theory from suitable low-energy measurements. The strong advantage of using EFTs in this approach is the simplification of the initial problem and the resummation of large logarithms.

In the bottom-up approach, however, the idea is trying to be agnostic about the UV completion of the SM. In this case, one can use many low-energy datasets to constrain a large number of SMEFT Wilson coefficients. In principle the goal of this approach is to perform a global fit to determine all of the SMEFT parameters. In practice, owing to the large number of free parameters, such a fit is currently unfeasible. These types of analyses consider only a certain subset of parameters based on general dynamical hypotheses and/or symmetry assumptions, such as the flavor symmetries discussed in Sec. III. Eventually constraints provided in this manner should still be used to constrain different BSM scenarios that simply have to be matched to the SMEFT, rather than having to perform the full analysis for every model individually.

Sometimes there is also no clear distinction between the two approaches. A key point is that performing an EFT analysis is especially useful if there is a signal for new physics. Without such a signal, one can put constraints only on the large parameter space of the SMEFT, gaining limited knowledge about the underlying structure of the new physics. This is particularly problematic, as not all of the SMEFT parameters are equally relevant for experimental observations in different BSM theories. In the absence of a new-physics signal, the constraints are more efficiently expressed as direct bounds on possible deviations from the SM for a given set of observables. In this respect, an interesting approach is that of pseudo-observables (Bardin, Grunewald, and Passarino, 1999; Passarino, Sturm, and Uccirati, 2010), i.e., the definition of a suitable set of on-shell amplitudes unambiguously connected to measurable quantities that can be characterized in general terms as deviations from the SM of short-distance origin. This approach, which was introduced to describe electroweak precision tests at the Z pole (Bardin, Grunewald, and Passarino, 1999) and later extended to Higgs physics (Passarino, Sturm, and Uccirati, 2010; Ghezzi *et al.*, 2015; Gonzalez-Alonso *et al.*, 2015; David and Passarino, 2016; Greljo *et al.*, 2016), can be viewed as an intermediate, consistent, and economical step between measurements and their possible EFT interpretation. In the absence of deviations from the SM, the EFT interpretation of data provides a useful guiding principle in model building, but the power of the EFT approach in predicting new effects and testing the validity of a given BSM hypothesis cannot be exploited.

In the following we discuss all of the steps involved in a new-physics SMEFT analysis. We also analyze for illustration one example each of a top-down and a bottom-up analysis.

B. Matching BSM models to the SMEFT

The matching of a BSM theory to the SMEFT is involved, and there are several variants. To expose the important points, we consider the matching procedure in the context of EFTs in general, as similar computations are required in all of the matching steps illustrated in Fig. 10. By matching a given UV theory to its corresponding low-energy EFT, we fix the value of all the Wilson coefficients of the EFT such that both theories reproduce the same physics in the low-energy limit. Therefore, the Wilson coefficients have to be determined as functions of the UV parameters, and constraints on the EFT coefficients can be directly translated into bounds on the BSM parameters. There are two different approaches, known as off-shell and on-shell matching, that allow us to ensure that two theories describe the same physics at low energies.

The most restrictive requirement that we can enforce is that the effective action Γ of both theories, taken as a function of the light fields ϕ only, agrees,

$$\Gamma_{\mathrm{UV}}[\phi] = \Gamma_{\mathrm{EFT}}[\phi]. \tag{6.1}$$

This ensures that all off-shell amplitudes with light external particles agree in the two theories at low energies. Therefore, this method is commonly known as off-shell matching. The matching condition (6.1) then determines the value of all Wilson coefficients in terms of the UV parameters. One way to determine the effective action is by calculating all relevant Feynman diagrams with external light fields. Unlike the usual computation of the effective action, where we need to consider all one-particle-irreducible diagrams, it is required in this case to compute all one-light-particle-irreducible (1LPI) Feynman diagrams, i.e., the diagrams that cannot be split in two by cutting any light internal line. This is because we consider the effective action as a function of light fields only. More on this "diagrammatic matching procedure" is provided in Sec. VI.B.1. An alternative approach to calculating the effective action is through its path integral representation, which we discuss in Sec. VI.B.2.

Requiring off-shell amplitudes to agree is actually more restrictive than necessary. It suffices to ensure that all physical observables computed in either theory agree, which is equivalent to equating the S matrices of UV and EFT for all scattering processes with only light particles in the external states,

$$\langle\phi|S_{\mathrm{UV}}|\phi\rangle = \langle\phi|S_{\mathrm{EFT}}|\phi\rangle. \tag{6.2}$$

This amounts to equating on-shell amplitudes and is therefore known as on-shell matching. We can again compute the S matrix diagrammatically, but unlike with the off-shell matching computation we now need to consider all contributing diagrams, not simply the 1LPI ones. This can significantly

increase the number of diagrams that need to be included in the computation. In addition, the matching of the reducible diagrams is computationally more challenging, which is why in practice off-shell matching is used most often.

The main advantage of on-shell matching is that it suffices to consider EFT operators from a minimal basis for the matching computation. This is not the case for off-shell matching, since for off-shell amplitudes further kinematical structures are allowed, and therefore additional operators need to be included. When discussing the construction of EFT bases in Sec. II.A.1, we used field redefinitions to reduce the operator list to a minimal basis. Recall that, to do so, we argued that the LSZ-formula guarantees that physical observables remain unchanged under field redefinitions. For off-shell matching, however, we do not compute physical observables. Therefore, we are not allowed to use the LSZ formula and have to use a larger set of operators, that is, a basis up to field redefinitions. Such an operator set is commonly referred to as a Green's basis. We discuss the diagrammatic off-shell matching procedure with a concrete example and mention the differences versus the on-shell computation. Afterward we provide an introduction to functional matching.

Before we continue with the different matching prescriptions, a comment on the calculation of the loop integrals is in order. Because loop integrals in the matching can depend on light m and heavy M mass scales, certain regions of the internal momentum k of the loop are enhanced. This is encapsulated in the method of expansion by regions (Beneke and Smirnov, 1998; Jantzen, 2011), which can be applied to all of the previously mentioned matching techniques. We can expand each integrand in the region where k is hard $(k \sim M \gg m)$ and where it is soft $(k \sim m \ll M)$. Performing both integrals separately over the full D-dimensional space and summing their results then yields the same outcome as computing the full integral and expanding afterward in powers of the ratio m/M. Applying the method of regions offers the advantage of separating the UV from the IR physics. By construction the full theory and its corresponding EFT describe the same low-energy dynamics, i.e., IR physics. This means that the soft region of the full theory integrals must be equal to the soft region of the corresponding EFT diagrams. Thus, we merely have to compute the hard region of all integrals to determine the matching conditions since they incorporate all of the short-distance dynamics that must be captured by the Wilson coefficients. Next we notice that the hard region of EFT integrals yields only scaleless integrals, which vanish in dimensional regularization, since the EFT depends only analytically on M. Therefore, we need only consider tree-level EFT diagrams with insertions of one-loop coefficients and full theory diagrams with at least one heavy propagator in the loop to obtain the full matching conditions; see Appendix A.1 and Manohar (2018) for more details.

1. Diagrammatic matching

To demonstrate the diagrammatic matching procedure, we work with a concrete example. Consider the extension of the SM by a heavy colored scalar S_1 transforming as $(\bar{\mathbf{3}}, \mathbf{1})_{1/3}$ under the SM gauge group. The S_1 leptoquark couples to both quarks and leptons (thus its name), and its BSM Lagrangian is

$$\mathcal{L}_{S_1} = \mathcal{L}_{\mathrm{SM}} + (D_\mu S_1)^\dagger (D^\mu S_1) - M_S^2 S_1^\dagger S_1 - [\lambda^L_{pr}(\bar{q}^c_p \varepsilon \ell_r) S_1 + \lambda^R_{pr}(\bar{u}^c_p e_r) S_1 + \mathrm{H.c.}], \tag{6.3}$$

where we neglect any direct coupling of the S_1 to the Higgs doublet H. For the off-shell matching we need to consider a Green's basis for the SMEFT, i.e., a basis of operators up to field redefinitions. Such a basis was given by Gherardi, Marzocca, and Venturini (2020), who also presented the full matching computation for the given model. Here we merely reproduce partial results of this derivation to illustrate the procedure.

To begin, we realize that for tree-level matching only interaction terms of the Lagrangian (6.3) with at most one heavy field can contribute. Operators with more heavy fields can contribute only at loop level. It is then obvious that only four-fermion operators are generated in the EFT at tree level. The resulting EFT Lagrangian is

$$\mathcal{L}_{\mathrm{EFT}} = \mathcal{L}_{\mathrm{SM}} + \sum_X \frac{[C_X^{(R)}]_{prst}}{\Lambda^2} [R_X]_{prst}, \tag{6.4}$$

where the sum runs over the "redundant" operators

$$[R_{q^c l}]_{prst} = (\bar{q}^c_{ip} \ell_{jr})(\bar{\ell}^j_s q^{c\,i}_t), \tag{6.5a}$$

$$[R'_{q^c l}]_{prst} = (\bar{q}^c_{ip} \ell_{jr})(\bar{\ell}^i_s q^{c\,j}_t), \tag{6.5b}$$

$$[R_{e^c u}]_{prst} = (\bar{e}^c_p u_r)(\bar{u}_s e^c_t), \tag{6.5c}$$

$$[R_{u^c e l q^c}]_{prst} = (\bar{u}^c_p e_r)\varepsilon_{ij}(\bar{\ell}^i_s q^{c\,j}_t) \tag{6.5d}$$

defined following the conventions used by Fuentes-Martin *et al.* (2023b). The Feynman diagrams in the UV and the EFT relevant to the matching are shown on the left- and right-hand sides of Fig. 11, respectively. Inserting the appropriate interaction terms from the UV and EFT Lagrangian, we can compute the corresponding amplitudes. Afterward we expand the UV amplitudes as power series in $1/M_S$. Here we work to mass dimension 6; thus, we need to truncate the results at $\mathcal{O}(M_S^{-2})$. We can then equate the amplitudes of both the EFT and the UV to find the matching conditions

$$[C^{(R)}_{q^c l}]_{prst} = -[C'^{(R)}_{q^c l}]_{prst} = \lambda^L_{pr}\lambda^{L*}_{ts}, \tag{6.6a}$$

$$[C^{(R)}_{e^c u}]_{prst} = \lambda^R_{rp}\lambda^{R*}_{st}, \tag{6.6b}$$

$$[C^{(R)}_{u^c e l q^c}]_{prst} = -\lambda^R_{pr}\lambda^{L*}_{ts}, \tag{6.6c}$$

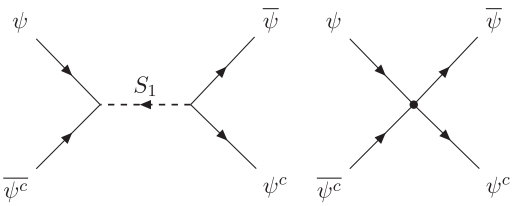

FIG. 11. Tree-level Feynman diagrams for the S_1 model (left) and the SMEFT (right) that are relevant to the matching of the four-fermion operators. The UV diagram has to be expanded in powers of $1/M_S$ before equating it to the EFT diagram.

where we also identify the new-physics scale Λ with the mass of the S_1 state: $\Lambda = M_S$.

For convenience we rewrite our result in the Warsaw basis. The operators in Eq. (6.5) are related to the operators $Q_{lq}^{(1,3)}$, Q_{eu}, and $Q_{lequ}^{(1,3)}$ of the Warsaw basis through the Fierz transformations (2.20). The matching conditions in the Warsaw basis read

$$[C_{lq}^{(1)}]_{prst} = \tfrac{1}{2}[C_{q^c l}^{(R)}]_{trps} + \tfrac{1}{4}[C_{q^c l}^{\prime(R)}]_{trps}, \tag{6.7a}$$

$$[C_{lq}^{(3)}]_{prst} = \tfrac{1}{4}[C_{q^c l}^{\prime(R)}]_{trps}, \tag{6.7b}$$

$$[C_{eu}]_{prst} = \tfrac{1}{2}[C_{e^c u}^{(R)}]_{rtsp}, \tag{6.7c}$$

$$[C_{lequ}^{(1)}]_{prst} = -4[C_{lequ}^{(3)}]_{prst} = -\tfrac{1}{2}[C_{u^c elq^c}^{(R)}]_{trps}, \tag{6.7d}$$

where evanescent operators can be ignored since we work at tree level. In this case there are no integration by parts relations or field redefinitions required to reduce the matching result to the Warsaw basis.

Next we perform the one-loop matching. Since the entire computations are lengthy and the full results were given by Gherardi, Marzocca, and Venturini (2020), we focus here on the contributions to the leptonic dipole operators

$$[Q_{eB}]_{pr} = (\bar{\ell}_p \sigma^{\mu\nu} e_r) H B_{\mu\nu}, \tag{6.8}$$

$$[Q_{eW}]_{pr} = (\bar{\ell}_p \sigma^{\mu\nu} e_r) \tau^I H W^I_{\mu\nu}, \tag{6.9}$$

which can be generated only at loop level. We choose to use on-shell matching, which allows us to single out the dipole matching contributions, for which the relevant diagrams are shown in Fig. 12. The first four rows display the diagrams of the UV theory, whereas the diagram in the last row is the only EFT diagram. Recall that, since we employ the method of regions, we have to consider only EFT tree diagrams with one-loop coefficients, not loop diagrams. After one expands in the hard loop-momentum region and performs the Dirac algebra, including the application of the spinor equations of motions and the Gordon identity, the diagrams in the third and fourth rows provide a local contribution to the leptonic dipole operators. If we had instead chosen off-shell matching, we would have had to consider further topologies that do not directly match to the dipole but do contribute to it only after field redefinitions are applied to reduce the Green's basis to the Warsaw basis. However, it is not straightforward to identify which topologies to consider, which is why we choose to work out this explicit contribution on shell.[34]

Computing and equating the amplitudes corresponding to the diagrams shown in Fig. 12, where for the UV amplitudes

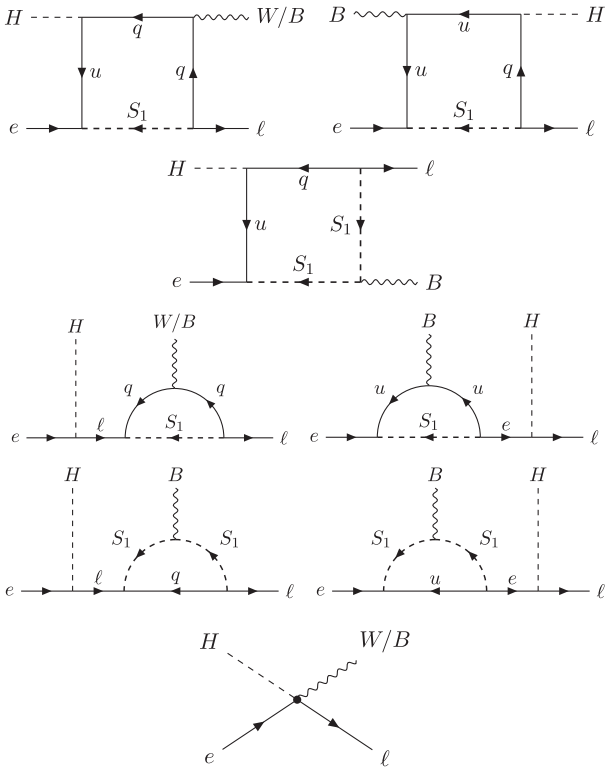

FIG. 12. One-loop diagrams relevant to the on-shell matching of the leptonic dipole operators for the S_1 model. The first four rows show the diagrams of the UV theory, whereas the last row contains the only EFT diagram that contributes when one uses the method of regions.

we keep only the terms with a Lorentz structure matching that of the dipole since the remaining terms will match onto other operators of the Warsaw basis that we are not interested in, we find at $\mathcal{O}(M_S^{-2})$ that

$$[C_{eB}]_{pr} = \frac{1}{16\pi^2}\frac{g_1}{8}\left\{-[Y_e]_{pt}\lambda_{st}^{R*}\lambda_{sr}^{R} + \lambda_{sp}^{L*}[Y_u^*]_{st}\lambda_{tr}^{R}\left[\frac{19}{2} + 5\log\left(\frac{\mu_m^2}{M_S^2}\right)\right]\right\} + [\Delta_{eB}]_{pr}, \tag{6.10}$$

$$[C_{eW}]_{pr} = \frac{1}{16\pi^2}\frac{g_2}{8}\left\{\lambda_{sp}^{L*}\lambda_{st}^{L}[Y_e]_{tr} - 3\lambda_{sp}^{L*}[Y_u^*]_{st}\lambda_{tr}^{R}\left[\frac{3}{2} + \log\left(\frac{\mu_m^2}{M_S^2}\right)\right]\right\} + [\Delta_{eW}]_{pr}, \tag{6.11}$$

where μ_m is the matching scale, which we can conveniently choose as $\mu_m = M_S$ to eliminate all logarithms in the matching conditions.[35]

However, since we work at the one-loop level now, we can no longer use the Fierz identities applied in the tree-level

[34] In the case of off-shell matching, we could also neglect the diagrams in the third and fourth rows of Fig. 12 since we have to consider only 1LPI diagrams. Their contribution would be shifted to the additional operators in the Green's basis that reduce to the dipole by applying field redefinitions such that the final results of the two methods agree.

[35] Other choices for μ_m are possible, but it should not be chosen too far from the mass threshold to avoid large logarithms and a worsening of the perturbative expansion.

matching in Eq. (6.7). As previously stated, these are intrinsically four-dimensional identities that must not be applied in combination with a computation in dimensional regularization, since they lead to evanescent operators. Instead, we apply the corrected one-loop Fierz transformations as discussed in Sec. II.A.5 and by Fuentes-Martin *et al.* (2023b)). These transformations effectively project the evanescent operators onto the physical four-dimensional Warsaw basis, allowing us to ignore evanescent contributions afterward. We focus on the dipole operator, whose additional contributions arising due to the evanescent operators generated by applying the $D=4$ Fierz identities in Eq. (6.7) are labeled by $\Delta_{eB/eW}$ in Eqs. (6.10) and (6.11). The corresponding shift of the action was derived in Sec. II.A.5 and is given by Eq. (2.32), with which we find that

$$[\Delta_{eB}]_{pr} = -\frac{1}{16\pi^2}\frac{5}{8} g_1 [Y_u^*]_{ts}(1-\xi_{\mathrm{rp}})[C^{(R)}_{u^c e l q^c}]_{srpt}, \tag{6.12}$$

$$[\Delta_{eW}]_{pr} = \frac{1}{16\pi^2}\frac{3}{8} g_2 [Y_u^*]_{ts}(1-\xi_{\mathrm{rp}})[C^{(R)}_{u^c e l q^c}]_{srpt}, \tag{6.13}$$

where ξ_{rp} is the parameter denoting the reading point ambiguity when using NDR to evaluate the loop integrals; see Sec. II.A.5 and Appendix A.2 for more details. For convenience we decide to read all EFT loop integrals ending with the EFT operator, as suggested by Fuentes-Martin *et al.* (2023b). As previously mentioned, we then have to follow this prescription for all subsequent computations within the EFT to obtain consistent results, regardless of the choice of reading point. The given prescription yields $\xi_{\mathrm{rp}}=1$ (which also agrees with the results obtained in the 't Hooft–Veltman scheme), and thus the evanescent contributions to the dipole happen to vanish. Nevertheless, there are additional nonvanishing and unambiguous evanescent contributions to further operators that we do not consider here. For more details on the reading point ambiguity, see Appendix A.2 and Fuentes-Martin *et al.* (2023b).

2. Functional matching

We now recap the functional formalism worked out by Dittmaier and Grosse-Knetter (1996), del Aguila, Kunszt, and Santiago (2016), Fuentes-Martin, Portoles, and Ruiz-Femenia (2016), Henning, Lu, and Murayama (2016, 2018), Zhang (2017), and Cohen, Lu, and Zhang (2021a) and employ it for a specific matching computation. We make use of the background-field method (Abbott, 1981; Abbott, Grisaru, and Schaefer, 1983; Denner, Weiglein, and Dittmaier, 1995; Denner, Dittmaier, and Weiglein, 1996) by separating all fields $\eta \to \hat{\eta}+\eta$ in a background-field configuration $\hat{\eta}$, which satisfies the classical equations of motion, and a pure quantum component η. In Feynman diagrams $\hat{\eta}$ then corresponds to tree-level lines, whereas η corresponds to lines in loops. Expanding the action to one-loop accuracy we find that

$$S[\hat{\eta}+\eta] = S[\hat{\eta}] + \frac{\sigma_{\eta_j}}{2}\bar{\eta}_i \frac{\delta^2 S}{\delta\bar{\eta}_i \delta\eta_j}\bigg|_{\eta=\hat{\eta}} \eta_j + \mathcal{O}(\eta^3), \tag{6.14}$$

where $\sigma_{\eta_j}=1$ if η_j is bosonic and $\sigma_{\eta_j}=-1$ if it is Grassmann due to anticommuting η_j to the right-hand side of Eq. (6.14). The linear term vanishes due to the equations of motion, and higher-order terms contribute only at two-loop order and beyond. We identify the term that is quadratic in the quantum fields as the fluctuation operator,

$$\Omega_{ij}[\hat{\eta}] = \sigma_{\eta_j}\frac{\delta^2 S}{\delta\bar{\eta}_i\delta\eta_j}\bigg|_{\eta=\hat{\eta}}. \tag{6.15}$$

The effective action of the theory is then given by

$$\exp(i\Gamma[\hat{\eta}]) = \int \mathcal{D}\eta \, \exp\left(iS[\hat{\eta}] + \frac{i}{2}\bar{\eta}_i\Omega_{ij}[\hat{\eta}]\eta_j + \mathcal{O}(\eta^3)\right). \tag{6.16}$$

Thus, we find the tree-level effective action $\Gamma^{(0)}[\hat{\eta}] = S^{(0)}[\hat{\eta}]$ and the one-loop effective action

$$\begin{aligned}\Gamma^{(1)}[\hat{\eta}] &= S^{(1)}[\hat{\eta}] - i\log\left(\mathrm{SDet}\Omega^{(0)}[\hat{\eta}]\right)^{-1/2} \\ &= S^{(1)}[\hat{\eta}] + \frac{i}{2}\mathrm{STr}\log\Omega^{(0)}[\hat{\eta}],\end{aligned} \tag{6.17}$$

where $S^{(1)}[\hat{\eta}]$ contains all local one-loop contributions; that is, in renormalizable theories $S^{(1)}[\hat{\eta}]$ contains only the counterterms required to renormalize the theory. In EFTs the one-loop induced Wilson coefficients are included in $S^{(1)}[\hat{\eta}]$ too. We furthermore introduce the superdeterminant (SDet) and the supertrace (STr), which are generalizations of the determinant and trace to operators with mixed spin. The supertrace is a trace over all internal degrees of freedom and therefore involves an integration over all loop momenta

$$\mathrm{STr}\,\log\Omega[\hat{\eta}] = \pm\int\frac{\mathrm{d}^D k}{(2\pi)^D}\langle k|\mathrm{tr}\,\log\Omega[\hat{\eta}]|k\rangle, \tag{6.18}$$

where tr denotes the regular trace over all internal degrees of freedom apart from momentum and the sign depends on the spin of the considered field, with $+$ $(-)$ for bosonic (fermionic) states. These operator traces can be evaluated using the so-called covariant derivative expansion (Chan, 1986; Gaillard, 1986; Cheyette, 1988). However, a discussion of the supertrace evaluation is beyond the scope of this review; see Henning, Lu, and Murayama (2016), Cohen, Lu, and Zhang (2021a), and Fuentes-Martin, König *et al.* (2021) for further details.

Since the path integral formulation allows one to compute the effective action, we can also use it to calculate the off-shell matching condition in Eq. (6.1). At tree level we find that

$$S^{(0)}_{\mathrm{EFT}}[\hat{\eta}_L] = S^{(0)}_{\mathrm{UV}}[\hat{\eta}_L, \hat{\eta}_H], \tag{6.19}$$

where we separate the fields into light $\hat{\eta}_L$ and heavy $\hat{\eta}_H$. The heavy background fields are understood as the solutions to their equations of motion as a power series in $1/M$, where M is their mass, so they can be entirely expressed in terms of the light fields $\hat{\eta}_H = \hat{\eta}_H[\hat{\eta}_L]$.

Taking the Lagrangian (6.3) of the S_1 leptoquark example, we find the equation of motion for S_1,

$$D^2 S_1 + M_S^2 S_1 - \lambda^{L*}_{pr}(\bar{\ell}_r \varepsilon q^c_p) + \lambda^{R*}_{pr}(\bar{e}_r u^c_p) = 0. \tag{6.20}$$

Its power series solution is given by

$$S_1 = \frac{1}{M_S^2}[\lambda_{pr}^{L*}(\overline{\ell}_r \varepsilon q_p^c) - \lambda_{pr}^{R*}(\bar{e}_r u_p^c)] + \mathcal{O}(M_S^{-4}). \tag{6.21}$$

Substituting this solution back into the Lagrangian (6.3) yields the same matching condition as in the diagrammatic computation shown in Eq. (6.5).

For the one-loop matching it is convenient to split the fluctuation operator into a kinetic and an interaction term,

$$\Omega_{ij} \equiv \delta_{ij}\Delta_i^{-1} - X_{ij}, \quad \text{with } \Delta_i^{-1} = \begin{cases} -(D^2 + M_i^2), \\ i\not{D} - M_i, \\ g^{\mu\nu}(D^2 + M_i^2), \end{cases} \tag{6.22}$$

for scalars, fermions, and vector bosons, respectively. For simplicity we use the Feynman gauge for the quantum fluctuations of the gauge fields. This does not imply any particular choice for the gauge of the background fields, which remain in the general R_ξ gauge (Henning, Lu, and Murayama, 2016). For more details on gauge fixing the SMEFT in the background-field method, see Helset, Paraskevas, and Trott (2018). The interaction terms X_{ij} are implicitly defined by Eq. (6.22). This allows one to write the one-loop effective action of the UV theory as

$$\Gamma_{\rm UV}^{(1)} = \frac{i}{2}\mathrm{STr}\,\log\Delta^{-1} + \frac{i}{2}\mathrm{STr}\,\log(1-\Delta X). \tag{6.23}$$

We can again apply the method of regions splitting $\Gamma_{\rm UV}^{(1)}$ into a hard and a soft part, which are computed by expanding the loop integrands in the soft and the hard momentum region, respectively. By construction we have $\Gamma_{\rm EFT}^{(1)}|_{\rm soft} = \Gamma_{\rm UV}^{(1)}|_{\rm soft}$, which ensures that both theories describe the same long-distance dynamics. Therefore, we find the one-loop EFT Lagrangian to be given by $\int \mathrm{d}^D x \mathcal{L}_{\rm EFT}^{(1)} = \Gamma_{\rm UV}^{(1)}|_{\rm hard}$, and thus

$$\int \mathrm{d}^D x\, \mathcal{L}_{\rm EFT}^{(1)} = \frac{i}{2}\mathrm{STr}\,\log\Delta^{-1}|_{\rm hard} + \frac{i}{2}\sum_{n=0}^{\infty}\frac{1}{n}\mathrm{STr}(\Delta X)^n|_{\rm hard}, \tag{6.24}$$

where we expand the logarithm in the latter term. This is the master formula for functional one-loop matching, expressing the EFT Lagrangian in terms of *log-type* and *power-type* supertraces. These can be evaluated using the covariant derivative expansion as discussed by Cohen, Lu, and Zhang, (2021a) and Fuentes-Martin, König *et al.* (2021). The main advantage of the functional formalism is that Eq. (6.24) directly yields all generated EFT operators and, unlike the diagrammatic approach, no *a priori* knowledge of an operator basis is required. However, the Lagrangian obtained using Eq. (6.24) is in a nonminimal form, and redundant operators need to be removed to recover the EFT in a minimal basis.

Computation of the previously discussed S_1 example using functional methods is tedious and thus not discussed here, but further details were given by Dedes and Mantzaropoulos (2021) and Fuentes-Martin, König *et al.* (2021).[36] However, this is a purely algebraic problem that can be solved by a computer. The *Mathematica* package `Matchete` (Fuentes-Martin *et al.*, 2023a) was the first tool to fully automize the functional one-loop matching.[37] Previously, the diagrammatic one-loop matching technique was automated in the `MatchMakerEFT` tool (Carmona *et al.*, 2022). This greatly simplifies phenomenological BSM analyses and opens the possibility of validating matching results with different methods. Another tool for one-loop matching is `CoDEx` (Das Bakshi, Chakrabortty, and Patra, 2019), which uses the universal one-loop effective action (UOLEA) method (Drozd *et al.*, 2016; Ellis *et al.*, 2016, 2017, 2020; Krämer, Summ, and Voigt, 2020), which is also based on the previously explained path integral approach. A more detailed discussion of the UOLEA technique is, however, beyond the scope of this review.

C. Renormalization group evolution

The Wilson coefficients of the SMEFT Lagrangian obtained from the matching are related to the UV parameters at the matching scale μ_m, which are usually taken at the mass threshold $\mu_m \sim M$. Next we have to evolve the coefficients down to the electroweak scale ($\sim m_W$) using the SMEFT RG equations. These have been computed by Jenkins, Manohar, and Trott (2013b, 2014) and Alonso, Jenkins *et al.* (2014) at one loop for the dimension-6 operators of the Warsaw basis shown in Table II. The RG equations of the baryon- and lepton-number-violating operators listed in Table IV, including operators with right-handed neutrinos, were derived by Alonso, Chang *et al.* (2014). The RG equations for the dimension-5 and dimension-7 operators were derived by Babu, Leung, and Pantaleone (1993), Liao and Ma (2016), Davidson, Gorbahn, and Leak (2018), and Liao and Ma (2019), whereas for dimension 8 only partial results are currently available (Chala *et al.*, 2021; Das Bakshi *et al.*, 2022). Results for specific sectors of the two-loop anomalous-dimension matrix were derived by Bern, Parra-Martinez, and Sawyer (2020) and Aebischer, Buras, and Kumar (2022). For some recent phenomenological analyses of SMEFT RG mixing effects, see Chala and Titov (2021), Aoude, Maltoni *et al.* (2022), Isidori, Pagès, and Wilsch (2022), and Kumar (2022). A careful analysis of the flavor structure of the 2499×2499 anomalous-dimension matrix of the SMEFT was presented by Machado, Renner, and Sutherland (2023).

An important feature of the RG evolution is the mixing of different operator classes. In particular, an operator that is not generated by the matching can obtain a nonvanishing

[36]For applications of the functional matching formalism to other simple BSM theories, see Dittmaier, Schuhmacher, and Stahlhofen (2021), Zhang and Zhou (2021), Du, Li, and Yu (2022), Li, Zhang, and Zhou (2022), and Liao and Ma (2022).

[37]Earlier codes such as `STrEAM` (Cohen, Lu, and Zhang, 2021b) and `SuperTracer` (Fuentes-Martin, König *et al.*, 2021) allow one to compute the supertraces but do not perform the full matching computation. In particular, they do not perform operator reductions on the resulting EFT Lagrangian. See also `MatchingTools` (Criado, 2018) for a pure tree-level matching implementation.

coefficient through the running. This leads to nontrivial relations among different operator types that need to be carefully considered in a phenomenological analysis.

As an example, we consider the RG evolution of the leptonic dipole operators in Eqs. (6.8) and (6.9) and the Yukawa interactions that are described by

$$\mu \frac{\mathrm{d}}{\mathrm{d}\mu}[C_X]_{pr} = \frac{1}{16\pi^2}[\beta_X]_{pr}, \tag{6.25}$$

with the beta functions given by

$$[\beta_{eB}]_{pr} = 3|y_t|^2[C_{eB}]_{pr} - 10 g_1 y_t^*[C^{(3)}_{lequ}]_{pr33}, \tag{6.26a}$$

$$[\beta_{eW}]_{pr} = 3|y_t|^2[C_{eW}]_{pr} + 6 g_2 y_t^*[C^{(3)}_{lequ}]_{pr33}, \tag{6.26b}$$

$$[\beta_{Y_e}]_{pr} = 3\lambda\frac{v^2}{\Lambda^2}([C_{eH}]_{pr} - y_t^*[C^{(1)}_{lequ}]_{pr33}) \approx 0, \tag{6.26c}$$

$$[\beta_{eH}]_{pr} = 9|y_t|^2[C_{eH}]_{pr} + 12 y_t^*|y_t|^2[C^{(1)}_{lequ}]_{pr33}, \tag{6.26d}$$

where for simplicity we keep only the numerically relevant terms, i.e., top Yukawa (y_t)-enhanced terms that are not multiplied by λ. Thus, we can write the Wilson coefficients at a low scale μ_l in terms of the coefficients at the matching scale μ_m with one-loop accuracy as

$$[C_X]_{pr}(\mu_l) = [C_X]_{pr}(\mu_m) + \frac{1}{16\pi^2}\log\left(\frac{\mu_l}{\mu_m}\right)[\beta_X]_{pr}. \tag{6.27}$$

The RG evolution of the Warsaw basis operators is also automated in computer programs such as `DSixTools` (Celis *et al.*, 2017; Fuentes-Martin, Ruiz-Femenia *et al.*, 2021) and `Wilson` (Aebischer, Kumar, and Straub, 2018), making a phenomenological analysis using the full 2499×2499 anomalous-dimension matrix of the $d = 6$ SMEFT feasible.

D. Low-energy constraints in the LEFT

Having discussed the matching of the BSM model defined in Eq. (6.3) to the dipole operators Q_{eB} and Q_{eW}, we now relate them to the photon dipole operator

$$[\mathcal{Q}_{e\gamma}]_{pr} = \frac{v}{\sqrt{2}}\bar{e}_p^L\sigma^{\mu\nu}e_r^R F_{\mu\nu}. \tag{6.28}$$

Equation (6.28) allows us to illustrate how the low-energy constraints on these effective operators can be used to constrain the high-energy couplings of the S_1 field.

To this end, we write the SMEFT Lagrangian in the broken phase[38]

$$\begin{aligned}\Delta\mathcal{L}^{\text{broken}} = &-[\mathcal{Y}_e]_{pr}\frac{v}{\sqrt{2}}(\bar{e}_p^L e_r^R) - [\mathcal{Y}_{he}]_{pr}\frac{h}{\sqrt{2}}(\bar{e}_p^L e_r^R)\\ &+\frac{[\mathcal{C}_{e\gamma}]_{pr}}{\Lambda^2}\frac{v}{\sqrt{2}}(\bar{e}_p^L\sigma^{\mu\nu}e_r^R)F_{\mu\nu}\\ &+\frac{[\mathcal{C}_{eZ}]_{pr}}{\Lambda^2}\frac{v}{\sqrt{2}}(\bar{e}_p^L\sigma^{\mu\nu}e_r^R)Z_{\mu\nu} + \cdots.\end{aligned} \tag{6.29}$$

In Eq. (6.29) we also include the mass term, the Yukawa, and the Z-boson dipole, where the last two are not phenomenologically relevant in this analysis.

Assuming that new physics is not affecting the electroweak symmetry-breaking pattern, i.e., assuming that the relations between quantities in the broken and unbroken phases are the same as in the SM (for example, $\bar{g}_1 = g_1$, $\bar{s}_\theta = s_\theta$, $v_T = v$), etc., we can use the results presented in Sec. V to relate the coefficients of the broken phase Lagrangian to those of the unbroken phase through

$$\begin{pmatrix}[\mathcal{C}_{e\gamma}]_{pr}\\ [\mathcal{C}_{eZ}]_{pr}\end{pmatrix} = \begin{pmatrix}c_\theta & -s_\theta\\ -s_\theta & -c_\theta\end{pmatrix}\begin{pmatrix}[C_{eB}]_{pr}\\ [C_{eW}]_{pr}\end{pmatrix}, \tag{6.30}$$

$$\begin{pmatrix}[\mathcal{Y}_e]_{pr}\\ [\mathcal{Y}_{he}]_{pr}\end{pmatrix} = \begin{pmatrix}1 & -\frac{1}{2}\\ 1 & -\frac{3}{2}\end{pmatrix}\begin{pmatrix}[Y_e]_{pr}\\ \frac{v^2}{\Lambda^2}[C_{eH}]_{pr}\end{pmatrix}, \tag{6.31}$$

where

$$c_\theta = \frac{g_2}{\sqrt{g_1^2+g_2^2}} = \frac{e}{g_1}, \qquad s_\theta = \frac{g_1}{\sqrt{g_1^2+g_2^2}} = \frac{e}{g_2}. \tag{6.32}$$

We can now combine our results for the relations to the broken phase, which are shown in Eqs. (6.30) and (6.31), with the RG evolution equations above the electroweak scale in Eqs. (6.26) and (6.27) to express the electromagnetic dipole and the mass Yukawa at the electroweak scale μ_w in terms of the SMEFT Wilson coefficients at the new-physics matching scale $\mu_m \sim \Lambda$,

$$\begin{aligned}[\mathcal{C}_{e\gamma}]_{pr}(\mu_w) = &(1 - 3\hat{L}y_t^2)[\mathcal{C}_{e\gamma}]_{pr}(\mu_m)\\ &+16\hat{L}y_t e[C^{(3)}_{lequ}]_{pr33}(\mu_m),\end{aligned} \tag{6.33}$$

$$\begin{aligned}[\mathcal{Y}_e]_{pr}(\mu_w) = &[Y_e]_{pr}(\mu_m) - \frac{v^2}{2\Lambda^2}[C_{eH}]_{pr}(\mu_m)\\ &+6\frac{v^2}{\Lambda^2}\hat{L}\left[y_t^3[C^{(1)}_{lequ}]_{pr33} + \frac{3}{4}y_t^2[C_{eH}]_{pr}\right]_{\mu_m},\end{aligned} \tag{6.34}$$

where we assume the Yukawa couplings to be real and define $\hat{L} \equiv (1/16\pi^2)\log(\mu_m/\mu_w)$. We find that the semileptonic triplet operator $Q^{(3)}_{lequ}$ can generate the electromagnetic dipole $\mathcal{Q}_{e\gamma}$ at the low scale, whereas the semileptonic singlet operator $Q^{(1)}_{lequ}$ as well as Q_{eH} runs into the mass terms $\mathcal{Y}_e$.

We can now investigate the RG evolution below the electroweak scale, which is given by (Jenkins, Manohar, and Stoffer, 2018a)

[38]Note that for convenience we use a different definition here for the Yukawa and mass matrices than we do in Eq. (5.10). Moreover, for the dipole operators we directly apply the SMEFT instead of the LEFT power counting.

$$\mu\frac{\mathrm{d}}{\mathrm{d}\mu}[\mathcal{C}_{e\gamma}]_{pr} = \frac{1}{16\pi^2}\frac{170}{9}e^2[\mathcal{C}_{e\gamma}]_{pr}, \tag{6.35}$$

$$\mu\frac{\mathrm{d}}{\mathrm{d}\mu}[\mathcal{Y}_e]_{pr} = -\frac{1}{16\pi^2}6e^2[\mathcal{Y}_e]_{pr}, \tag{6.36}$$

where we consider all other operators to be turned off,[39] and thus we only have the self-renormalization of the dipole and the mass term, which leave the flavor structure unchanged. Note also that the LEFT dipole operator in Eq. (6.28) is a dimension-5 operator; thus, in principle we had to consider double insertions of this operator for the RG evolution. However, from the matching conditions (6.10) and (6.11) we know that such contribution is of the order of M_S^{-4} in the SMEFT power counting and can thus be neglected. Equation (6.35) then allows one to evolve the photon dipole to the low-energy scales of experimental measurements, which for muons is $\mu_l \sim m_\mu$. Note that in this case it is not required to integrate out any other particles, such as the b quark, since they do not affect the RG evolution in good approximation due to their small Yukawa couplings.

Experimental measurements usually constrain couplings in the mass basis, whereas our Wilson coefficients are given in the generic flavor basis of the UV theory. Thus, rotating the fermion fields to the mass basis is the last missing piece of our analysis. To do this, we need to diagonalize the mass matrix $[\mathcal{Y}_e]_{pr}$, which is determined in terms of the SMEFT operators in Eq. (6.31). Assume that the mass term is diagonalized (diag $= U_L\mathcal{Y}_e U_R^\dagger$) while rotating the lepton fields by

$$e'_L = U_L e_L, \qquad e'_R = U_R e_R, \tag{6.37}$$

where $U_{L,R}$ are unitary matrices and $e'_{L,R}$ denote the mass-basis fields. The mass-basis dipole $\mathcal{C}'_{e\gamma}$ is then given by

$$\mathcal{C}'_{e\gamma} = U_L\mathcal{C}_{e\gamma}U_R^\dagger. \tag{6.38}$$

The most sensitive probe of this operator is the lepton flavor-violating transition $\mu \to e\gamma$; however, the anomalous magnetic moment of the muon $(g-2)_\mu$ is also interesting, especially given the tension of the recent FNAL measurement (Abi *et al.*, 2021) with the SM prediction by Aoyama *et al.* (2020), which is summarized in Eq. (1.9). For mere illustrative purposes, we take the latter result as the reference input of our analysis, despite the recent doubts on its validity mentioned in Sec. I.B.1. Taking into account the upper bound on the branching ratio $\mathcal{B}(\mu^+ \to e^+\gamma)$ determined by the MEG experiment (Baldini *et al.*, 2016), we can then write

$$\mathcal{B}(\mu^+ \to e^+\gamma) = \frac{m_\mu^3 v^2}{8\pi\Gamma_\mu}\frac{|[\mathcal{C}'_{e\gamma}]_{12}|^2 + |[\mathcal{C}'_{e\gamma}]_{21}|^2}{\Lambda^4} < 4.2\times10^{-13} \quad (90\%\ \text{C.L.}), \tag{6.39}$$

$$\Delta a_\mu \equiv a_\mu^{\mathrm{Exp}} - a_\mu^{\mathrm{SM}} = -\frac{4m_\mu}{e}\frac{v}{\sqrt{2}}\frac{\mathrm{Re}[\mathcal{C}'_{e\gamma}]_{22}}{\Lambda^2} = (251\pm59)\times10^{-11}, \tag{6.40}$$

which leads to

$$\left|\frac{[\mathcal{C}'_{e\gamma}]_{12(21)}}{\Lambda^2}\right| \lesssim 2.1\times10^{-10}\ \mathrm{TeV}^{-2}, \tag{6.41}$$

$$\frac{\mathrm{Re}[\mathcal{C}'_{e\gamma}]_{22}}{\Lambda^2} \simeq -1.0\times10^{-5}\ \mathrm{TeV}^{-2}. \tag{6.42}$$

We can now combine all of our results: the low-energy constraints in Eqs. (6.41) and (6.42), the rotation to the mass basis (6.38), the LEFT RG equations (6.35) and (6.36), the EWSB relations (6.30) and (6.31), the SMEFT running (6.26), and the matching conditions (6.10) and (6.11), where the last three results were already combined[40] in Eqs. (6.33) and (6.34).

For simplicity, we also consider $[C_{eH}]_{pr} = 0$, which holds at tree level in the considered S_1 model. We also assume Y_e to be diagonal such that the mass matrix is already diagonal and such that we can set $U_{L,R} = \mathbb{1}$. Note that this is a strong assumption on a marginal operator appearing in the UV, and in general we have to consider rotation matrices $U_{L,R} \neq \mathbb{1}$. The resulting constraints on the S_1 couplings, assuming that these are real quantities, are shown in Fig. 13, where we set the leptoquark mass to $M_S = 2$ TeV. In the upper panel of Fig. 13, the constraints derived from the Δa_μ measurement are shown, whereas the lower panel shows the constraints from the $\mu \to e\gamma$ decay, where we set $\lambda^R_{31} = 0$ for simplicity. In addition, couplings to quarks other than top quarks are neglected, as they are not y_t enhanced.

The scales of the two panels of Fig. 13 are much different, signaling that underlying models able to explain the $(g-2)_\mu$ anomaly, while being consistent with $\mu \to e\gamma$, require a peculiar flavor-alignment mechanism. A more detailed phenomenological analysis of the given model and a discussion of the implied flavor structure were given by Isidori, Pagès, and Wilsch (2022); see also Aebischer, Dekens *et al.* (2021).

There are also tools automating large parts of such analyses. For example, the `flavio` package (Straub, 2018) has a large set of low-energy measurements implemented that can be used to constrain the Wilson coefficients. In addition, the SMEFT-to-LEFT matching as well as the RG evolution in both EFTs is available in the code [through the `Wilson` package (Aebischer, Kumar, and Straub, 2018); see also `DsixTools` (Celis *et al.*, 2017)]. A global likelihood based on the data available in `flavio` can be constructed with the `smelli` package (Aebischer, Kumar *et al.*, 2019), which can simplify the analyses.

[39]For the SMEFT, the only numerically relevant contributions in the running are due to the y_t-enhanced terms. In the LEFT, however, the top quark is integrated out and top loops cannot contribute; thus, no such RG effects are present below the electroweak scale.

[40]Note that we choose $\xi_{\mathrm{rp}} = 1$ for convenience, which fixes the NDR reading point that has to be used in all consecutive EFT calculations.

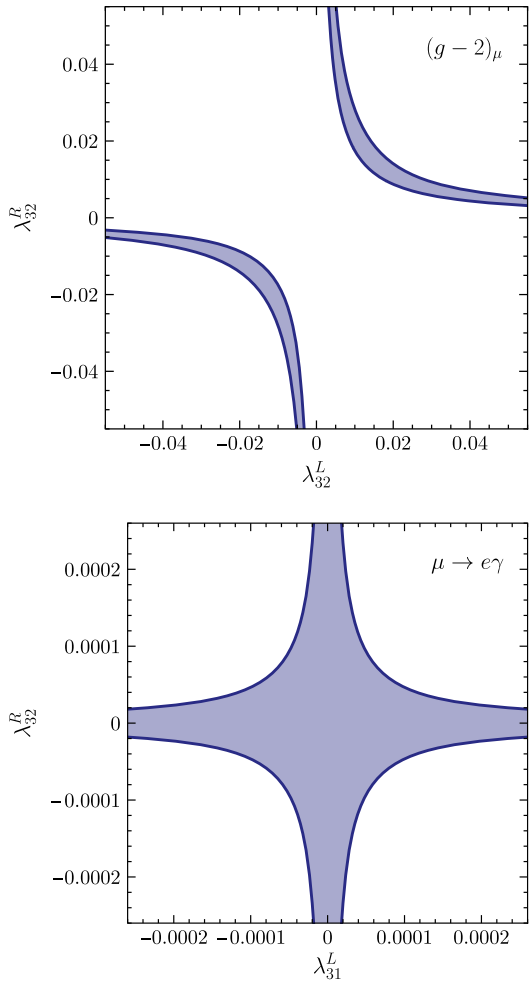

FIG. 13. Constraints on the S_1 leptoquark couplings derived (bottom panel) from the measurements of the $\mu \to e\gamma$ transition and (top panel) from the $(g-2)_\mu$ measurement. The leptoquark mass is chosen as $M_S = 2$ TeV, and only top-Yukawa-enhanced contributions are considered in the numerical analysis. See the text for more details.

E. SMEFT at high-p_T and global fits

While the SMEFT (in combination with the LEFT) is practical for relating low-energy measurements to UV parameters, it can also be used to analyze measurements from higher energies in a model independent way. This makes it a powerful tool for combined analyses of multiple datasets from various types of processes at different energy scales. This is particularly advantageous in light of the plethora of measurements of different processes performed at the LHC and the Large Electron-Positron (LEP) collider. We can use the SMEFT for phenomenological analyses of all of these observables in Higgs physics (Corbett *et al.*, 2013, 2015; Ellis, Sanz, and You, 2014), diboson physics (Butter *et al.*, 2016; Biekoetter, Corbett, and Plehn, 2019; Gomez-Ambrosio, 2019; Grojean, Montull, and Riembau, 2019; Brivio *et al.*, 2020), and top physics (Hartland *et al.*, 2019; Aoude, El Faham *et al.*, 2022; Aoude, Maltoni *et al.*, 2022), as well as for electroweak precision studies (Han and Skiba, 2005; Efrati, Falkowski, and Soreq, 2015; Falkowski and Riva, 2015; Falkowski and Straub, 2020; Bresó-Pla, Falkowski, and González-Alonso, 2021; Almeida *et al.*, 2022) and Drell-Yan tails (Allwicher *et al.*, 2023a; Greljo *et al.*, 2023). Global fits considering multiple components of the aforementioned datasets were performed by Ellis *et al.* (2018, 2021), da Silva Almeida *et al.* (2019), and Ethier *et al.* (2021); see also Dawson, Homiller, and Lane (2020). Such combined analyses of different types of data are necessary since in any reasonable new-physics model multiple SMEFT operators are generated when the heavy particles are integrated out (Jiang and Trott, 2017). These operators can contribute to different processes that can be probed at various energies. In addition, RG mixing can generate further operators contributing to even more processes. Therefore, to carefully evaluate the plausibility of a given BSM theory, it is not enough to look at only a single measurement: we have to perform a global SMEFT fit.

One of the main challenges of these fits is the large number of free parameters in the SMEFT. Thus, one has to apply some simplifying assumptions to reduce the degrees of freedom in a fit. For example, one can decide only to look at a specific set of operators that is particularly relevant for a given set of observables (for example, those involving only top and bottom quarks and electroweak gauge bosons). Moreover, one can apply some flavor-symmetry assumptions as discussed in Sec. III.C. As shown in Table V, the latter allow us to significantly lower the number of parameters that we have to fit while still allowing us to describe the SM flavor structure at a good approximation.

On the one hand, if experimental data show deviations from the SM predictions, global fits are essential to determine the best-fit values of all relevant Wilson coefficients in order to be simultaneously compatible with multiple possibly correlated measurements. On the other hand, if no clear signal of new physics is present in the data, global fits allow us to put upper bounds on the coefficients only. In general the constraints obtained depend on the assumptions entering the fit. Since a truly global fit with all 2499 parameters of the $d = 6$ SMEFT is unfeasible, a selection of certain operators, for example, by choosing a specific flavor symmetry, has to be made. Therefore, keep in mind that the results of the simplified fit cannot necessarily be applied to generic BSM scenarios.

As an illustration of the present state of the art of global fits, in Fig. 14 we report the results of one of the most updated and extensive global analyses of SMEFT coefficients (Ellis *et al.*, 2021). The results are obtained while considering all of the relevant operators constrained by electroweak precision observables, diboson processes, and top-physics measurements from the LHC. The flavor symmetries $U(3)^5$ and $U(3)^3 \times U(2)^2$ are employed; see Sec. III.C. The results for each Wilson coefficient are obtained by marginalizing over the remaining ones. Despite not being fully generic, the number of independent coefficients that are varied at the same time is impressive. One of the most important messages emerging from this analysis is that, under motivated flavor-symmetry assumptions, the present data are compatible with an effective cutoff scale for the SMEFT in the few-TeV domain.

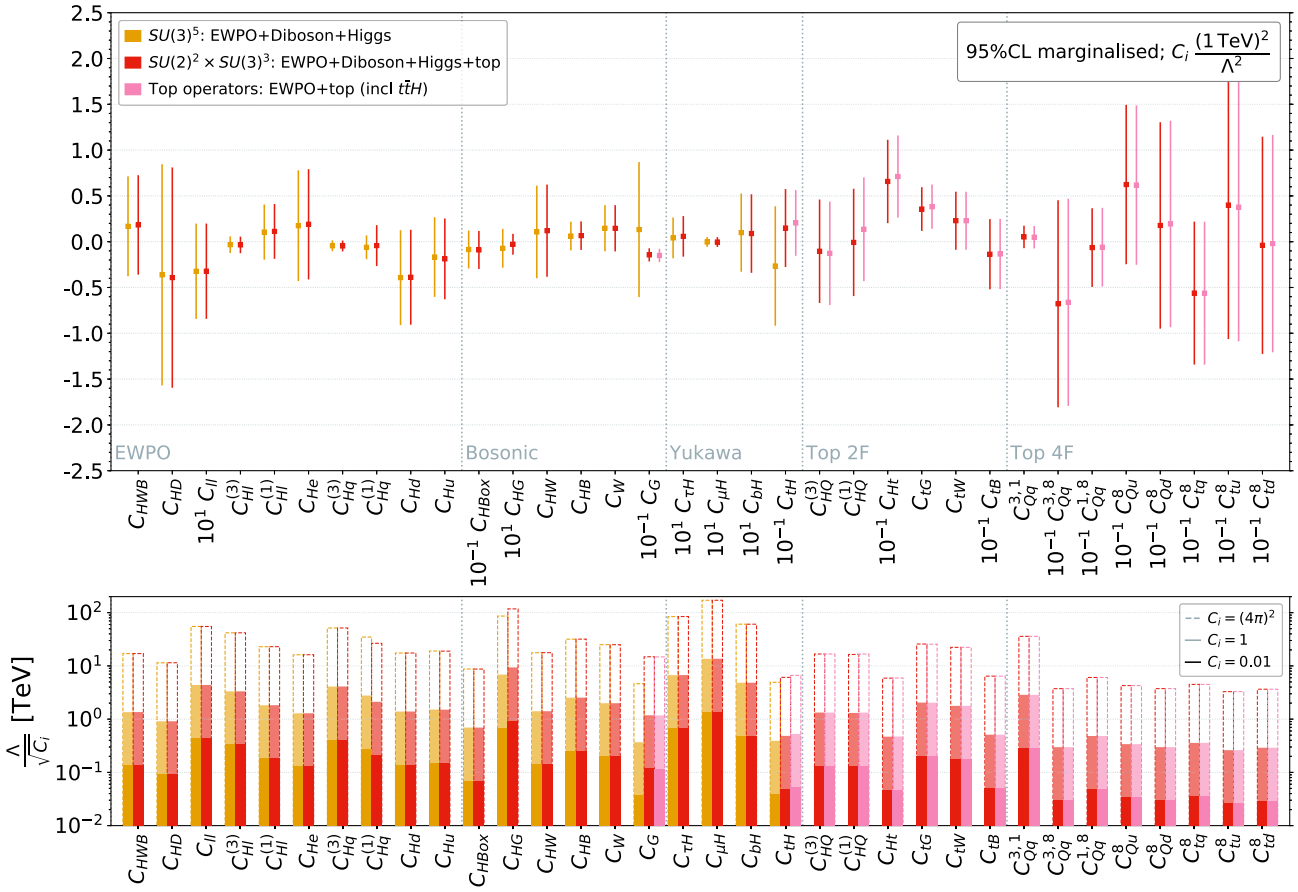

FIG. 14. Bounds on SMEFT effective coefficients obtained by Ellis *et al.* (2021). Top panel: bounds on the coefficients assuming a reference effective scale of 1 TeV. Bottom panel: corresponding bounds on the effective scales for different reference hypotheses for the Wilson coefficients. The light yellow points are obtained in the $\mathrm{U}(3)^5$ symmetric limit. The remaining points are obtained employing the $\mathrm{U}(3)^3 \times \mathrm{U}(2)_u \times \mathrm{U}(2)_q$ flavor symmetry, which allows us to treat top-physics observables separately.

1. Drell-Yan tails

In this section we analyze the specific case of the Drell-Yan process $pp \to \ell^+\ell^-$, which represents a good example of a high-energy transition constraining SMEFT Wilson coefficients. In the SM this process is mediated by the photon and the Z boson, whereas in the SMEFT the dominant contributions are given by four-fermion operators (ψ^4), dipole operators ($\psi^2 XH$), and operators modifying the Z-boson couplings ($\psi^2 H^2 D$). The relevant tree-level Feynman diagrams are shown in Fig. 15. The left diagram shows the SM contribution, and the center diagram shows the contribution by the ψ^4 contact interactions. The diagram for the $\psi^2 XH$ and $\psi^2 H^2 D$ operators is similar to the SM diagram, with the SM interaction vertices replaced by the respective SMEFT

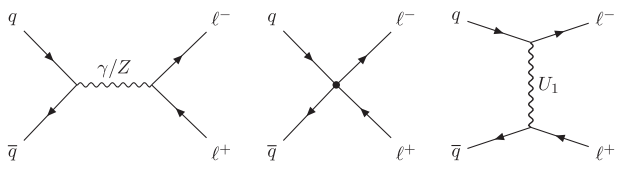

FIG. 15. Tree-level Feynman diagrams contributing to the Drell-Yan process in (left image) the SM, (center image) the SMEFT, and (right image) the U_1 leptoquark model.

interactions. The dominant contribution depends on the energy range that we are investigating. The operators modifying the Z-boson couplings can best be probed at the Z pole, i.e., for invariant masses of the dilepton system of around $m_{\ell\ell} \sim m_Z$. At higher energies the four-fermion contact interaction yields the dominant contribution since its amplitude is energy enhanced compared to the SM. This is what allows us to probe effects due to the exchange of resonances with a mass even above the center-of-mass energy of the collider, as pointed out by Greljo and Marzocca (2017).

In the following, we focus on the high-p_T constraints on ψ^4 operators involving mainly third-generation fermions, which have received considerable interest in the recent literature (Faroughy, Greljo, and Kamenik, 2017; Dawson, Giardino, and Ismail, 2019; Greljo, Camalich, and Ruiz-Álvarez, 2019; Alioli *et al.*, 2020; Angelescu, Faroughy, and Sumensari, 2020; Fuentes-Martin, Greljo *et al.*, 2020; Boughezal, Mereghetti, and Petriello, 2021; Endo *et al.*, 2022; Allwicher *et al.*, 2023a, 2023b; Boughezal, Huang, and Petriello, 2023; Greljo *et al.*, 2023). We also consider measurements of low-energy meson decays that are mediated by the same effective operators. Therefore, we can utilize the SMEFT framework to combine these complementary high-p_T and low-energy constraints to assess the validity of a given BSM scenario. The first analysis of this type, which focused on light-generation

four-fermion operators, was presented by Cirigliano, Gonzalez-Alonso, and Graesser (2013).

In this example, we consider the U_1 vector leptoquark contributing to the Drell-Yan process (see the right diagram in Fig. 15) and to charged-current semileptonic B-meson decays with the underlying $b \to c\tau\nu$ transition. We follow the discussion presented by Aebischer, Isidori *et al.* (2023). The example is particularly interesting due to the deviations currently observed in these low-energy decays, known as the B-anomalies, which were mentioned in Sec. I.B.2. We are especially interested in the lepton-flavor-universality ratios $R_{D^{(*)}}$ defined in Eq. (1.10), which currently show a 3.1σ discrepancy from the SM expectation (Amhis *et al.*, 2023b).[41]

Consider the U_1 Lagrangian

$$\mathcal{L}_{U_1} = \mathcal{L}_{\rm SM} - \tfrac{1}{2} U^\dagger_{\mu\nu} U^{\mu\nu} + M_U^2 U^\dagger_\mu U^\mu + (U_\mu J^\mu + \text{H.c.}), \tag{6.43}$$

$$J^\mu = \frac{g_U}{\sqrt{2}} [\beta^L_{pr} (\bar{q}_p \gamma^\mu \ell_r) + \beta^R_{pr} (\bar{d}_p \gamma^\mu e_r)]. \tag{6.44}$$

Integrating out the U_1 field at tree level using its equation of motion $U_\mu = -J^\dagger_\mu / M_U^2 + \mathcal{O}(M_U^{-4})$, we find that

$$\mathcal{L}_{\rm EFT} = \mathcal{L}_{\rm SM} - \frac{1}{M_U^2} J^\dagger_\mu J^\mu. \tag{6.45}$$

Using the Fierz identities in Eqs. (2.20) and (2.21), we then find the EFT Lagrangian in the Warsaw basis,

$$\mathcal{L}_{\rm W} = \mathcal{L}_{\rm SM} - \frac{g_U^2}{2M_U^2} \left\{ \frac{1}{2} \beta^L_{pr} \beta^{L*}_{st} ([Q^{(1)}_{lq}]_{trps} + [Q^{(3)}_{lq}]_{trps}) + \beta^R_{pr} \beta^{R*}_{st} [Q_{ed}]_{trps} - (2\beta^R_{pr} \beta^{L*}_{st} [Q_{ledq}]_{trps} + \text{H.c.}) \right\}. \tag{6.46}$$

Note that since we restrict our analysis to tree level, we do not have to consider evanescent contributions here.

This Lagrangian provides the appropriate description for interactions at energies above the electroweak scale but below M_U. Thus, we can use it to describe the tails of Drell-Yan distributions where we consider events with $200\ \text{GeV} \lesssim m_{\ell\ell} \lesssim M_U$. For a discussion of the EFT validity in the case where the EFT cutoff scale M_U is not sufficiently high, see the end of this section and Allwicher *et al.* (2023a).

The event yield $\mathcal{N}$ in a given bin of the measured $m_{\ell\ell}$ distribution can then be schematically written as

$$\mathcal{N} = \mathcal{L}_{\rm int} (\mathcal{A} \times \epsilon) \int_{m^2_{\ell\ell,\min}}^{m^2_{\ell\ell,\max}} \mathrm{d}s \frac{\mathrm{d}\sigma}{\mathrm{d}s}, \tag{6.47}$$

where $\mathcal{L}_{\rm int}$ is the integrated luminosity and $\mathcal{A} \times \epsilon$ parametrizes the acceptance and efficiency of the detector and has to be extracted using Monte Carlo simulations. The cross section σ is computed as a function of the Wilson coefficients or new-physics couplings, thus allowing them to be constrained. For more details, see Allwicher *et al.* (2023a). The event yields can also be automatically extracted using codes like `HighPT` (Allwicher *et al.*, 2023b) and `flavio` (Greljo *et al.*, 2023).

The operators in Eq. (6.46) also contribute to low-energy processes. In particular, $[Q^{(3)}_{lq}]_{3323}$ and $[Q_{ledq}]_{3332}$ can contribute to the $b \to c\tau\nu$ transitions that we are interested in. The relevant low-energy Lagrangian can be written as

$$\mathcal{L}_{b\to c} = -\frac{4G_F}{\sqrt{2}} V_{23} [(1 + \mathcal{C}^c_{LL})(\bar{c}_L \gamma^\mu b_L)(\bar{\tau}_L \gamma_\mu \nu_L) - 2\mathcal{C}^c_{LR} (\bar{c}_L b_R)(\bar{\tau}_R \nu_L)], \tag{6.48}$$

where G_F is Fermi's constant and $V_{23} = V_{cb}$ is a CKM matrix element. The coefficients are related to the Warsaw basis Wilson coefficients by

$$\mathcal{C}^c_{LL} = -\frac{1}{\sqrt{2} G_F} \frac{1}{M_U^2} \sum_{k=1}^{3} \frac{[C^{(3)}_{lq}]_{33k3} V_{2k}}{V_{23}}, \tag{6.49}$$

$$\mathcal{C}^c_{LR} = \frac{1}{4\sqrt{2} G_F} \frac{1}{M_U^2} \sum_{k=1}^{3} \frac{[C^*_{ledq}]_{333k} V_{2k}}{V_{23}}, \tag{6.50}$$

where we assume that the flavor basis of the new physics is given by the down-quark and charged-lepton mass basis such that we can write

$$q_p = \begin{pmatrix} V^*_{rp} u^L_r \\ d^L_p \end{pmatrix}, \quad u_p = u^R_p, \quad d_p = d^R_p, \quad \ell_p = \begin{pmatrix} \nu^L_p \\ e^L_p \end{pmatrix}, \quad e_p = e^R_p. \tag{6.51}$$

Following Cornella *et al.* (2021), we can express the lepton-flavor-universality ratios $R_{D^{(*)}}$ in terms of these parameters as

$$\frac{R_D}{R_D^{\rm SM}} = |1 + \mathcal{C}^c_{LL}|^2 - 3.0 \text{Re}[(1 + \mathcal{C}^c_{LL}) \mathcal{C}^{c*}_{LR}] + 4.12 |\mathcal{C}^c_{LR}|^2, \tag{6.52}$$

$$\frac{R_{D^*}}{R_{D^*}^{\rm SM}} = |1 + \mathcal{C}^c_{LL}|^2 - 0.24 \text{Re}[(1 + \mathcal{C}^c_{LL}) \mathcal{C}^{c*}_{LR}] + 0.16 |\mathcal{C}^c_{LR}|^2. \tag{6.53}$$

As numerical input we use the world average for the experimental measurements and the SM predictions for these observables as provided by the HFLAV Collaboration (Amhis *et al.*, 2023a; Amhis *et al.*, 2023b), respectively,

$$R_D = 0.356 \pm 0.029, \qquad R_D^{\rm SM} = 0.298(4), \tag{6.54}$$

$$R_{D^*} = 0.284 \pm 0.013, \qquad R_{D^*}^{\rm SM} = 0.254(5). \tag{6.55}$$

The LEFT beta functions of the coefficients are given by (Jenkins, Manohar, and Stoffer, 2018a)

$$\beta_{\mathcal{C}^c_{LL}} = -4e^2 \mathcal{C}^c_{LL}, \qquad \beta_{\mathcal{C}^c_{LR}} = (\tfrac{4}{3} e^2 - 8 g_3^2) \mathcal{C}^c_{LR}. \tag{6.56}$$

[41] Note that while the fate of this anomaly (as with any anomaly) is unclear, the discussion presented here remains an illustrative example of a SMEFT analysis.

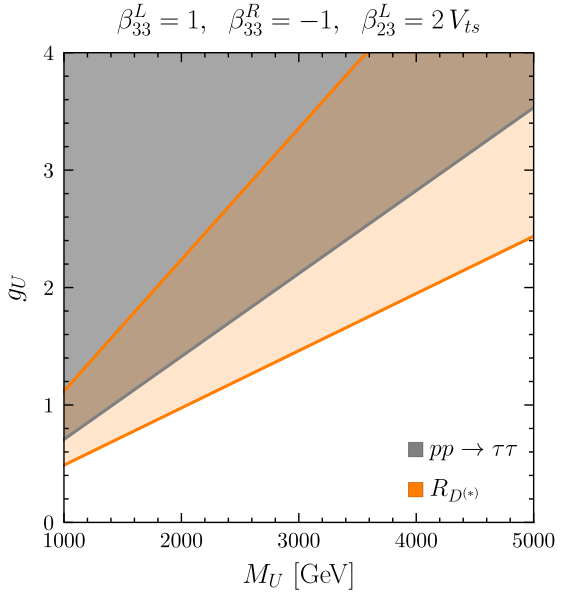

FIG. 16. Constraints on the U_1 model in the plane coupling g_U vs mass M_U. Shown in light orange is the region preferred by the low-energy fit of the $R_{D^{(*)}}$ anomalies, and in dark gray we show the parameter space excluded by the ATLAS search (Aad *et al.*, 2020) for new physics in $pp \to \tau\tau$ scatterings. Both constraints are given at 95% C.L.

We use the LEFT RG equations[42] to directly run the low-energy coefficients from the scale $\mu \sim m_b$ up to $\mu = 1$ TeV, which is the appropriate scale for measurements of the high-p_T Drell-Yan tails at the LHC. There we directly match to the SMEFT and neglect the SMEFT running in good approximation since it yields only a small logarithmic contribution.

To perform the combined fit of the high-p_T Drell-Yan data and the low-energy measurements of $R_{D^{(*)}}$, we assume that all couplings except for $\beta_{33}^{L/R}$ and β_{23}^L vanish, i.e., the U_1 couples dominantly to the third generation. Furthermore, we choose to set $\beta_{33}^L = -\beta_{33}^R = 1$ and $\beta_{23}^L = 2V_{ts}$, adopting the hypothesis of a minimal breaking of the flavor symmetry (Aebischer, Isidori *et al.*, 2023). The combined constraints on the U_1 model in the plane coupling versus mass are shown in Fig. 16. We used the `HighPT` package (Allwicher *et al.*, 2023b) to derive the constraints from the Drell-Yan search for new physics in $pp \to \tau\tau$ scattering by the ATLAS Collaboration (Aad *et al.*, 2020). The 95% C.L. region preferred by our previously discussed low-energy constraint is shown in light orange, whereas the region excluded at 95% C.L. by the LHC is shown in dark gray. In combination, only a fraction of parameter space is left viable, thus showing the complementarity of the low- and high-energy constraints.[43] For more details on this analysis, see Cornella *et al.* (2021) and Aebischer, Isidori *et al.* (2023).

In the case of low masses of the leptoquark ($M_U \sim 1$ TeV), one might question the validity of the EFT approach to Drell-Yan measurements since the kinematical distributions contain events with corresponding center-of-mass energies $\sqrt{s}$ of the same order. Therefore, the EFT expansion in s/M_U^2 can converge poorly, or even break down. To improve the convergence, one can include higher-dimensional operators. We can fit them as additional free parameters, marginalize over them,[44] or we can match them to the parameters of a given UV model, such as the U_1 leptoquark, depending on the scenario that we are considering. If we are too close to the mass threshold of the heavy BSM states, there might be no way to analyze the high-energy data apart from using a concrete UV model. However, in this case the model independence of the EFT approach might be less important as the signal for a concrete new-physics model should be stronger. A discussion of the EFT validity in Drell-Yan tails was provided by Allwicher *et al.* (2023a). For more details, see Sec. II.C.1 and Brivio *et al.* (2022).

VII. CONCLUSION

The standard model has set a natural and successful framework for the qualitative and quantitative understanding of the elementary particles and their interactions. It has been possible to calculate its predictions with great precision, allowing comparisons with similar progress on the experimental side. However, as stated in the Introduction, there are a number of observational and theoretical issues with the SM, such as neutrino masses, baryon asymmetry, a natural bridge to gravity, and the instability of the Higgs quadratic term. This is why it is widely believed, and we share this point of view, that the SM is the remnant of a more complete theory with new degrees of freedom showing up at a higher energy scale. By this statement we imply not that there cannot also be other light states beyond the SM ones but that the SM fields are embedded in a more complete QFT with heavy fields in the UV, addressing many current open issues.

The strong agreement between experiment and theory, which in various cases reaches the subpercent level, suggests that the energy scale where new heavy particles will appear, and where the SM will manifestly become an incomplete description of nature, is well above the electroweak scale. This fact does not prevent the observation of effects related to the new degrees of freedom in current and near-future experiments. However, these effects will be indirect manifestation of new physics, and their interpretation in terms of hypothetical new dynamics requires a suitable effective theory approach.

In this review we examined the EFT approach to physics beyond the SM, focusing, in particular, on the linear realization of the mechanism of electroweak symmetry breaking, i.e., the SMEFT. Given that all measurements of the 125 GeV scalar particle discovered at the LHC are consistent with the properties

[42]The dominant contribution is due to the strong coupling constant $\alpha_s = g_3^2/4\pi$, which runs as $\alpha_s(\mu) = 4\pi/\beta_0 \ln(\mu^2/\Lambda_{\rm QCD}^2)$ at one loop with the one-loop QCD beta function β_0.

[43]CMS data currently indicate a 3σ excess of events in $pp \to \tau\bar{\tau}$, which is highly compatible with a possible U_1 contribution in this parameter region (CMS Collaboration, 2023).

[44]Note that when marginalizing over $d = 8$ operators no correlation among the $d = 6$ and 8 operators is assumed, which is not true in concrete BSM scenarios. In particular, the interference of $d = 6$ and 8 operators with the SM amplitude are allowed to have opposite signs, thus leading to cancellations.

expected for the SM Higgs boson, the SMEFT emerges as the most natural EFT approach to physics beyond the SM. In Sec. II we extensively reviewed the construction of the basis of effective operators, the power counting, and various other technical aspects of this EFT. In Sec. IV we illustrated the more general approach represented by the HEFT and the possibility of a nonlinear realization of the mechanism of electroweak symmetry breaking. This is an option that, despite not being favored by current data, cannot be excluded at present.

An important role in effective field theories is played by exact and approximate symmetries emerging in the low-energy limit of the theory, the so-called accidental symmetries. We reviewed this aspect in Sec. III, focusing, in particular, on flavor symmetries, which represent the vast majority of possible global symmetries in the SMEFT. As we argued, in the absence of flavor symmetries the SMEFT approach is not particularly useful: severe bounds from flavor-violating observables would imply a very high scale of new physics, rendering the entire construction not particularly appealing. However, with the help of motivated hypotheses about a symmetry and symmetry breaking resulting from general dynamical hypothesis in the UV, it is possible to consistently reduce the bounds on the new-physics scales and provide an *a posteriori* justification for the observed mass hierarchies. In this theoretically motivated limit, we can both reduce the number of free parameters of the SMEFT and combine information from flavor-changing and flavor-violating processes.

In Sec. V, and especially in Sec. VI, we discussed the techniques used to put the SMEFT at work in analyzing data and possibly extracting information about physics beyond the SM. These involved a large array of theoretical concepts and methods developed in recent decades, which we brought together here. From the use of low-energy effective theories valid below the electroweak scale to the running of the SMEFT, and finally to the matching to explicit beyond-the-SM theories. We reviewed various technical aspects of this workflow, both from a bottom-up perspective and in top-down approaches. We expect that the noteworthy progress of these calculations will continue in the immediate future.

The SMEFT is already a mature subject, and many studies exist in the literature, including reviews such as that by Brivio and Trott (2019). However, most of the existing studies are focused mainly on the use of this tool in setting bounds on possible new-physics scenarios.

In this review we emphasized the advantage of using the SMEFT in the case of a "positive" signal of new physics. While new-physics bounds can be efficiently set, in many cases, directly at the level of the observables, the full power of the EFT approach manifests itself in the presence of a new-physics signal. In this case the SMEFT, which is a consistent QFT, allows us to connect a signal in one observable to those in other processes and possibly recognize the underlying origin of the new dynamics. We illustrated this chain via two specific examples in Sec. VI that were inspired by "anomalies" (i.e., deviations from the SM predictions) present in current data: the $(g-2)_\mu$ anomaly and the deviation from lepton-flavor universality in $b \to c\ell\nu$ decays. While none of these effects are statistically compelling, we analyzed them since they provide a clear and general illustration of the power of the EFT approach.

This leads us to the important question of how to design a strategy for future experiments and where to focus theoretical work. A general analysis of all experimental results aiming at a global fit to all the 2499 SMEFT dimension-6 coefficients is neither a viable nor a particularly useful option. It is hardly feasible because of the large dimension of the parameter space while also not being especially illuminating, given that in realistic models only a subset of the operators play a relevant phenomenological role. A more purposeful strategy is to work out the main features of representative classes of models as UV conditions on the SMEFT, correspondingly identify the relevant subsets of operators, and then proceed to a comparison with experiments. As discussed in Sec. VI, the new generation of automated tools for the matching, RG evolution, and computation of experimental observables in the involved EFTs make such an approach feasible. An important role in the data-theory comparison is also played by formulating hypotheses on flavor symmetries and corresponding symmetry-breaking terms. These symmetries not only reduce the number of relevant free parameters but also allow us to consider more compelling new-physics scenarios in the few-TeV energy range that can be probed directly by current and near-future experiments, as shown in Fig. 5.

Concerning experimental work, a fruitful direction is to investigate possible differences between the HEFT and the SMEFT. As discussed at the end of Sec. IV.A, progress has been made in constructing UV models that cannot be described by the SMEFT. Correspondingly some experimental signatures that would signal a breakdown of the SMEFT description were also identified. A comprehensive strategy for how to distinguish between the two effective theories could lead to meaningful results in the near future.

The applicability of the SMEFT rests on the validity of the effective theory approach. This itself relies on the hypothesis of having identified all degrees of freedom and symmetries relevant at low energies. In this respect, the wide class of SM extensions with light new degrees of freedom, such as axions or axionlike particles, is not entirely covered by the SMEFT described here. In such models we can imagine that the BSM physics produces two low-energy sectors, one of which is the SM and the other of which is in the world of light particles (such as axions). These two sectors are necessarily weakly coupled to each other and generate low-energy axion physics. In this sense, the SMEFT is part (probably the major part) of a larger effective theory. The inclusion of additional light particles is conceptually simple once the symmetry properties of the new fields are specified; see Agrawal *et al.* (2021), Bauer *et al.* (2021), and Galda, Neubert, and Renner (2021).

More generally EFT approaches are based on the concept of scale separation, a key paradigm that has guided the progress in particle physics for several decades. The absence of TeV-scale new physics, as expected from naive EFT considerations, has stimulated theorists to consider alternatives to this paradigm; see Giudice (2019). While this is an interesting possibility, our knowledge of TeV-scale physics is still far from complete. The possibility of new physics just around the corner of the current energy and precision frontiers remains a well-motivating option, and the SMEFT represents the most suitable tool to analyze it.

ACKNOWLEDGMENTS

We are grateful to Ilaria Brivio, Wilfried Buchmüller, and Peter Stoffer for the useful comments on the manuscript. D. W. thanks the Centre for High Energy Physics (CHEP) at the Indian Institute of Science for the hospitality. This project has received funding from the European Research Council (ERC) under the European Union's Horizon 2020 research and innovation program, Grant Agreement No. 833280 (FLAY), and from the Swiss National Science Foundation (SNF) under Contract 200020_204428.

APPENDIX: DIMENSIONAL REGULARIZATION IN THE SMEFT

As in any QFT, divergences can occur in the computation of one-loop diagrams in EFTs, which need to be regulated. Afterward the theory can be renormalized and physical predictions can be derived. By far the most commonly used regularization scheme in SMEFT computations is dimensional regularization, which we also use throughout this review, where we work in $D = 4 - 2\epsilon$ spacetime dimensions. The most common renormalization scheme for SMEFT computations is the $\overline{\text{MS}}$ scheme, which we also use in most of this work. The only exception is when we deal with evanescent operators, where we choose to work in an evanescent free version of $\overline{\text{MS}}$; see Sec. II.A.5. To be precise, we work in a modified version of $\overline{\text{MS}}$ that contains additional finite counterterms that compensate for the effects of evanescent operators to physical observables, so they can be neglected in all computations.

In the following, we discuss two topics related to the use of dimensional regularization. First, we discuss the method of regions that is often used in EFT computations, for example, when computing one-loop matching conditions. Second, we comment on the issue of chiral fermions in dimensional regularization, i.e., the generalization of the γ^5 matrix to D dimensions.

1. The method of regions

The method of expansion by regions (Beneke and Smirnov, 1998; Jantzen, 2011) simplifies the calculation of multiscale loop integrals. Loop integrals can depend on several different scales (for example, masses or external momenta), each defining an integration region. For each scale we can expand the loop integrand in the quantities that are small in the respective region and then perform the resulting integral over the entire D-dimensional space. The method of regions states that doing this for all regions and summing the results yields the same answer as performing the full original integral and expanding afterward.

As an example, consider the loop integral

$$\mathcal{I} = \int \frac{\mathrm{d}^D k}{(2\pi)^D} \frac{1}{k^2 - M^2} \frac{1}{k^2 - m^2} = \frac{i}{16\pi^2} \left[\frac{1}{\epsilon} + \log\left(\frac{\mu^2}{M^2}\right) + 1 + \frac{m^2}{M^2} \log\left(\frac{m^2}{M^2}\right) \right] + \mathcal{O}(M^{-4}), \tag{A1}$$

which entails two regions called soft ($k \sim m$) and hard ($k \sim M$). Expanding the propagators in the soft ($k^2 \sim m^2 \ll M^2$) and hard ($k^2 \sim M^2 \gg m^2$) regions before the integration

$$\frac{1}{k^2 - M^2} = -\frac{1}{M^2} \left[1 + \frac{k^2}{M^2} + \mathcal{O}\left(\frac{k^4}{M^4}\right) \right], \tag{A2}$$

$$\frac{1}{k^2 - m^2} = \frac{1}{k^2} \left[1 + \frac{m^2}{k^2} + \mathcal{O}\left(\frac{m^4}{k^4}\right) \right], \tag{A3}$$

we find the corresponding integrals in each region,

$$\mathcal{I}|_{\text{soft}} = -\frac{1}{M^2} \int \frac{\mathrm{d}^D k}{(2\pi)^D} \left[\frac{1}{k^2 - m^2} + \cdots \right] = -\frac{i}{16\pi^2} \frac{m^2}{M^2} \left[\frac{1}{\epsilon} + \log\left(\frac{\mu^2}{m^2}\right) + 1 \right] + \mathcal{O}(M^{-4}), \tag{A4}$$

$$\mathcal{I}|_{\text{hard}} = \int \frac{\mathrm{d}^D k}{(2\pi)^D} \frac{1}{k^2} \frac{1}{k^2 - M^2} \left[1 + \frac{m^2}{k^2} + \cdots \right] = \frac{i}{16\pi^2} \left[\frac{1}{\epsilon} + \log\left(\frac{\mu^2}{M^2}\right) + 1 \right] \left(1 + \frac{m^2}{M^2} \right) + \mathcal{O}(M^{-4}). \tag{A5}$$

Thus, we find working at the order $\mathcal{O}(M^{-2})$,

$$\mathcal{I} = \mathcal{I}|_{\text{hard}} + \mathcal{I}|_{\text{soft}} + \mathcal{O}(M^{-4}), \tag{A6}$$

as dictated by the method of regions.

As discussed in Sec. VI.B, the method of regions provides a powerful tool for EFT matching computations. These are multiscale problems, and applying this method allows for a separation of the hard UV dynamics from the soft IR behavior. In these computations we have to determine Green's functions in the UV theory and the corresponding EFT. In both theories we can split these into hard and soft regions. Since we require both theories to describe the same IR physics, the soft regions of both theories (which describe the low-energy dynamics) must agree. Thus, the one-loop matching conditions for the EFT Wilson coefficients are determined solely by the hard regions encoding the UV dynamics. However, since the EFT by definition does not contain any UV scales, its hard scale loop integrals must be scaleless and thus vanish exactly in dimensional regularization. This holds for all integrals apart from

$$\int \frac{\mathrm{d}^D k}{(2\pi)^D} \frac{1}{k^4} = \frac{i}{16\pi^2} \left(\frac{1}{\epsilon_{\text{UV}}} - \frac{1}{\epsilon_{\text{IR}}} \right) = 0, \tag{A7}$$

which vanishes only since we identify $\epsilon_{\text{UV}} = \epsilon_{\text{IR}}$ by analytic continuation in dimensional regularization. Therefore, it is sufficient to consider only the hard region of the Green's functions of the UV theory, which contains all of the information required to determine the EFT Wilson coefficients. The entire procedure of applying the method of regions is schematically shown in Fig. 17.

Figure 17 also highlights the connection of the different UV and IR divergences encountered in the computation.

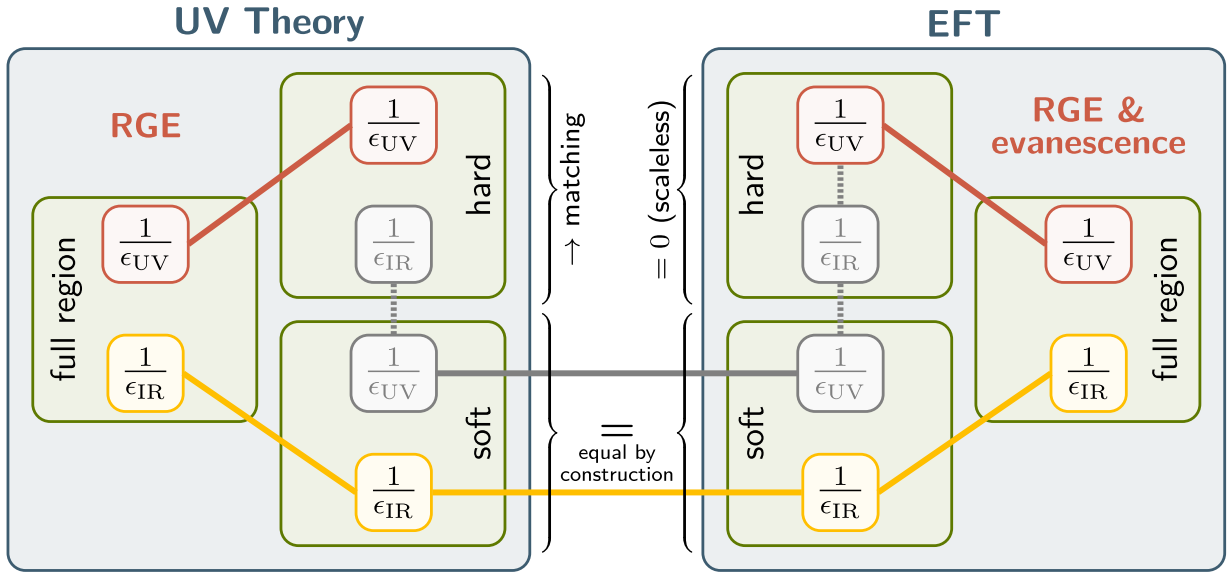

FIG. 17. Illustration of the method of regions applied for EFT matching. The separation of the full integration region into hard and soft regions (green frames) is shown for the UV theory and the corresponding EFT. For each region the UV (IR) poles are highlighted in red (yellow) at the top (bottom) of each box. The UV divergences require counterterms and allow one to extract the RGE and the contributions of evanescent operators. The artificial divergences introduced by the method of region are shown in gray and cancel between the soft and the hard region as indicated by the dashed lines connecting them. Divergences that are equal are connected by a solid line, whereas divergences that have the same magnitude but opposite sign are linked by dashed lines. The soft region of both theories are equal by construction, and the hard region of the EFT contains only scaleless integrals and thus vanishes in dimensional regularization.

The UV poles (red) and IR poles (yellow) of a theory must match the corresponding poles in the hard and soft regions, respectively. However, applying the method of regions introduces additional artificial divergences (gray) into both regions. But, since the sum of both regions must yield back the full solution, these must cancel between the soft and hard regions. Recall that the UV and IR poles of the hard EFT region must also cancel due to Eq. (A7). In Fig. 17 canceling divergences are connected by dashed lines, whereas equal poles are linked by solid lines. When performing a computation, we use the renormalized versions of these theories; i.e., we introduce counterterms canceling the UV poles. As previously mentioned, for a matching computation we need only compute the hard region of the UV theory. The $\epsilon_{\rm UV}$ poles of this region are canceled by the appropriate counterterms, and from Fig. 17 we see that the artificial IR poles provide the exact counterterms to cancel the UV poles of the resulting EFT. Thus, the EFT is automatically renormalized.

Note that the method of regions is also useful for extracting only the UV divergences of a theory since these are entirely encoded in its hard region. Therefore, it simplifies the extraction of the RG equations of a theory, and also the computation of the physical effect of the evanescent operators (see Sec. II.A.5), since both are entirely determined by $\epsilon_{\rm UV}$.

2. Treatment of γ_5 in D dimensions

When one works in D dimensions, the Dirac algebra is infinite dimensional for noninteger D, as mentioned in Sec. II.A.5. While the usual Dirac matrices are defined by interpolation of the D-dimensional Dirac basis γ^μ for $\mu \in \{0, \ldots, D = 2n\}$ with an integer $n \geq 2$, the γ_5 matrix is not easily generalizable to $D \neq 4$ dimensions. This is due to the intrinsically four-dimensional relation $\gamma_5 = -(i/4!)\varepsilon_{\mu\nu\rho\sigma}\gamma^\mu\gamma^\nu\gamma^\rho\gamma^\sigma$ linking it to the Levi-Civita tensor that can be defined only for $D = 4$. Thus, any regularization and renormalization scheme must provide a prescription for treating γ_5 in dimensional regularization.

Throughout this review, we have employed the (semi)naive dimensional regularization scheme, which assumes that the four-dimensional anticommutation relations (Nicolai and Townsend, 1980; Kreimer, 1990; Korner, Kreimer, and Schilcher, 1992)

$$\{\gamma^\mu, \gamma^\nu\} = 2g^{\mu\nu}, \quad \{\gamma^\mu, \gamma_5\} = 0, \quad \gamma_5^2 = \mathbb{1} \tag{A8}$$

also hold away from $D = 4$. This is inconsistent with the cyclicity of the trace and $\mathrm{tr}(\gamma^\mu\gamma^\nu\gamma^\rho\gamma^\sigma\gamma_5) \neq 0$. To reproduce the correct four-dimensional limit, we formally substitute

$$\mathrm{tr}(\gamma^\mu\gamma^\nu\gamma^\rho\gamma^\sigma\gamma_5) = -4i\varepsilon^{\mu\nu\rho\sigma} \tag{A9}$$

with $\varepsilon^{0123} = +1$. This breaks the cyclicity of traces with six or more γ^μ matrices and an odd number of γ_5, thus introducing a reading point ambiguity. That means that these traces depend on which γ matrix is put first or last in the trace. For example, when computing the Feynman diagrams in Fig. 2 with insertions of the operator $Q^{(3)}_{lequ}$, we find, depending on where we start reading the closed fermion loop, the two Dirac traces

$$\mathrm{tr}_1 \equiv \mathrm{tr}(\gamma^\alpha\gamma^\rho\gamma^\sigma\gamma_\alpha\gamma^\mu\gamma^\nu\gamma_5) = 4i(4-D)\epsilon^{\mu\nu\rho\sigma}, \tag{A10}$$

$$\mathrm{tr}_2 \equiv \mathrm{tr}(\gamma^\rho\gamma^\sigma\gamma_\alpha\gamma^\mu\gamma^\nu\gamma_5\gamma^\alpha) = -4i(4-D)\epsilon^{\mu\nu\rho\sigma}, \tag{A11}$$

which can be shown using Eq. (A9) and $\gamma^\alpha\gamma^\mu\gamma^\nu\gamma_\alpha = 4g^{\mu\nu}\mathbb{1} - (4-D)\gamma^\mu\gamma^\nu$. We thus find that

$$\mathrm{tr}_1 - \mathrm{tr}_2 = \mathcal{O}(\epsilon) \neq 0, \tag{A12}$$

which contradicts the cyclicity of the trace. In EFT analyses using the NDR scheme, we must therefore carefully apply a consistent reading point prescription throughout all computations to obtain consistent results (Fuentes-Martin, König *et al.*, 2021; Carmona *et al.*, 2022; Fuentes-Martin *et al.*, 2023b).

To avoid the ambiguities related to the reading point of Dirac traces, one can resort to the 't Hooft–Veltman (HV) scheme ('t Hooft and Veltman, 1972; Breitenlohner and Maison, 1977), which is the only γ_5 scheme that has proven to be self-consistent to all orders. In this scheme we define

$$\{\gamma^\mu, \gamma_5\} = 0 \quad \text{for } \mu \in \{0,1,2,4\}, \tag{A13}$$

$$[\gamma^\mu, \gamma_5] = 0 \quad \text{otherwise}. \tag{A14}$$

While being the only known self-consistent scheme, HV comes with a subtlety in that it breaks chiral symmetry and thus the Ward identities, which need to be restored by finite renormalizations. In addition, the HV scheme is computationally more expensive than NDR due to the splitting of the Dirac algebra into a four- and a $(D-4)$-dimensional part. We therefore stick to the NDR scheme throughout this review, which is sufficient for the topics discussed here. For a more detailed discussion of regularization schemes in D dimensions and the problems of extending γ_5 to D dimensions, see Jegerlehner (2001), Gnendiger *et al.* (2017), and references therein.

REFERENCES

Aad, Georges, *et al.* (ATLAS Collaboration), 2012, "Observation of a new particle in the search for the standard model Higgs boson with the ATLAS detector at the LHC," Phys. Lett. B **716**, 1–29.

Aad, Georges, *et al.* (ATLAS Collaboration), 2020, "Search for Heavy Higgs Bosons Decaying into Two Tau Leptons with the ATLAS Detector Using pp Collisions at $\sqrt{s} = 13$ TeV," Phys. Rev. Lett. **125**, 051801.

Aaij, R., *et al.* (LHCb Collaboration), 2023, "Test of Lepton Universality in $b \to s\ell^+\ell^-$ Decays," Phys. Rev. Lett. **131**, 051803.

Abbott, L. F., 1981, "The background field method beyond one loop," Nucl. Phys. **B185**, 189–203.

Abbott, L. F., Marcus T. Grisaru, and Robert K. Schaefer, 1983, "The background field method and the S matrix," Nucl. Phys. **B229**, 372–380.

Abi, B., *et al.* (Muon $g-2$), 2021, "Measurement of the Positive Muon Anomalous Magnetic Moment to 0.46 ppm," Phys. Rev. Lett. **126**, 141801.

Adams, Allan, Nima Arkani-Hamed, Sergei Dubovsky, Alberto Nicolis, and Riccardo Rattazzi, 2006, "Causality, analyticity and an IR obstruction to UV completion," J. High Energy Phys. 10, 014.

Aebischer, Jason, Christoph Bobeth, Andrzej J. Buras, and Jacky Kumar, 2020, "SMEFT ATLAS of $\Delta F = 2$ transitions," J. High Energy Phys. 12, 187.

Aebischer, Jason, Christoph Bobeth, Andrzej J. Buras, Jacky Kumar, and Mikołaj Misiak, 2021, "General non-leptonic $\Delta F = 1$ WET at the NLO in QCD," J. High Energy Phys. 11, 227.

Aebischer, Jason, Andrzej J. Buras, and Jacky Kumar, 2022, "NLO QCD renormalization group evolution for nonleptonic $\Delta F = 2$ transitions in the SMEFT," Phys. Rev. D **106**, 035003.

Aebischer, Jason, Andrzej J. Buras, and Jacky Kumar, 2023, "Simple rules for evanescent operators in one-loop basis transformations," Phys. Rev. D **107**, 075007.

Aebischer, Jason, Wouter Dekens, Elizabeth E. Jenkins, Aneesh V. Manohar, Dipan Sengupta, and Peter Stoffer, 2021, "Effective field theory interpretation of lepton magnetic and electric dipole moments," J. High Energy Phys. 07, 107.

Aebischer, Jason, Matteo Fael, Alexander Lenz, Michael Spannowsky, and Javier Virto, 2019, Eds., "Computing tools for the SMEFT," arXiv:1910.11003v1.

Aebischer, Jason, Gino Isidori, Marko Pesut, Ben A. Stefanek, and Felix Wilsch, 2023, "Confronting the vector leptoquark hypothesis with new low- and high-energy data," Eur. Phys. J. C **83**, 153.

Aebischer, Jason, Jacky Kumar, Peter Stangl, and David M. Straub, 2019, "A global likelihood for precision constraints and flavour anomalies," Eur. Phys. J. C **79**, 509.

Aebischer, Jason, Jacky Kumar, and David M. Straub, 2018, "`Wilson`: A `Python` package for the running and matching of Wilson coefficients above and below the electroweak scale," Eur. Phys. J. C **78**, 1026.

Aebischer, Jason, and Marko Pesut, 2022, "One-loop Fierz transformations," J. High Energy Phys. 10, 090.

Aebischer, Jason, Marko Pesut, and Zachary Polonsky, 2023, "Dipole operators in Fierz identities," Phys. Lett. B **842**, 137968.

Aebischer, Jason, *et al.*, 2023, "Computing tools for effective field theories," arXiv:2307.08745.

Agrawal, Prateek, *et al.*, 2021, "Feebly-interacting particles: FIPs 2020 workshop report," Eur. Phys. J. C **81**, 1015.

Aguilar-Saavedra, J. A., 2009a, "A minimal set of top anomalous couplings," Nucl. Phys. **B812**, 181–204.

Aguilar-Saavedra, J. A., 2009b, "A minimal set of top-Higgs anomalous couplings," Nucl. Phys. **B821**, 215–227.

Alexandrou, C., *et al.* (Extended Twisted Mass Collaboration), 2023, "Lattice calculation of the short and intermediate time-distance hadronic vacuum polarization contributions to the muon magnetic moment using twisted-mass fermions," Phys. Rev. D **107**, 074506.

Alioli, Simone, Radja Boughezal, Emanuele Mereghetti, and Frank Petriello, 2020, "Novel angular dependence in Drell-Yan lepton production via dimension-8 operators," Phys. Lett. B **809**, 135703.

Allwicher, Lukas, Darius A. Faroughy, Florentin Jaffredo, Olcyr Sumensari, and Felix Wilsch, 2023a, "Drell-Yan tails beyond the standard model," J. High Energy Phys. 03, 064.

Allwicher, Lukas, Darius. A. Faroughy, Florentin Jaffredo, Olcyr Sumensari, and Felix Wilsch, 2023b, "`HighPT`: A tool for high-p_T Drell-Yan tails beyond the standard model," Comput. Phys. Commun. **289**, 108749.

Almeida, Eduardo da Silva, Alexandre Alves, Oscar J. P. Éboli, and M. C. Gonzalez-Garcia, 2022, "Electroweak legacy of the LHC run II," Phys. Rev. D **105**, 013006.

Alonso, R., M. B. Gavela, L. Merlo, S. Rigolin, and J. Yepes, 2013, "The effective chiral Lagrangian for a light dynamical 'Higgs particle,'" Phys. Lett. B **722**, 330–335.

Alonso, Rodrigo, Hsi-Ming Chang, Elizabeth E. Jenkins, Aneesh V. Manohar, and Brian Shotwell, 2014, "Renormalization group evolution of dimension-six baryon number violating operators," Phys. Lett. B **734**, 302–307.

Alonso, Rodrigo, Elizabeth E. Jenkins, and Aneesh V. Manohar, 2016a, "A geometric formulation of Higgs effective field theory: Measuring the curvature of scalar field space," Phys. Lett. B **754**, 335–342.

Alonso, Rodrigo, Elizabeth E. Jenkins, and Aneesh V. Manohar, 2016b, "Sigma models with negative curvature," Phys. Lett. B **756**, 358–364.

Alonso, Rodrigo, Elizabeth E. Jenkins, and Aneesh V. Manohar, 2016c "Geometry of the scalar sector," J. High Energy Phys. 08, 101.

Alonso, Rodrigo, Elizabeth E. Jenkins, Aneesh V. Manohar, and Michael Trott, 2014, "Renormalization group evolution of the standard model dimension six operators III: Gauge coupling dependence and phenomenology," J. High Energy Phys. 04, 159.

Alonso, Rodrigo, and Mia West, 2022, "Roads to the standard model," Phys. Rev. D **105**, 096028.

Amhis, Yasmine Sara, *et al.* (Heavy Flavor Averaging Group Collaboration), 2023a, "Preliminary average of $R(D)$ and $R(D^*)$ for winter 2023," https://hflav-eos.web.cern.ch/hflav-eos/semi/winter23_prel/html/RDsDsstar/RDRDs.html.

Amhis, Yasmine Sara, *et al.* (Heavy Flavor Averaging Group Collaboration Collaboration), 2023b, "Averages of b-hadron, c-hadron, and τ-lepton properties as of 2021," Phys. Rev. D **107**, 052008.

Ananthanarayan, B., M. S. A. Alam Khan, and Daniel Wyler, 2023, "Chiral perturbation theory: Reflections on effective theories of the standard model," Indian J. Phys. **97**, 3245–3267.

Angelescu, Andrei, Darius A. Faroughy, and Olcyr Sumensari, 2020, "Lepton flavor violation and dilepton tails at the LHC," Eur. Phys. J. C **80**, 641.

Aoude, Rafael, Hesham El Faham, Fabio Maltoni, and Eleni Vryonidou, 2022, "Complete SMEFT predictions for four top quark production at hadron colliders," J. High Energy Phys. 10, 163.

Aoude, Rafael, Fabio Maltoni, Olivier Mattelaer, Claudio Severi, and Eleni Vryonidou, 2022, "Renormalisation group effects on SMEFT interpretations of LHC data," arXiv:2212.05067.

Aoyama, T., *et al.*, 2020, "The anomalous magnetic moment of the muon in the standard model," Phys. Rep. **887**, 1–166.

Appelquist, Thomas, and Claude W. Bernard, 1980, "Strongly interacting Higgs bosons," Phys. Rev. D **22**, 200.

Appelquist, Thomas, and Claude W. Bernard, 1981, "The nonlinear σ model in the loop expansion," Phys. Rev. D **23**, 425.

Appelquist, Thomas, and J. Carazzone, 1975, "Infrared singularities and massive fields," Phys. Rev. D **11**, 2856.

Arzt, C., M. B. Einhorn, and J. Wudka, 1995, "Patterns of deviation from the standard model," Nucl. Phys. **B433**, 41–66.

Arzt, Christopher, 1995, "Reduced effective Lagrangians," Phys. Lett. B **342**, 189–195.

Azatov, Aleksandr, Roberto Contino, Camila S. Machado, and Francesco Riva, 2017, "Helicity selection rules and noninterference for BSM amplitudes," Phys. Rev. D **95**, 065014.

Babu, K. S., Chung Ngoc Leung, and James T. Pantaleone, 1993, "Renormalization of the neutrino mass operator," Phys. Lett. B **319**, 191–198.

Baglio, Julien, Sally Dawson, Samuel Homiller, Samuel D. Lane, and Ian M. Lewis, 2020, "Validity of standard model EFT studies of VH and VV production at NLO," Phys. Rev. D **101**, 115004.

Baldini, A. M., *et al.* (MEG Collaboration), 2016, "Search for the lepton flavour violating decay $\mu^+ \to e^+\gamma$ with the full dataset of the MEG experiment," Eur. Phys. J. C **76**, 434.

Banta, Ian, Timothy Cohen, Nathaniel Craig, Xiaochuan Lu, and Dave Sutherland, 2022, "Non-decoupling new particles," J. High Energy Phys. 02, 029.

Barbieri, Riccardo, 2019, "The paradox of the standard model," arXiv:1707.05637.

Barbieri, Riccardo, Dario Buttazzo, Filippo Sala, and David M. Straub, 2012, "Flavour physics from an approximate $U(2)^3$ symmetry," J. High Energy Phys. 07, 181.

Barbieri, Riccardo, Gino Isidori, Joel Jones-Perez, Paolo Lodone, and David M. Straub, 2011, "U(2) and minimal flavour violation in supersymmetry," Eur. Phys. J. C **71**, 1725.

Bardin, Dmitri Yu., Martin Grunewald, and Giampiero Passarino, 1999, "Precision calculation project report," arXiv:hep-ph/9902452.

Barducci, D., *et al.*, 2018, "Interpreting top-quark LHC measurements in the standard-model effective field theory," arXiv:1802.07237.

Bauer, Martin, Matthias Neubert, Sophie Renner, Marvin Schnubel, and Andrea Thamm, 2021, "The low-energy effective theory of axions and ALPs," J. High Energy Phys. 04, 063.

Bellazzini, Brando, Joan Elias Miró, Riccardo Rattazzi, Marc Riembau, and Francesco Riva, 2021, "Positive moments for scattering amplitudes," Phys. Rev. D **104**, 036006.

Beneke, M., and Vladimir A. Smirnov, 1998, "Asymptotic expansion of Feynman integrals near threshold," Nucl. Phys. **B522**, 321–344.

Bennett, G. W., *et al.* (Muon $g-2$ Collaboration), 2006, "Final report of the muon E821 anomalous magnetic moment measurement at BNL," Phys. Rev. D **73**, 072003.

Bern, Zvi, Julio Parra-Martinez, and Eric Sawyer, 2020, "Structure of two-loop SMEFT anomalous dimensions via on-shell methods," J. High Energy Phys. 10, 211.

Bernard, Veronique, 2008, "Chiral perturbation theory and baryon properties," Prog. Part. Nucl. Phys. **60**, 82–160.

Biekoetter, Anke, Tyler Corbett, and Tilman Plehn, 2019, "The Gauge-Higgs legacy of the LHC run II," SciPost Phys. **6**, 064.

Blankenburg, Gianluca, Gino Isidori, and Joel Jones-Perez, 2012, "Neutrino masses and LFV from minimal breaking of $U(3)^5$ and $U(2)^5$ flavor symmetries," Eur. Phys. J. C **72**, 2126.

Boggia, Michele, Raquel Gomez-Ambrosio, and Giampiero Passarino, 2016, "Low energy behaviour of standard model extensions," J. High Energy Phys. 05, 162.

Bona, Marcella, *et al.*, 2022, "Unitarity triangle global fits testing the standard model: UTfit 2021 SM update," Proc. Sci. EPS-HEP2021, 512.

Bonnefoy, Quentin, Emanuele Gendy, Christophe Grojean, and Joshua T. Ruderman, 2022, "Beyond Jarlskog: 699 invariants for CP violation in SMEFT," J. High Energy Phys. 08, 032.

Bonnefoy, Quentin, Emanuele Gendy, Christophe Grojean, and Joshua T. Ruderman, 2023, "Opportunistic CP violation," J. High Energy Phys. 06, 141.

Bordone, Marzia, Oscar Catà, and Thorsten Feldmann, 2020, "Effective theory approach to new physics with flavour: General framework and a leptoquark example," J. High Energy Phys. 01, 067.

Borsanyi, Sz., *et al.*, 2021, "Leading hadronic contribution to the muon magnetic moment from lattice QCD," Nature (London) **593**, 51–55.

Boughezal, Radja, Yingsheng Huang, and Frank Petriello, 2022, "Exploring the SMEFT at dimension eight with Drell-Yan transverse momentum measurements," Phys. Rev. D **106**, 036020.

Boughezal, Radja, Yingsheng Huang, and Frank Petriello, 2023, "Impact of high invariant-mass Drell-Yan forward-backward asymmetry measurements on SMEFT fits," arXiv:2303.08257.

Boughezal, Radja, Emanuele Mereghetti, and Frank Petriello, 2021, "Dilepton production in the SMEFT at $\mathcal{O}(1/\Lambda^4)$," Phys. Rev. D **104**, 095022.

Boyd, J. T., 2022, "LHC run-2 and future prospects," CERN Yellow Rep. Sch. Proc. **5**, 247.

Breitenlohner, P., and D. Maison, 1977, "Dimensional renormalization and the action principle," Commun. Math. Phys. **52**, 11–38.

Bresó-Pla, Víctor, Adam Falkowski, and Martín González-Alonso, 2021, "A_{FB} in the SMEFT: Precision Z physics at the LHC," J. High Energy Phys. 08, 021.

Brivio, I., T. Corbett, O. J. P. Éboli, M. B. Gavela, J. Gonzalez-Fraile, M. C. Gonzalez-Garcia, L. Merlo, and S. Rigolin, 2014, "Disentangling a dynamical Higgs," J. High Energy Phys. 03, 024.

Brivio, I., J. Gonzalez-Fraile, M. C. Gonzalez-Garcia, and L. Merlo, 2016, "The complete HEFT Lagrangian after the LHC run I," Eur. Phys. J. C **76**, 416.

Brivio, Ilaria, Sebastian Bruggisser, Fabio Maltoni, Rhea Moutafis, Tilman Plehn, Eleni Vryonidou, Susanne Westhoff, and C. Zhang, 2020, "O new physics, where art thou? A global search in the top sector," J. High Energy Phys. 02, 131.

Brivio, Ilaria, Sally Dawson, Jorge de Blas, Gauthier Durieux, Pierre Savard, Ansgar Denner, Ayres Freitas, Chris Hays, Ben Pecjak, and Alessandro Vicini, 2021, "Electroweak input parameters," arXiv:2111.12515.

Brivio, Ilaria, and Michael Trott, 2017, "Scheming in the SMEFT … and a reparameterization invariance!," J. High Energy Phys. 07, 148.

Brivio, Ilaria, and Michael Trott, 2019, "The standard model as an effective field theory," Phys. Rep. **793**, 1–98.

Brivio, Ilaria, *et al.*, 2022, "Truncation, validity, uncertainties," arXiv:2201.04974.

Buchalla, G., O. Cata, A. Celis, and C. Krause, 2017, "Standard model extended by a heavy singlet: Linear vs. nonlinear EFT," Nucl. Phys. **B917**, 209–233.

Buchalla, Gerhard, Andrzej J. Buras, and Markus E. Lautenbacher, 1996, "Weak decays beyond leading logarithms," Rev. Mod. Phys. **68**, 1125–1144.

Buchalla, Gerhard, Oscar Catà, and Claudius Krause, 2014, "Complete electroweak chiral Lagrangian with a light Higgs at NLO," Nucl. Phys. **B880**, 552–573.

Buchmüller, W., B. Lampe, and N. Vlachos, 1987, "Contact interactions and the Callan-Gross relation," Phys. Lett. B **197**, 379–382.

Buchmüller, W., and D. Wyler, 1986, "Effective Lagrangian analysis of new interactions and flavor conservation," Nucl. Phys. **B268**, 621–653.

Buras, Andrzej, 2020, *Gauge Theory of Weak Decays* (Cambridge University Press, Cambridge, England).

Buras, Andrzej J., 2003, "Minimal flavor violation," Acta Phys. Pol. B **34**, 5615–5668 [arXiv:hep-ph/0310208v1].

Buras, Andrzej J., and Peter H. Weisz, 1990, "QCD nonleading corrections to weak decays in dimensional regularization and 't Hooft–Veltman schemes," Nucl. Phys. **B333**, 66–99.

Butter, Anja, Oscar J. P. Éboli, J. Gonzalez-Fraile, M. C. Gonzalez-Garcia, Tilman Plehn, and Michael Rauch, 2016, "The Gauge-Higgs legacy of the LHC run I," J. High Energy Phys. 07, 152.

Callan, Jr., Curtis G., Sidney R. Coleman, J. Wess, and Bruno Zumino, 1969, "Structure of phenomenological Lagrangians. II," Phys. Rev. **177**, 2247–2250.

Carmona, Adrian, Achilleas Lazopoulos, Pablo Olgoso, and Jose Santiago, 2022, "`MatchMakerEFT`: Automated tree-level and one-loop matching," SciPost Phys. **12**, 198.

Cè, Marco, *et al.*, 2022, "Window observable for the hadronic vacuum polarization contribution to the muon $g-2$ from lattice QCD," Phys. Rev. D **106**, 114502.

Celis, Alejandro, Javier Fuentes-Martin, Avelino Vicente, and Javier Virto, 2017, "`DsixTools`: The standard model effective field theory toolkit," Eur. Phys. J. C **77**, 405.

Chala, Mikael, Guilherme Guedes, Maria Ramos, and Jose Santiago, 2021, "Towards the renormalisation of the standard model effective field theory to dimension eight: Bosonic interactions I," SciPost Phys. **11**, 065.

Chala, Mikael, and Jose Santiago, 2022, "Positivity bounds in the standard model effective field theory beyond tree level," Phys. Rev. D **105**, L111901.

Chala, Mikael, and Arsenii Titov, 2021, "Neutrino masses in the standard model effective field theory," Phys. Rev. D **104**, 035002.

Chan, Lai-Him, 1986, "Derivative Expansion for the One-Loop Effective Actions with Internal Symmetry," Phys. Rev. Lett. **57**, 1199.

Chatrchyan, Serguei, *et al.* (CMS Collaboration), 2012, "Observation of a new boson at a mass of 125 GeV with the CMS experiment at the LHC," Phys. Lett. B **716**, 30–61.

Cheyette, Oren, 1988, "Effective action for the standard model with large Higgs mass," Nucl. Phys. **B297**, 183–204.

Chivukula, R. Sekhar, and Howard Georgi, 1987, "Composite technicolor standard model," Phys. Lett. B **188**, 99–104.

Cirigliano, Vincenzo, Martin Gonzalez-Alonso, and Michael L. Graesser, 2013, "Non-standard Charged current interactions: Beta decays versus the LHC," J. High Energy Phys. 02, 046.

CMS Collaboration, 2023, "Search for a third-generation leptoquark coupled to a τ lepton and a b quark through single, pair, and nonresonant production in proton-proton collisions at $\sqrt{s} = 13$ TeV," Reports No. CMS-EXO-19-016 and No. CERN-EP-2023-144 [arXiv:2308.07826].

Cohen, Timothy, Nathaniel Craig, Xiaochuan Lu, and Dave Sutherland, 2021, "Is SMEFT enough?," J. High Energy Phys. 03, 237.

Cohen, Timothy, Xiaochuan Lu, and Zhengkang Zhang, 2021a, "Functional prescription for EFT matching," J. High Energy Phys. 02, 228.

Cohen, Timothy, Xiaochuan Lu, and Zhengkang Zhang, 2021b, "STrEAMlining EFT Matching," SciPost Phys. **10**, 098.

Colangelo, G., A. X. El-Khadra, M. Hoferichter, A. Keshavarzi, C. Lehner, P. Stoffer, and T. Teubner, 2022, "Data-driven evaluations of Euclidean windows to scrutinize hadronic vacuum polarization," Phys. Lett. B **833**, 137313.

Coleman, Sidney R., J. Wess, and Bruno Zumino, 1969, "Structure of phenomenological Lagrangians. I," Phys. Rev. **177**, 2239–2247.

Contino, Roberto, Adam Falkowski, Florian Goertz, Christophe Grojean, and Francesco Riva, **2016**, "On the validity of the effective field theory approach to SM precision tests," J. High Energy Phys. 07, 144.

Contino, Roberto, Margherita Ghezzi, Christophe Grojean, Margarete Muhlleitner, and Michael Spira, 2013, "Effective Lagrangian for a light Higgs-like scalar," J. High Energy Phys. 07, 035.

Corbett, Tyler, O. J. P. Eboli, J. Gonzalez-Fraile, and M. C. Gonzalez-Garcia, 2013, "Robust determination of the Higgs couplings: Power to the data," Phys. Rev. D **87**, 015022.

Corbett, Tyler, Oscar J. P. Eboli, Dorival Goncalves, J. Gonzalez-Fraile, Tilman Plehn, and Michael Rauch, **2015**, "The Higgs legacy of the LHC run I," J. High Energy Phys. 08, 156.

Corbett, Tyler, O. J. P. Éboli, and M. C. Gonzalez-Garcia, 2015, "Unitarity constraints on dimension-six operators," Phys. Rev. D **91**, 035014.

Corbett, Tyler, O. J. P. Éboli, and M. C. Gonzalez-Garcia, 2017, "Unitarity constraints on dimension-six operators II: Including fermionic operators," Phys. Rev. D **96**, 035006.

Corbett, Tyler, Andreas Helset, Adam Martin, and Michael Trott, 2021, "EWPD in the SMEFT to dimension eight," J. High Energy Phys. 06, 076.

Corbett, Tyler, Andreas Helset, and Michael Trott, 2020, "Ward identities for the standard model effective field theory," Phys. Rev. D **101**, 013005.

Cornella, Claudia, Darius A. Faroughy, Javier Fuentes-Martin, Gino Isidori, and Matthias Neubert, 2021, "Reading the footprints of the B-meson flavor anomalies," J. High Energy Phys. 08, 050.

Craig, Nathaniel, Minyuan Jiang, Ying-Ying Li, and Dave Sutherland, 2020, "Loops and trees in generic EFTs," J. High Energy Phys. 08, 086.

Criado, J. C., and M. Pérez-Victoria, 2019, "Field redefinitions in effective theories at higher orders," J. High Energy Phys. 03, 038.

Criado, Juan C., 2018, "`MatchingTools`: A `Python` library for symbolic effective field theory calculations," Comput. Phys. Commun. **227**, 42–50.

D'Ambrosio, G., G. F. Giudice, G. Isidori, and A. Strumia, 2002, "Minimal flavor violation: An effective field theory approach," Nucl. Phys. **B645**, 155–187.

Das Bakshi, Supratim, Joydeep Chakrabortty, and Sunando Kumar Patra, 2019, "`CoDEx`: Wilson coefficient calculator connecting SMEFT to UV theory," Eur. Phys. J. C **79**, 21.

Das Bakshi, Supratim, Mikael Chala, Álvaro Díaz-Carmona, and Guilherme Guedes, 2022, "Towards the renormalisation of the standard model effective field theory to dimension eight: Bosonic interactions II," Eur. Phys. J. Plus **137**, 973.

Dashen, Roger F., and M. Weinstein, 1969, "Soft pions, chiral symmetry, and phenomenological Lagrangians," Phys. Rev. **183**, 1261–1291.

da Silva Almeida, Eduardo, Alexandre Alves, N. Rosa Agostinho, Oscar J. P. Éboli, and M. C. Gonzalez-Garcia, 2019, "Electroweak sector under scrutiny: A combined analysis of LHC and electroweak precision data," Phys. Rev. D **99**, 033001.

David, André, and Giampiero Passarino, 2016, "Through precision straits to next standard model heights," Rev. Phys. **1**, 13–28.

Davidson, Sacha, Martin Gorbahn, and Matthew Leak, 2018, "Majorana neutrino masses in the renormalization group equations for lepton flavor violation," Phys. Rev. D **98**, 095014.

Davies, C. T. H., *et al.* (Fermilab Lattice, MILC, and HPQCD Collaborations), 2022, "Windows on the hadronic vacuum polarization contribution to the muon anomalous magnetic moment," Phys. Rev. D **106**, 074509.

Dawson, S., P. P. Giardino, and A. Ismail, 2019, "Standard model EFT and the Drell-Yan process at high energy," Phys. Rev. D **99**, 035044.

Dawson, Sally, Samuel Homiller, and Samuel D. Lane, 2020, "Putting standard model EFT fits to work," Phys. Rev. D **102**, 055012.

de Blas, J., M. Ciuchini, E. Franco, A. Goncalves, S. Mishima, M. Pierini, L. Reina, and L. Silvestrini, 2022, "Global analysis of electroweak data in the standard model," Phys. Rev. D **106**, 033003.

de Blas, J., J. C. Criado, M. Perez-Victoria, and J. Santiago, 2018, "Effective description of general extensions of the standard model: The complete tree-level dictionary," J. High Energy Phys. 03, 109.

Dedes, A., W. Materkowska, M. Paraskevas, J. Rosiek, and K. Suxho, 2017, "Feynman rules for the standard model effective field theory in R_ξ-gauges," J. High Energy Phys. 06, 143.

Dedes, Athanasios, and Kostas Mantzaropoulos, 2021, "Universal scalar leptoquark action for matching," J. High Energy Phys. 11, 166.

Dekens, Wouter, and Peter Stoffer, 2019, "Low-energy effective field theory below the electroweak scale: Matching at one loop," J. High Energy Phys. 10, 197.

del Aguila, Francisco, Zoltan Kunszt, and Jose Santiago, 2016, "One-loop effective Lagrangians after matching," Eur. Phys. J. C **76**, 244.

Denner, Ansgar, Stefan Dittmaier, and Georg Weiglein, 1996, "The background field formulation of the electroweak standard model," Acta Phys. Pol. B **27**, 3645–3660 [arXiv:hep-ph/ 9609422].

Denner, Ansgar, Georg Weiglein, and Stefan Dittmaier, 1995, "Application of the background field method to the electroweak standard model," Nucl. Phys. **B440**, 95–128.

Distler, Jacques, Benjamin Grinstein, Rafael A. Porto, and Ira Z. Rothstein, 2007, "Falsifying Models of New Physics via WW Scattering," Phys. Rev. Lett. **98**, 041601.

Dittmaier, Stefan, and Carsten Grosse-Knetter, 1996, "Integrating out the standard Higgs field in the path integral," Nucl. Phys. **B459**, 497–536.

Dittmaier, Stefan, Sebastian Schuhmacher, and Maximilian Stahlhofen, 2021, "Integrating out heavy fields in the path integral using the background-field method: General formalism," Eur. Phys. J. C **81**, 826.

Donoghue, John F., 2009, "When EFTs fail," Proc. Sci. EFT09, 001 [arXiv:0909.0021].

Donoghue, John F., Eugene Golowich, and Barry R. Holstein, 2014, *Dynamics of the Standard Model*, 2nd ed., Vol. 2 (Oxford University Press, New York).

Drozd, Aleksandra, John Ellis, Jérémie Quevillon, and Tevong You, 2016, "The universal one-loop effective action," J. High Energy Phys. 03, 180.

Du, Yong, Xu-Xiang Li, and Jiang-Hao Yu, 2022, "Neutrino seesaw models at one-loop matching: Discrimination by effective operators," J. High Energy Phys. 09, 207.

Dugan, Michael J., and Benjamin Grinstein, 1991, "On the vanishing of evanescent operators," Phys. Lett. B **256**, 239–244.

Dvali, Gia, Andre Franca, and Cesar Gomez, 2012, "Road signs for UV-completion," arXiv:1204.6388.

Efrati, Aielet, Adam Falkowski, and Yotam Soreq, 2015, "Electroweak constraints on flavorful effective theories," J. High Energy Phys. 07, 018.

Einhorn, Martin B., and Jose Wudka, 2013, "The bases of effective field theories," Nucl. Phys. **B876**, 556–574.

Elias-Miró, J., J. R. Espinosa, E. Masso, and A. Pomarol, 2013a, "Higgs windows to new physics through $d = 6$ operators: Constraints and one-loop anomalous dimensions," J. High Energy Phys. 11, 066.

Elias-Miró, J., J. R. Espinosa, E. Masso, and A. Pomarol, 2013b, "Renormalization of dimension-six operators relevant for the Higgs decays $h \to \gamma\gamma, \gamma Z$," J. High Energy Phys. 08, 033.

Elias-Miró, Joan, Christophe Grojean, Rick S. Gupta, and David Marzocca, 2014, "Scaling and tuning of EW and Higgs observables," J. High Energy Phys. 05, 019.

Ellis, John, Maeve Madigan, Ken Mimasu, Veronica Sanz, and Tevong You, 2021, "Top, Higgs, diboson and electroweak fit to the standard model effective field theory," J. High Energy Phys. 04, 279.

Ellis, John, Christopher W. Murphy, Verónica Sanz, and Tevong You, 2018, "Updated global SMEFT fit to Higgs, diboson and electroweak data," J. High Energy Phys. 06, 146.

Ellis, John, Veronica Sanz, and Tevong You, 2014, "Complete Higgs sector constraints on dimension-6 operators," J. High Energy Phys. 07, 036.

Ellis, Sebastian A. R., Jérémie Quevillon, Pham Ngoc Hoa Vuong, Tevong You, and Zhengkang Zhang, 2020, "The fermionic universal one-loop effective action," J. High Energy Phys. 11, 078.

Ellis, Sebastian A. R., Jeremie Quevillon, Tevong You, and Zhengkang Zhang, 2016, "Mixed heavy-light matching in the universal one-loop effective action," Phys. Lett. B **762**, 166–176.

Ellis, Sebastian A. R., Jérémie Quevillon, Tevong You, and Zhengkang Zhang, 2017, "Extending the universal one-loop effective action: Heavy-light coefficients," J. High Energy Phys. 08, 054.

Endo, Motoi, Syuhei Iguro, Teppei Kitahara, Michihisa Takeuchi, and Ryoutaro Watanabe, 2022, "Non-resonant new physics search at the LHC for the $b \to c\tau\nu$ anomalies," J. High Energy Phys. 02, 106.

Ethier, Jacob J., Giacomo Magni, Fabio Maltoni, Luca Mantani, Emanuele R. Nocera, Juan Rojo, Emma Slade, Eleni Vryonidou, and Cen Zhang, 2021, "Combined SMEFT interpretation of Higgs, diboson, and top quark data from the LHC," J. High Energy Phys. 11, 089.

Falkowski, Adam, 2023, "Lectures on SMEFT," Eur. Phys. J. C **83**, 656.

Falkowski, Adam, and Riccardo Rattazzi, 2019, "Which EFT?," J. High Energy Phys. 10, 255.

Falkowski, Adam, and Francesco Riva, 2015, "Model-independent precision constraints on dimension-6 operators," J. High Energy Phys. 02, 039.

Falkowski, Adam, and David Straub, 2020, "Flavourful SMEFT likelihood for Higgs and electroweak data," J. High Energy Phys. 04, 066.

Faroughy, Darius A., Admir Greljo, and Jernej F. Kamenik, 2017, "Confronting lepton flavor universality violation in B decays with high-p_T tau lepton searches at LHC," Phys. Lett. B **764**, 126–134.

Faroughy, Darius A., Gino Isidori, Felix Wilsch, and Kei Yamamoto, 2020, "Flavour symmetries in the SMEFT," J. High Energy Phys. 08, 166.

Feldmann, Thorsten, and Thomas Mannel, 2008, "Large Top-Quark Mass and Nonlinear Representation of Flavor Symmetry," Phys. Rev. Lett. **100**, 171601.

Feldmann, Thorsten, Thomas Mannel, and Steffen Schwertfeger, 2015, "Renormalization group evolution of flavour invariants," J. High Energy Phys. 10, 007.

Fermi, E., 1934, "Versuch einer Theorie der β-Strahlen. I [An attempt of a theory of β-radiation. I]," Z. Phys. **88**, 161–177.

Feruglio, F., 1993, "The chiral approach to the electroweak interactions," Int. J. Mod. Phys. A **08**, 4937–4972.

Feruglio, Ferruccio, 2021, "A note on gauge anomaly cancellation in effective field theories," J. High Energy Phys. 03, 128.

Fierz, Markus, 1937, "Zur Fermischen Theorie des β-Zerfalls [On the Fermi theory of β-decay]," Z. Phys. **104**, 553.

Fonseca, Renato M., 2017, "The `Sym2Int` program: Going from symmetries to interactions," J. Phys. Conf. Ser. **873**, 012045.

Fonseca, Renato M., 2020, "Enumerating the operators of an effective field theory," Phys. Rev. D **101**, 035040.

Fox, Patrick J., Zoltan Ligeti, Michele Papucci, Gilad Perez, and Matthew D. Schwartz, 2008, "Deciphering top flavor violation at the LHC with B factories," Phys. Rev. D **78**, 054008.

Froggatt, C. D., and Holger Bech Nielsen, 1979, "Hierarchy of quark masses, cabibbo angles and CP violation," Nucl. Phys. **B147**, 277–298.

Fuentes-Martin, Javier, Admir Greljo, Jorge Martin Camalich, and José David Ruiz-Alvarez, 2020, "Charm physics confronts high-p_T lepton tails," J. High Energy Phys. 11, 080.

Fuentes-Martin, Javier, Gino Isidori, Julie Pagès, and Kei Yamamoto, 2020, "With or without U(2)? Probing non-standard flavor and helicity structures in semileptonic B decays," Phys. Lett. B **800**, 135080.

Fuentes-Martin, Javier, Matthias König, Julie Pagès, Anders Eller Thomsen, and Felix Wilsch, 2021, "`SuperTracer`: A calculator of functional supertraces for one-loop EFT matching," J. High Energy Phys. 04, 281.

Fuentes-Martin, Javier, Matthias König, Julie Pagès, Anders Eller Thomsen, and Felix Wilsch, 2023a, "A proof of concept for `Matchete`: An automated tool for matching effective theories," Eur. Phys. J. C **83**, 662.

Fuentes-Martin, Javier, Matthias König, Julie Pagès, Anders Eller Thomsen, and Felix Wilsch, 2023b, "Evanescent operators in one-loop matching computations," J. High Energy Phys. 02, 031.

Fuentes-Martin, Javier, Jorge Portoles, and Pedro Ruiz-Femenia, 2016, "Integrating out heavy particles with functional methods: A simplified framework," J. High Energy Phys. 09, 156.

Fuentes-Martin, Javier, Pedro Ruiz-Femenia, Avelino Vicente, and Javier Virto, 2021, "`DsixTools 2.0`: The effective field theory toolkit," Eur. Phys. J. C **81**, 167.

Gaillard, M. K., 1986, "The effective one loop Lagrangian with derivative couplings," Nucl. Phys. **B268**, 669–692.

Galda, Anne Mareike, Matthias Neubert, and Sophie Renner, 2021, "ALP-SMEFT interference," J. High Energy Phys. 06, 135.

Gasser, J., and H. Leutwyler, 1984, "Chiral perturbation theory to one loop," Ann. Phys. (N.Y.) **158**, 142.

Gasser, J., and H. Leutwyler, 1985, "Chiral perturbation theory: Expansions in the mass of the strange quark," Nucl. Phys. **B250**, 465–516.

Gavela, B. M., E. E. Jenkins, A. V. Manohar, and L. Merlo, 2016, "Analysis of general power counting rules in effective field theory," Eur. Phys. J. C **76**, 485.

Georgi, H., 1993, "Effective field theory,"Annu. Rev. Nucl. Part. Sci. **43**, 209–252.

Georgi, Howard, 1991, "On-shell effective field theory," Nucl. Phys. **B361**, 339–350.

Georgi, Howard, and Sheldon L. Glashow, 1972, "Gauge theories without anomalies," Phys. Rev. D **6**, 429.

Gerard, J. M., 1983, "Fermion mass spectrum in $\mathrm{SU}(2)_L \times \mathrm{U}(1)$," Z. Phys. C **18**, 145.

Gherardi, Valerio, David Marzocca, and Elena Venturini, 2020, "Matching scalar leptoquarks to the SMEFT at one loop," J. High Energy Phys. 07, 225.

Ghezzi, Margherita, Raquel Gomez-Ambrosio, Giampiero Passarino, and Sandro Uccirati, 2015, "NLO Higgs effective field theory and κ-framework," J. High Energy Phys. 07, 175.

Giudice, G. F., C. Grojean, A. Pomarol, and R. Rattazzi, 2007, "The strongly-interacting light Higgs," J. High Energy Phys. 06, 045.

Giudice, Gian Francesco, 2019, "The dawn of the post-naturalness era," arXiv:1710.07663.

Gnendiger, C., *et al.*, 2017, "To d, or not to d: Recent developments and comparisons of regularization schemes," Eur. Phys. J. C **77**, 471.

Gomez-Ambrosio, Raquel, 2019, "Studies of dimension-six EFT effects in vector boson scattering," Eur. Phys. J. C **79**, 389.

Gonzalez-Alonso, Martin, Admir Greljo, Gino Isidori, and David Marzocca, 2015, "Pseudo-observables in Higgs decays," Eur. Phys. J. C **75**, 128.

Gonzalez-Garcia, M. C., and Michele Maltoni, 2008, "Phenomenology with massive neutrinos," Phys. Rep. **460**, 1–129.

Gráf, Lukáš, Brian Henning, Xiaochuan Lu, Tom Melia, and Hitoshi Murayama, 2023, "Hilbert series, the Higgs mechanism, and HEFT," J. High Energy Phys. 02, 064.

Greljo, Admir, Jorge Martin Camalich, and José David Ruiz-Álvarez, 2019, "Mono-τ Signatures at the LHC Constrain Explanations of B-Decay Anomalies," Phys. Rev. Lett. **122**, 131803.

Greljo, Admir, Gino Isidori, Jonas M. Lindert, and David Marzocca, 2016, "Pseudo-observables in electroweak Higgs production," Eur. Phys. J. C **76**, 158.

Greljo, Admir, and David Marzocca, 2017, "High-p_T dilepton tails and flavor physics," Eur. Phys. J. C **77**, 548.

Greljo, Admir, Ajdin Palavrić, and Anders Eller Thomsen, **2022**, "Adding flavor to the SMEFT," J. High Energy Phys. 10, 010.

Greljo, Admir, Jakub Salko, Aleks Smolkovič, and Peter Stangl, 2023, "Rare b decays meet high-mass Drell-Yan," J. High Energy Phys. 05, 087.

Grinstein, Benjamin, and Michael Trott, 2007, "A Higgs-Higgs bound state due to new physics at a TeV," Phys. Rev. D **76**, 073002.

Grinstein, Benjamin, and Mark B. Wise, 1991, "Operator analysis for precision electroweak physics," Phys. Lett. B **265**, 326–334.

Grojean, Christophe, Marc Montull, and Marc Riembau, 2019, "Diboson at the LHC vs LEP," J. High Energy Phys. 03, 020.

Grossman, Yuval, and Yossi Nir, 2023, *The Standard Model: From Fundamental Symmetries to Experimental Tests* (Princeton University Press, Princeton, NJ).

Grzadkowski, B., M. Iskrzynski, M. Misiak, and J. Rosiek, 2010, "Dimension-six terms in the standard model Lagrangian," J. High Energy Phys. 10, 085.

Grzadkowski, Bohdan, Zenro Hioki, Kazumasa Ohkuma, and Jose Wudka, 2004, "Probing anomalous top quark couplings induced by dimension-six operators at photon colliders," Nucl. Phys. **B689**, 108–126.

Guedes, G., P. Olgoso, and J. Santiago, 2023, "Towards the one loop IR/UV dictionary in the SMEFT: One loop generated operators from new scalars and fermions," arXiv:2303.16965.

Hagiwara, Kaoru, S. Ishihara, R. Szalapski, and D. Zeppenfeld, 1993, "Low-energy effects of new interactions in the electroweak boson sector," Phys. Rev. D **48**, 2182–2203.

Haller, Johannes, Andreas Hoecker, Roman Kogler, Klaus Mönig, Thomas Peiffer, and Jörg Stelzer, 2018, "Update of the global electroweak fit and constraints on two-Higgs-doublet models," Eur. Phys. J. C **78**, 675.

Haller, Johannes, Andreas Hoecker, Roman Kogler, Klaus Mönig, and Jörg Stelzer, 2022, "Status of the global electroweak fit with `Gfitter` in the light of new precision measurements," Proc. Sci. ICHEP2022, 897 [arXiv:2211.07665].

Han, Zhenyu, and Witold Skiba, 2005, "Effective theory analysis of precision electroweak data," Phys. Rev. D **71**, 075009.

Hartland, Nathan P., Fabio Maltoni, Emanuele R. Nocera, Juan Rojo, Emma Slade, Eleni Vryonidou, and Cen Zhang, 2019, "A Monte Carlo global analysis of the standard model effective field theory: The top quark sector," J. High Energy Phys. 04, 100.

Hays, Chris, Andreas Helset, Adam Martin, and Michael Trott, 2020, "Exact SMEFT formulation and expansion to $\mathcal{O}(v^4/\Lambda^4)$," J. High Energy Phys. 11, 087.

Hays, Chris, Adam Martin, Verónica Sanz, and Jack Setford, 2019, "On the impact of dimension-eight SMEFT operators on Higgs measurements," J. High Energy Phys. 02, 123.

Helset, Andreas, and Andrew Kobach, 2020, "Baryon number, lepton number, and operator dimension in the SMEFT with flavor symmetries," Phys. Lett. B **800**, 135132.

Helset, Andreas, Adam Martin, and Michael Trott, 2020, "The geometric standard model effective field theory," J. High Energy Phys. 03, 163.

Helset, Andreas, Michael Paraskevas, and Michael Trott, 2018, "Gauge Fixing the Standard Model Effective Field Theory," Phys. Rev. Lett. **120**, 251801.

Henning, Brian, Xiaochuan Lu, Tom Melia, and Hitoshi Murayama, 2017a, "2, 84, 30, 993, 560, 15456, 11962, 261485, … : Higher dimension operators in the SM EFT," J. High Energy Phys. 08, 016.

Henning, Brian, Xiaochuan Lu, Tom Melia, and Hitoshi Murayama, 2017b, "Operator bases, S-matrices, and their partition functions," J. High Energy Phys. 10, 199.

Henning, Brian, Xiaochuan Lu, and Hitoshi Murayama, 2016, "How to use the standard model effective field theory," J. High Energy Phys. 01, 023.

Henning, Brian, Xiaochuan Lu, and Hitoshi Murayama, 2018, "One-loop matching and running with covariant derivative expansion," J. High Energy Phys. 01, 123.

Herrlich, Stefan, and Ulrich Nierste, 1995, "Evanescent operators, scheme dependences and double insertions," Nucl. Phys. **B455**, 39–58.

't Hooft, Gerard, and M. J. G. Veltman, 1972, "Regularization and renormalization of gauge fields," Nucl. Phys. **B44**, 189–213.

Ignatov, F. V., *et al.* (CMD-3 Collaboration), 2023, "Measurement of the $e^+e^- \to \pi^+\pi^-$ cross section from threshold to 1.2 GeV with the CMD-3 detector," arXiv:2302.08834.

Isidori, Gino, 2010, "Effective theories of electroweak symmetry breaking," Proc. Sci. CD09, 073 [arXiv:0911.3219].

Isidori, Gino, Aneesh V. Manohar, and Michael Trott, 2014, "Probing the nature of the Higgs-like boson via $h \to V\mathcal{F}$ decays," Phys. Lett. B **728**, 131–135.

Isidori, Gino, Yosef Nir, and Gilad Perez, 2010, "Flavor physics constraints for physics beyond the standard model," Annu. Rev. Nucl. Part. Sci. **60**, 355.

Isidori, Gino, Julie Pagès, and Felix Wilsch, 2022, "Flavour alignment of new physics in light of the $(g-2)_\mu$ anomaly," J. High Energy Phys. 03, 011.

Isidori, Gino, and Frederic Teubert, 2014, "Status of indirect searches for new physics with heavy flavour decays after the initial LHC run," Eur. Phys. J. Plus **129**, 40.

Isidori, Gino, and Michael Trott, 2014, "Higgs form factors in associated production," J. High Energy Phys. 02, 082.

Jaffredo, Florentin, 2022, "Revisiting mono-tau tails at the LHC," Eur. Phys. J. C **82**, 541.

Jantzen, Bernd, 2011, "Foundation and generalization of the expansion by regions," J. High Energy Phys. 12, 076.

Jegerlehner, F., 2001, "Facts of life with γ_5," Eur. Phys. J. C **18**, 673–679.

Jenkins, Elizabeth E., Aneesh V. Manohar, and Peter Stoffer, 2018a, "Low-energy effective field theory below the electroweak scale: Anomalous dimensions," J. High Energy Phys. 01, 084.

Jenkins, Elizabeth E., Aneesh V. Manohar, and Peter Stoffer, 2018b, "Low-energy effective field theory below the electroweak scale: Operators and matching," J. High Energy Phys. 03, 016.

Jenkins, Elizabeth E., Aneesh V. Manohar, and Michael Trott, 2013a, "On gauge invariance and minimal coupling," J. High Energy Phys. 09, 063.

Jenkins, Elizabeth E., Aneesh V. Manohar, and Michael Trott, 2013b, "Renormalization group evolution of the standard model dimension

six operators I: Formalism and λ dependence," J. High Energy Phys. 10, 087.
Jenkins, Elizabeth E., Aneesh V. Manohar, and Michael Trott, 2014, "Renormalization group evolution of the standard model dimension six operators II: Yukawa dependence," J. High Energy Phys. 01, 035.
Jiang, Yun, and Michael Trott, 2017, "On the non-minimal character of the SMEFT," Phys. Lett. B **770**, 108–116.
Kagan, Alexander L., Gilad Perez, Tomer Volansky, and Jure Zupan, 2009, "General minimal flavor violation," Phys. Rev. D **80**, 076002.
Kobach, Andrew, 2016, "Baryon number, lepton number, and operator dimension in the standard model," Phys. Lett. B **758**, 455–457.
Korner, J. G., D. Kreimer, and K. Schilcher, 1992, "A practicable γ_5 scheme in dimensional regularization," Z. Phys. C **54**, 503–512.
Krämer, Michael, Benjamin Summ, and Alexander Voigt, 2020, "Completing the scalar and fermionic universal one-loop effective action," J. High Energy Phys. 01, 079.
Kreimer, Dirk, 1990, "The γ_5 problem and anomalies: A Clifford algebra approach," Phys. Lett. B **237**, 59–62.
Kumar, Jacky, 2022, "Renormalization group improved implications of semileptonic operators in SMEFT," J. High Energy Phys. 01, 107.
Lang, Jannis, Stefan Liebler, Heiko Schäfer-Siebert, and Dieter Zeppenfeld, 2021, "Effective field theory versus UV-complete model: Vector boson scattering as a case study," Eur. Phys. J. C **81**, 659.
Lee, Benjamin W., C. Quigg, and H. B. Thacker, 1977a, "The Strength of Weak Interactions at Very High Energies and the Higgs Boson Mass," Phys. Rev. Lett. **38**, 883–885.
Lee, Benjamin W., C. Quigg, and H. B. Thacker, 1977b, "Weak interactions at very high energies: The role of the Higgs boson mass," Phys. Rev. D **16**, 1519.
Lehman, Landon, 2014, "Extending the standard model effective field theory with the complete set of dimension-7 operators," Phys. Rev. D **90**, 125023.
Lehman, Landon, and Adam Martin, 2016, "Low-derivative operators of the standard model effective field theory via Hilbert series methods," J. High Energy Phys. 02, 081.
Lehmann, H., K. Symanzik, and W. Zimmermann, 1955, "On the formulation of quantized field theories," Nuovo Cimento **1**, 205–225.
Leung, Chung Ngoc, S. T. Love, and S. Rao, 1986, "Low-energy manifestations of a new interaction scale: Operator analysis," Z. Phys. C **31**, 433.
Li, Hao-Lin, Yu-Han Ni, Ming-Lei Xiao, and Jiang-Hao Yu, 2022, "The bottom-up EFT: Complete UV resonances of the SMEFT operators," J. High Energy Phys. 11, 170.
Li, Hao-Lin, Zhe Ren, Jing Shu, Ming-Lei Xiao, Jiang-Hao Yu, and Yu-Hui Zheng, 2021, "Complete set of dimension-eight operators in the standard model effective field theory," Phys. Rev. D **104**, 015026.
Li, Hao-Lin, Zhe Ren, Ming-Lei Xiao, Jiang-Hao Yu, and Yu-Hui Zheng, 2021a, "Complete set of dimension-nine operators in the standard model effective field theory," Phys. Rev. D **104**, 015025.
Li, Hao-Lin, Zhe Ren, Ming-Lei Xiao, Jiang-Hao Yu, and Yu-Hui Zheng, 2021b, "Low energy effective field theory operator basis at $d \leq 9$," J. High Energy Phys. 06, 138.
Li, Hao-Lin, Zhe Ren, Ming-Lei Xiao, Jiang-Hao Yu, and Yu-Hui Zheng, 2022, "Operators for generic effective field theory at any dimension: On-shell amplitude basis construction," J. High Energy Phys. 04, 140.
Li, Xu, Di Zhang, and Shun Zhou, 2022, "One-loop matching of the type-II seesaw model onto the standard model effective field theory," J. High Energy Phys. 04, 038.
Liao, Yi, and Xiao-Dong Ma, 2016, "Renormalization group evolution of dimension-seven baryon- and lepton-number-violating operators," J. High Energy Phys. 11, 043.
Liao, Yi, and Xiao-Dong Ma, 2019, "Renormalization group evolution of dimension-seven operators in standard model effective field theory and relevant phenomenology," J. High Energy Phys. 03, 179.
Liao, Yi, and Xiao-Dong Ma, 2020, "An explicit construction of the dimension-9 operator basis in the standard model effective field theory," J. High Energy Phys. 11, 152.
Liao, Yi, and Xiao-Dong Ma, 2022, "One-loop matching of scotogenic model onto standard model effective field theory up to dimension 7," J. High Energy Phys. 12, 053.
Liao, Yi, Xiao-Dong Ma, and Quan-Yu Wang, 2020, "Extending low energy effective field theory with a complete set of dimension-7 operators," J. High Energy Phys. 08, 162.
Llewellyn Smith, C. H., 1973, "High-energy behavior and gauge symmetry," Phys. Lett. **46B**, 233–236.
Longhitano, Anthony C., 1980, "Heavy Higgs bosons in the Weinberg-Salam model," Phys. Rev. D **22**, 1166.
Longhitano, Anthony C., 1981, "Low-energy impact of a heavy Higgs boson sector," Nucl. Phys. **B188**, 118–154.
Machado, Camila S., Sophie Renner, and Dave Sutherland, 2023, "Building blocks of the flavourful SMEFT RG," J. High Energy Phys. 03, 226.
Maltoni, Fabio, Luca Mantani, and Ken Mimasu, 2019, "Top-quark electroweak interactions at high energy," J. High Energy Phys. 10, 004.
Maltoni, Fabio, Luca Mantani, and Ken Mimasu, 2020, "Modified interactions in the top-quark electroweak sector: Exploiting unitarity violating effects at the amplitude level to probe new physics," Proc. Sci. EPS-HEP2019, 652 [arXiv:1910.05053].
Manohar, Aneesh, and Howard Georgi, 1984, "Chiral quarks and the nonrelativistic quark model," Nucl. Phys. **B234**, 189–212.
Manohar, Aneesh V., 2013, "An exactly solvable model for dimension six Higgs operators and $h \to \gamma\gamma$," Phys. Lett. B **726**, 347–351.
Manohar, Aneesh V., 2018, "Introduction to effective field theories," in *Effective Field Theory in Particle Physics and Cosmology*, Proceedings of the Les Houches Summer School, Session CVIII, edited by Sacha Davidson, Paolo Gambino, Mikko Laine, Matthias Neubert, and Christophe Salomon (Oxford University Press, New York), https://academic.oup.com/book/44246/chapter-abstract/372561858?redirectedFrom=fulltext.
Marzocca, David, Ui Min, and Minho Son, **2020**, "Bottom-flavored mono-tau tails at the LHC," J. High Energy Phys. 12, 035.
Murphy, Christopher W., 2020, "Dimension-8 operators in the standard model eective field theory," J. High Energy Phys. 10, 174.
Murphy, Christopher W., 2021, "Low-energy effective field theory below the electroweak scale: Dimension-8 operators," J. High Energy Phys. 04, 101.
Nicolai, H., and P. K. Townsend, 1980, "Anomalies and supersymmetric regularization by dimensional reduction," Phys. Lett. **93B**, 111–115.
Nikolidakis, Emanuel, and Christopher Smith, 2008, "Minimal flavor violation, seesaw, and R parity," Phys. Rev. D **77**, 015021.
Nishi, C. C., 2005, "Simple derivation of general Fierz-like identities," Am. J. Phys. **73**, 1160–1163.
Passarino, Giampiero, 2017, "Field reparametrization in effective field theories," Eur. Phys. J. Plus **132**, 16.

Passarino, Giampiero, Christian Sturm, and Sandro Uccirati, 2010, "Higgs pseudo-observables, second Riemann sheet and all that," Nucl. Phys. **B834**, 77–115.

Pich, Antonio, Ignasi Rosell, Joaquin Santos, and Juan Jose Sanz-Cillero, 2017, "Fingerprints of heavy scales in electroweak effective Lagrangians," J. High Energy Phys. 04, 012.

Politzer, H. David, 1980, "Power corrections at short distances," Nucl. Phys. **B172**, 349–382.

Remmen, Grant N., and Nicholas L. Rodd, 2019, "Consistency of the standard model effective field theory," J. High Energy Phys. 12, 032.

Remmen, Grant N., and Nicholas L. Rodd, 2022, "Signs, spin, SMEFT: Sum rules at dimension six," Phys. Rev. D **105**, 036006.

Ren, Zhe, and Jiang-Hao Yu, 2022, "A complete set of the dimension-8 Green's basis operators in the standard model effective field theory," arXiv:2211.01420.

Skiba, Witold, 2010, "Effective field theory and precision electroweak measurements," arXiv:1006.2142.

Smolkovič, Aleks, Michele Tammaro, and Jure Zupan, 2019, "Anomaly free Froggatt-Nielsen models of flavor," J. High Energy Phys. 10, 188.

Stoffer, Peter, 2023, "Effective field theories for particle physics," https://www.physik.uzh.ch/en/teaching/PHY578/HS2022.html.

Straub, David M., 2018, "`flavio`: A `Python` package for flavour and precision phenomenology in the standard model and beyond," arXiv:1810.08132.

Sun, Hao, Yi-Ning Wang, and Jiang-Hao Yu, 2022, "Hilbert series and operator counting on the Higgs effective field theory," arXiv:2211.11598.

Sun, Hao, Ming-Lei Xiao, and Jiang-Hao Yu, 2023a, "Complete NLO operators in the Higgs effective field theory," J. High Energy Phys. 05, 043.

Sun, Hao, Ming-Lei Xiao, and Jiang-Hao Yu, 2023b, "Complete NNLO operator bases in Higgs effective field theory," J. High Energy Phys. 04, 086.

Tracas, N., and N. Vlachos, 1982, "Two loop calculations in QCD and the $\Delta I = 1/2$ rule in nonleptonic weak decays," Phys. Lett. **115B**, 419.

Weinberg, Steven, 1967, "Dynamical Approach to Current Algebra," Phys. Rev. Lett. **18**, 188–191.

Weinberg, Steven, 1979a, "Baryon and Lepton Nonconserving Processes," Phys. Rev. Lett. **43**, 1566–1570.

Weinberg, Steven, 1979b, "Phenomenological Lagrangians," Physica (Amsterdam) **96A**, 327–340.

Weinberg, Steven, 1980a, "Effective gauge theories," Phys. Lett. **91B**, 51–55.

Weinberg, Steven, 1980b, "Varieties of baryon and lepton nonconservation," Phys. Rev. D **22**, 1694.

Weinberg, Steven, 2010, "Effective field theory, past and future," Proc. Sci. CD09, 001 [arXiv:0908.1964].

Weinberg, Steven, 2016, "Effective field theory, past and future," Int. J. Mod. Phys. A **31**, 1630007.

Wilson, K. G., 1983, "The renormalization group and critical phenomena," Rev. Mod. Phys. **55**, 583–600.

Wilson, Kenneth G., 1969, "Non-Lagrangian models of current algebra," Phys. Rev. **179**, 1499–1512.

Yamashita, Kimiko, Cen Zhang, and Shuang-Yong Zhou, 2021, "Elastic positivity vs extremal positivity bounds in SMEFT: A case study in transversal electroweak gauge-boson scatterings," J. High Energy Phys. 01, 095.

Zhang, Cen, and Shuang-Yong Zhou, 2019, "Positivity bounds on vector boson scattering at the LHC," Phys. Rev. D **100**, 095003.

Zhang, Di, and Shun Zhou, 2021, "Complete one-loop matching of the type-I seesaw model onto the standard model effective field theory," J. High Energy Phys. 09, 163.

Zhang, Zhengkang, 2017, "Covariant diagrams for one-loop matching," J. High Energy Phys. 05, 152.